Removal of Hexavalent Chromium from Water

Using Manganese Oxide Sorbents

BY

SNOVER PUNIA

B.S., Loyola University, 2010

THESIS

submitted as partial fulfillment of the requirements
for the degree of Master of Science in Civil Engineering
in the Graduate College of the
University of Illinois at Chicago, 2017

Chicago, Illinois

Defense Committee:
Amid Khodadoust, Chair and Advisor
Krishna Reddy
Sybil Derrible

This thesis is dedicated to
my mother, Rita Kaur Punia,
for all her love, encouragement,
and support.

ACKNOWLEDGEMENTS

I would first and foremost like to extend my sincerest thanks to my research advisor, Professor Khodadoust, for giving me the opportunity to work with him. His guidance and expertise has been of great assistance to my knowledge of environmental science and remediation. The way he helped me to construct the methodology of my master's research will benefit me in my future work as well. I am very appreciative for his limitless patience and support throughout my research work.

I would also like to thank Professor Krishna R. Reddy and Professor Sybil Derrible for serving on my thesis committee and offering their professional opinions. Additionally, I am thankful to my colleagues, Hamed, Lisha, Soheil, and Raja for all their help and encouragement in completing my thesis. I would like to extend my appreciation to all my family for their support. Finally, I would like to express my gratitude to my fiancé, Alejandro Trujillo, for his encouragement and support.

TABLE OF CONTENTS

TABLE OF CONTENTS (continued)

TABLE OF CONTENTS (continued)

TABLE OF CONTENTS (continued)

LIST OF TABLES

I. RESEARCH BACKGROUND

II. ISOTHERM AND KINETIC STUDIES

LIST OF TABLES (continued)

LIST OF TABLES (continued)

LIST OF FIGURES

I. RESEARCH BACKGROUND

LIST OF FIGURES (continued)

II. ISOTHERM AND KINETIC STUDIES

LIST OF FIGURES (continued)

III. pH, CO-EXISTING IONS, ZETA POTENTIAL, AND REGENERATION STUDIES

LIST OF FIGURES (continued)

LIST OF FIGURES (continued)

SUMMARY

The increasing occurrence of hexavalent chromium [Cr (VI)] in water resources worldwide and recent evidence for genotoxic and carcinogenic effects of Cr (VI) by ingestion have heightened concern for this contaminant in drinking water. The current U.S. EPA maximum contaminant level (MCL) is 0.1 mg/L for total chromium. In contaminated water, Cr (VI) levels are typically three to five times the U.S. EPA limit and have been mainly traced to the leaking of industrial waste products such as stainless steel, electroplating, pigments, dyes, and leather tanning. The health concerns have not only led to a global trend towards more stringent regulations, but to the subsequent need for more effective and less expensive technologies for removal of Cr (VI).

The conventional methods for Cr (VI) removal, which include Cr (VI) reduction and precipitation, ion exchange, and membrane filtration, have several drawbacks such as high capital and operational cost, production of chemical sludge and sludge disposal problems. Adsorption has been considered as an effective but less expensive and simpler technology for the removal of Cr(VI) from water. Manganese oxide based sorbents have shown promise as low-cost adsorbents. In this study, the feasibility and application of manganese (III) oxide (Mn_2O_3) powder and two manganese-aluminum coated sands (New MCS and X MCS) were evaluated as potential sorbents for the removal of Cr (VI) from water. The processes were investigated by batch technique at room temperature and the adsorption data were analyzed using adsorption equilibrium equations and adsorption kinetic models. The Cr (VI) adsorption capacities and reaction rates were determined. The effect of pH and co- existing ions on adsorption of Cr(VI) was investigated. The reuse and regeneration of sorbent was also evaluated.

The Cr (VI) adsorption characteristics were best described using the Freundlich adsorption equation. The Dubinin-Radushkevich adsorption equation parameters showed that the Cr (VI) adsorption was predominately physical and reversible in nature. The mainly physical nature of adsorption also correlated with the rapid kinetics of Cr (VI) adsorption, particularly in case of the MCS adsorbents. Both Mn_2O_3 and MCS sorbents effectively adsorbed Cr (VI) within the pH range of 2 to 10. The adsorption of Cr (VI) was found to be slightly enhanced in the presence of Ca^{2+} and was suppressed in the presence of 0.1 mM PO_4^{3-}, 0.5 mM HCO_3^- , or 1 mM SO_4^{2-} concentrations. The reuse potential of the MCS adsorbents was greater than that of Mn_2O_3; New MCS showed potential for further reuse and Cr (VI) removal after regeneration using 0.001 N NaOH. The analysis of the point of zero charge (PZC) of Mn_2O_3 indicated that Cr (VI) anions were most likely adsorbed as inner-sphere complexes, while the more alkaline PZC of the MCS sorbents supported the formation of weakly bound Cr (VI) in outer-sphere complexes.

The adsorption capacity and kinetics were favorable for using Mn_2O_3 and MCS as sorbents for the removal of Cr (VI) from water. The application of MCS sorbents for Cr (VI) removal can offer the following advantages: lower cost, faster kinetics, wider effective pH range, greater stability under competing ion conditions and sorbent reuse potential. It is recommended that the MCS sorbents be developed further to improve the Cr (VI) adsorption capacity. The surface complex structures can be confirmed from spectroscopic studies in future work, and the sand coating mixture and consistency can be optimized for future preparations of the MCS sorbents.

Chapter I

I. RESEARCH BACKGROUND

1. INTRODUCTION

Hexavalent chromium Cr (VI) is a serious environmental concern due to its high toxicity and mobility, and difficult removal from industrial wastewater [1]. Moreover, it is a strong oxidizing agent that is carcinogenic. It distributes rapidly through soil and groundwater and when in the presence of an environmental reductant such as Fe (II) and organic substances, converts to trivalent chromium Cr (III), the dominant form of chromium Cr found in nature [1-5]. Cr (VI), however, can also be resistant to reduction [2].

1.1. Chromium mass distribution

Cr is found in carbonaceous meteorites at 3.1 parts per thousand by mass, in the sun at 20 ppm by mass, in the universe at 15 ppm by mass, in crustal rocks, stream water, and seawater on earth at 140 ppm, 1 ppb, and 0.6 ppb by mass [1]. Humans have 30 ppb Cr by mass. Chromium (III) oxide (Cr_2O_3) is the ten most abundant compound in Earth's crust and chromite [(Mg, Fe^{2+}) $(Cr, Al, Fe^{3+})_2 O_4$] is the principal ore mineral. Cr (VI) minerals are categorized in the following Dana mineral classes: carbonates-hydroxyl, carbonates-halogen, anhydrous chromates, compound chromates, phosphates, borates, iodates, or sulfides, hydroxides and oxides containing hydroxyl, and multiple oxides with Nb, Ta, and Ti.

1.1.1. Natural sources of chromium

Volcanic eruptions, erosion of soils and rocks, airborne sea salt particles, and smoke from forest wildfires are the natural sources of Cr. The alteration and weathering of ultramafic rocks are found to be the prominent cause of naturally elevated concentrations of Cr (VI) in soils and groundwater globally [6-11]. A recent study showed that frequent appearances of high Cr (VI) concentrations throughout Greece occur on or near ultramafic rocks as depicted in Figure 1[12]. Naturally occurring Cr (VI) concentrations ranging from 4 µg/L to 700 µg/L have been reported; those exceeding the World Health Organization's maximum contaminant level for drinking water are found in ground and surface waters from New Caledonia, California, Italy, and Mexico [6].

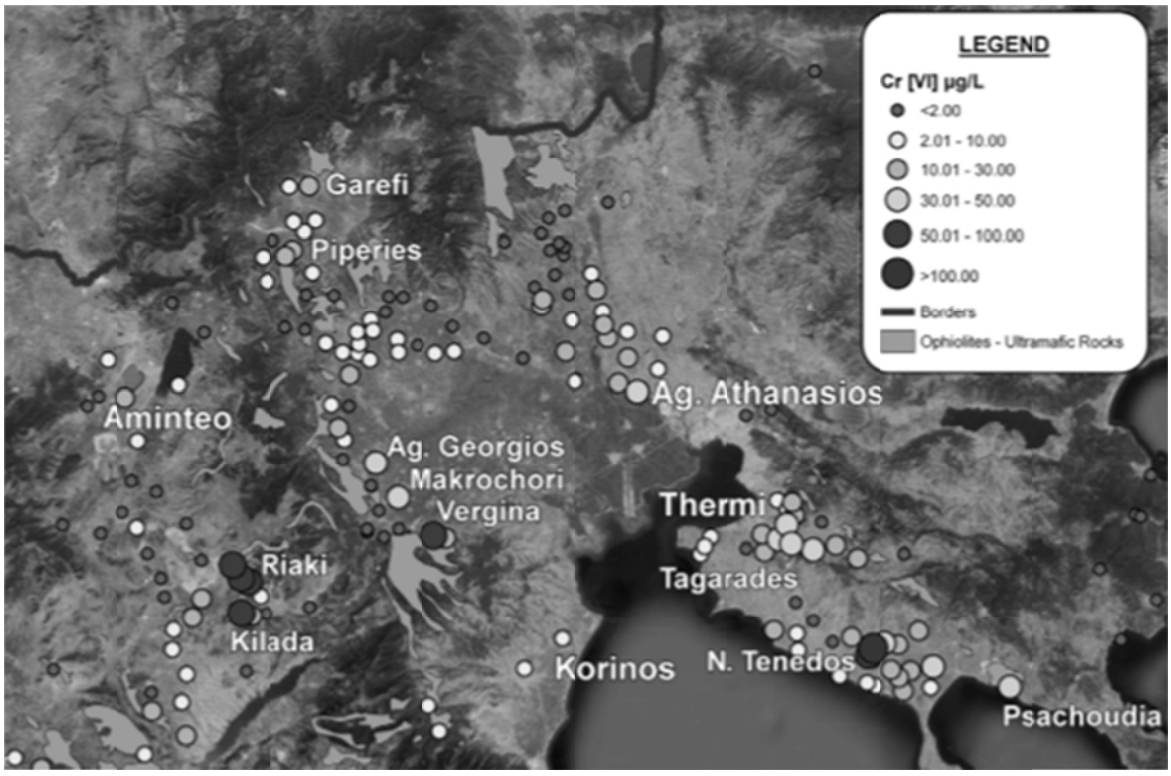

Fig. 1. Cr (VI) concentrations in central and western Macedonia [12].

1.1.2. Anthropogenic sources of chromium

Increased levels of Cr (VI) are also found in areas of intense industrial activity. The waste products of stainless steel, electroplating, dyes, pigments, wood preservation, and leather tanning manufacturing processes specifically contain Cr (VI) compounds such as chromic acid that frequently leak into soil and groundwater [1]. Table 1 below shows reported Cr (VI) concentrations of wastewater effluents ranging from 3.7 mg/L to 3,950 mg/L, which are much higher than naturally occurring Cr(VI) concentrations [6].

Table 1. Industrial wastewater containing Cr (VI) [6].

Industry	**Cr (VI) concentration (mg/L)**
Hardware factory	60
Chrome tanning plant	3.7
Electroplating plant	1.0
Electropolishing plant	42.8
Tannery plant	3,950
Tannery plant	100
Tannery plant	1,770
Electroplating plant	20.7
Electroplating plant	75.4
Tannery plant	8.3

1.1.3. Health effects of Cr (VI)

Studies indicate that acute and chronic exposure through inhalation of ambient air, ingestion of food and drinking water containing Cr, or dermal contact may result in adverse health effects for the general population [13]. Acute to high concentration inhalation exposure may result in gastrointestinal and neurological effects. Chronic exposure to high levels by inhalation or ingestion may affect the liver, kidney, gastrointestinal and immune systems, or blood. Ingestion of high levels can also cause gastrointestinal effects such as abdominal pain, vomiting, and hemorrhage. Acute dermal exposure causes skin burns whereas chronic exposure may cause contact dermatitis, sensitivity, and skin ulcerations. Developmental abnormalities in mice and reproductive effects by the ingestion route have also been reported. The EPA has classified Cr (VI) as a known human carcinogen by the inhalation route only.

1.1.4. Regulatory concentrations

The current USEPA MCL for total Cr in drinking water is 0.1 mg/L and is based on the assumption that Cr (VI) is not carcinogenic when ingested [14]. The World Health Organization recommends a more stringent MCL of 0.05 mg/L for total Cr due to the uncertainty of relevant studies. The California EPA established a MCL of 0.010 mg/L for Cr (VI) on July 1, 2014 based on the potential for Cr (VI) carcinogenic effects when ingested [15]. More studies are needed to determine the actual health risks. Also, total Cr rather than Cr (VI) is commonly regulated to avoid the underestimation of health risks [1]. In Tables 2 and 3, drinking water and wastewater U.S. and worldwide regulations are presented.

Table 2. Drinking water regulations [1].

Compound	Country	Standard (mg/L)
Total Cr	Kazakhstan	0.0031
Total Cr	Germany	0.05
Cr (VI)	Japan	0.05
Total Cr	United Kingdom	0.05
Total Cr	South Africa	0.1
Total Cr	U.S.	0.1

Table 3. Wastewater regulations [1].

Scenario	Country	Standard (mg/L)
Cr (VI)	Kazakhstan	0.005-0.03
Cr (VI) for freshwater-continuous (maximum)	U.S.	0.01 (0.015)
Cr (VI) for leather industry	Germany	0.05
Cr (VI) for salt water -continuous (maximum)	U.S.	0.05 (1.1)
Cr (VI) if total mass flow is > 1 g/day	France	0.1
Cr (VI) for metal or chemical industry	Germany	0.1
Total Cr if total mass flow is 5 g/day	France	0.5
Total Cr max for metal of chemical industry	Germany	0.5
Cr (VI) public water systems	Japan	0.5
Total Cr	South Africa	0.5
Total Cr max for leather industry	Germany	1
Total Cr in public water system	Japan	2
Range for estuary and coastal water, based on water hardness, receptors salmonid and cyprinid	U.K.	5-250

1.2. Chromium chemistry

Several chemical forms of Cr can exist with oxidation numbers ranging from -2 to +6 [1]. However, only the +3 and +6 states are stable in the environment exhibiting vastly different transport characteristics [16]. Cr (VI) compounds as compared with Cr (III) are more soluble, mobile, and bioavailable. The distribution between Cr (III) and Cr (VI) compounds depends on solution pH, Cr concentration, and redox potential (Eh) as depicted in the Pourbaix diagram given in Fig. 2 [17]. The diagram shows that Cr (VI) is stable in oxidizing conditions whereas Cr (III) predominates more under reducing conditions. Also despite variations in pH, Cr (VI) does not show any insoluble species. Therefore, to form a Cr solid phase for easy separation from solution, the oxidation state must be changed by altering redox conditions. This is the common treatment method for Cr (VI) removal. It must be noted that the kinetics of redox reactions also affect Cr (VI) and Cr (III) distribution [18]. The speciation of Cr (VI) entities is presented next to further understand the following Cr (VI) transport processes: redox, precipitation, and adsorption.

1.2.1. Chromium (VI) speciation in aqueous systems

The following Cr (VI) species are found in various equilibria depending on solution pH and total Cr (VI) concentration: $[H_2CrO_4]$, $[HCrO_4]^-$, $[CrO_4]^{2-}$, and $[Cr_2O_7]^{2-}$. This dependence is illustrated in Fig. 3 and Table 4. In Fig. 3, three pH regions in the predominance zone diagram may be distinguished for Cr (VI) species: (i) pH<0.9, where H_2CrO_4 is a significant species, (ii) pH 0.9 to 6.4, where $HCrO_4^-$ predominates and (iii) pH > 6.4, where CrO_4^{2-} predominates [17].

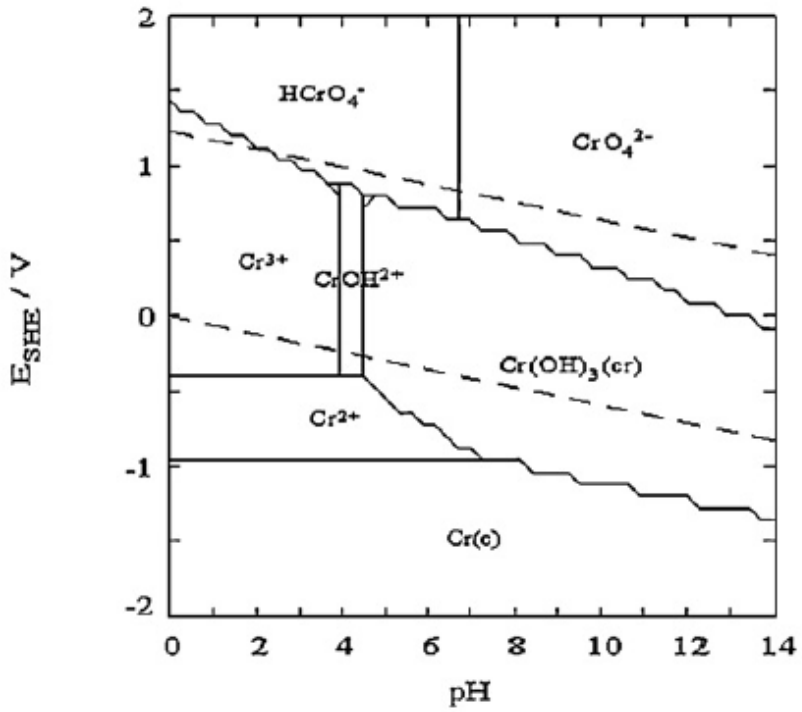

Fig. 2. Pourbaix diagram for Cr chemical species in aqueous solution. $[CrO_4]^2 = 2.00$ mM, I = 0.005 M, and T = 25 °C [17].

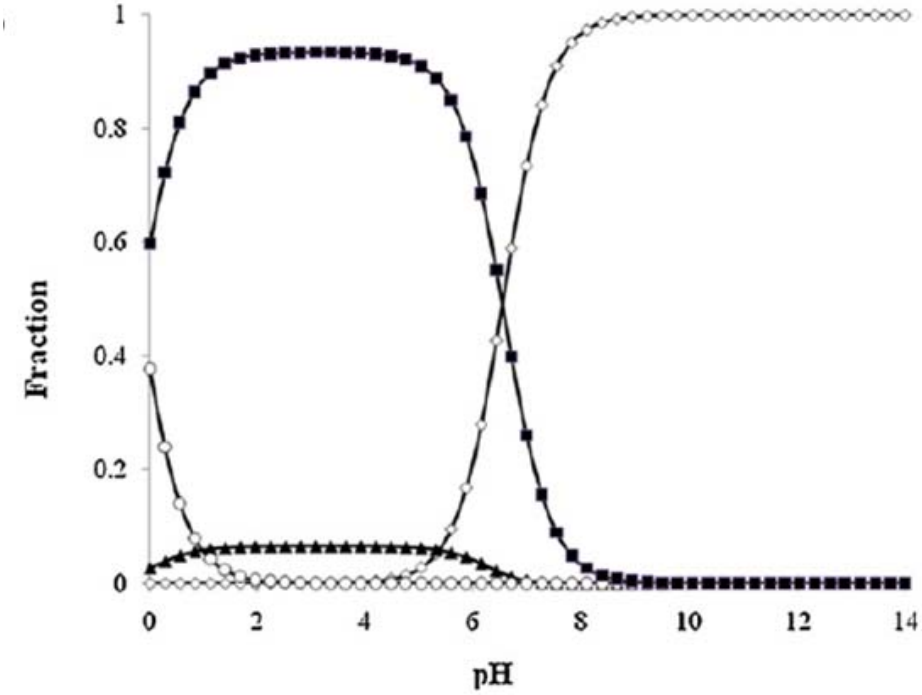

Fig. 3. Prodominance zone diagram for Cr(VI) chemical species in aqueous solution. (◊) CrO_4^{2-}, (▲) $Cr_2O_7^{2-}$, (○) H_2CrO4, and (■) $HCrO_4^-$ [17].

The published abundances of Cr (VI) species at concentrations of about 5 mg/L and 500 mg/L and different pH are tabulated in Table 4 [19]. This data shows that the formation of $Cr_2O_7^{2-}$ ions requires Cr (VI) concentrations greater than 500 mg/L and acidic environments, which is uncommon in natural waters within the normal pH range of 6 to 8. For concentrations greater than 1000 mg/, $Cr_2O_7^{2-}$ ions are found to dominate in acidic environments [1].

Table 4. Calculated abundances of Cr (VI) species in aqueous solution at pH 1-8 and total Cr (VI) concentrations (C) in the range 10^{-2} to 10^{-5} M [19].

		Abundance (%)			
pH	**C (M)**	**H_2CrO_4**	**$HCrO_4^-$**	**CrO_4^{2-}**	**$Cr_2O_7^{2-}$**
1	**10^{-2}**	27.3	49.1	0.0	23.6
	10^{-4}	35.6	64.0	0.0	0.4
	10^{-5}	35.7	64.3	0.0	0.0
2	**10^{-2}**	3.4	60.6	0.0	36.0
	10^{-4}	5.0	94.0	0.0	1.0
	10^{-5}	5.0	95.0	0.0	0.0
3	**10^{-2}**	0.3	62.0	0.0	37.7
	10^{-4}	0.5	98.5	0.0	1.0
	10^{-5}	0.6	99.3	0.0	0.1
4	**10^{-2}**	0.0	62.1	0.2	37.7
	10^{-4}	0.0	98.7	0.3	1.0
	10^{-5}	0.0	99.3	0.3	0.4
5	**10^{-2}**	0.0	61.3	2.0	36.7
	10^{-4}	0.0	96.0	3.0	1.0
	10^{-5}	0.0	96.8	3.1	0.1
6	**10^{-2}**	0.0	54.1	17.3	28.6
	10^{-4}	0.0	75.3	24.0	0.7
	10^{-5}	0.0	75.7	24.2	0.1
7	**10^{-2}**	0.0	22.6	72.4	5.0
	10^{-4}	0.0	23.6	76.2	0.0
	10^{-5}	0.0	23.8	76.2	0.0
8	**10^{-2}**	0.0	3.0	96.9	0.1
	10^{-4}	0.0	3.0	97.0	0.0
	10^{-5}	0.0	3.0	97.0	0.0

$[H_2CrO_4]$ is characterized as strong acid [3] and $[HCrO_4]^-$ a weak acid. The reported logarithmic acid dissociation constants (pKa) for hydrogen chromate and chromic acid equilibria are given in Table 5 [20-24]. The reported pKa values are shown to vary.

Table 5. pKa Values for chromic acid and hydrogen chromate at 25 ˚C.

Equilibrium	pKa	Reference
$[H_2CrO_4] \Leftrightarrow H^+ + [HCrO_4]^-$	-0.98	[20]
	0.74	[21]
	0.75	[3]
$[HCrO_4]^- \Leftrightarrow H^+ + [CrO_4]^{2-}$	6.49	[22-23]
	5.8	[24]

1.2.2. Mobility in the environment

In slightly acidic to alkaline environments, redox reactions can significantly affect Cr transport; labile Cr (VI) species rapidly reduce to usually insoluble Cr (III) in the presence of Fe (II) or manganese (II) [1]. The main Cr (VI) retention mechanisms then are precipitation and sorption because of the changes oxidation state (Eh) or in pH [25]. Precipitation specifically refers to the transformation of Cr (III) to a solid (3-dimensional) phase whereas sorption is the accumulation of Cr ions at the solid phase-aqueous phase interface.

1.2.2.1. Oxidation and reduction reactions

The physical and chemical properties of Cr are altered by redox reactions in the environment. The major redox couples in natural aquatic environments are [26-27].

- H_2O/O_2 (aq)
- Mn (II)/Mn(IV)
- NO_2/NO_3
- Fe (II)/Fe(III)
- S^{2-}/SO_4^{2-}
- CH_4/ CO_2

Cr (VI) in groundwater can travel large distances due to high solubility and enter an area with low Eh where it becomes immobile by reduction and precipitation to Cr (III). Organic matter or dissolved sulfides may be present in such an area and readily reduce Cr (VI), especially where pH is low. Only a few oxidizing agents are found at sufficient concentrations in groundwater to oxidize Cr (III) to Cr (VI). The rate and amount of Cr (III) oxidation is increased in low pH. Manganese oxides present as grain coatings in subsurface, deposits in cracks, finely disseminated grains, or result from bacterial activities are responsible for most Cr (III) oxidation in aquatic environments [16, 1].

1.2.2.2.Precipitation-dissolution

Earlier it was shown that CrO_4^{2-} and $Cr_2O_7^{2-}$ are water soluble at all pH value indicating that there are no significant solubility constraints on Cr (VI) concentrations. CrO_4^{2-} can, however, exist as an insoluble salt of the following divalent cations: Ba^{2+}, Sr^{2+}, Pb^{2+}, Zn^{2+}, and Cu^{2+} [1].

These salts vary significantly in solubility and rates of precipitation/dissolution reactions, which are pH dependent.

1.2.2.3. Sorption-desorption

The relative sorption of metals onto soil decreases in the following order: lead > antimony > copper > chromium > zinc > nickel > cobalt > cadmium [28]. Mn, Al, Fe oxides and hydroxides, clay minerals, and colloids can adsorb CrO_4^{2-} and $HCrO_4^-$ ions [5]. Sorption of Cr to soil depends on the clay, iron (III) oxide, and organic content of the soil [1]. The sorption of Cr (VI) decreases with the decrease in number of positively charged exchange sites and increasing soil pH [29]. The effect of competing anions on Cr (VI) is drastic and varies depending on their dissolved concentration of competing anions, affinities for solid surface, and surface site concentrations. The leaching of Cr (VI) from soils implies that the sorption can also be a reversible process. Cr sorption onto an interstitial lattice of goethite (FeOOH) on the other hand is an example of irreversible sorption; in this case Cr (VI) is not bioavailable to plants and animals [30].

1.3. Treatment processes for chromium (VI)

The above water quality standards can be achieved through treatment. The current treatment processes capable of removing Cr (VI) include chemical reduction and precipitation, ion exchange, membrane filtration, and activated carbon adsorption [31-32]. The treatment process is selected based on published literature regarding process effectiveness, technical complexity,

cost, and local circumstances [33]. This section describes each process and discusses the advantages of application as well as potential limitations.

1.3.1. Chemical reduction and precipitation

The goal of chemical reduction is to convert Cr (VI) to the less toxic and more thermodynamically stable Cr (III), which can then be precipitated as a solid and separated from solution by sedimentation or filtration. Chemical reduction involves the addition of electron donors such as S, Fe (II), or Fe (0) and pH adjustment to less than 3.0 to optimize Cr (VI) and electron donor electrostatic interactions for rapid reduction. Chemical precipitation of Cr (III) at pH 8.0 or higher follows by addition of calcium hydroxide or sodium hydroxide. The Cr (III) precipitate can finally be removed and disposed. Fig. 4 shows a chemical reduction and precipitation process flow chart [34].

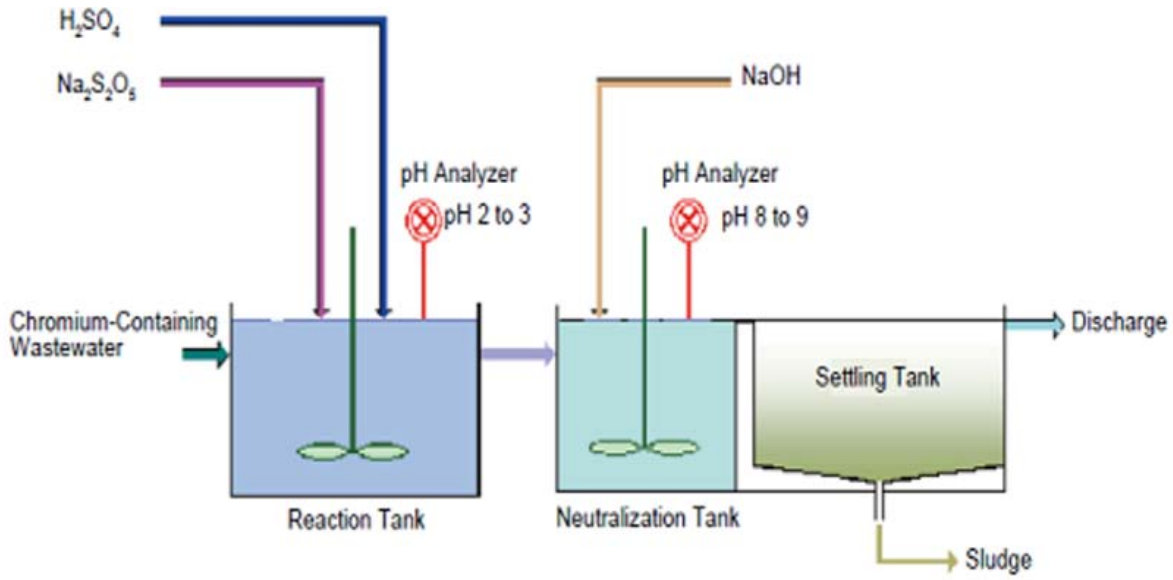

Fig. 4. Chemical reduction and precipitation process [34].

Several studies have shown the potential for reduction processes. It was recently reported that fluidized zero valent iron (ZVI) attained 99.9% chromate removal from an electroplating wastewater containing 418 mg/L Cr (VI) at pH 2.0 with a hydraulic detention time of 5.6 min [35]. Another study used ferrous sulfate for Cr (VI) reduction and evaluated the hydroxide precipitation process using $Ca(OH)_2$. It was found that maximum precipitation of Cr (III) occurred at pH 8.7 and that the chromate concentration was reduced from 30 mg/L to 0.01 mg/L. A later study revealed that lime precipitation was enhanced when using fly ash as the seed material and 100 mg/L of Cr (VI) decreased to 0.08 mg/L [31].

Although this technique is effective, simple, and inexpensive to operate, a disadvantage is that large amounts of residual sludge are generated and necessitate transport, disposal, and additional costs. These residues may also be susceptible to acid leaching. Furthermore, the system is not

suitable for treating low concentrations of Cr (VI). Finally, foreign ions may be introduced to the effluent and require further treatment.

1.3.2. Ion exchange

The physical process of ion exchange involves selective removal of Cr (V) anions when water is passed through one or more fixed beds containing anion exchange resins. Once the exchange capacity of the beds is exhausted, the beds are regenerated and reused. Selective resins for Cr (VI) removal have been investigated in several studies. Sapari et al [36] reported 100% removal efficiency using a strongly basic anion resin in hydroxide form and 5% NaOH regenerant for a mixed plating rinse wastewater containing 9.8 mg/L Cr (VI). Lin et al. [37] demonstrated efficient and continuous recovery of chromic acid from a synthetic waste acid solution containing 750 mg/L using strong base anionic (OH-type) and strong acid cationic (H-type) ion exchange resins in a multi-step ion exchange process (shown in figure). The OH-type resin was first used to capture chromic acid, which was converted to sodium chromate by NaOH solution. The H-type resin was then used to convert sodium chromate back to chromic acid, which was recovered by HCl solution. A treatment capacity of 100 mg/L was reported.

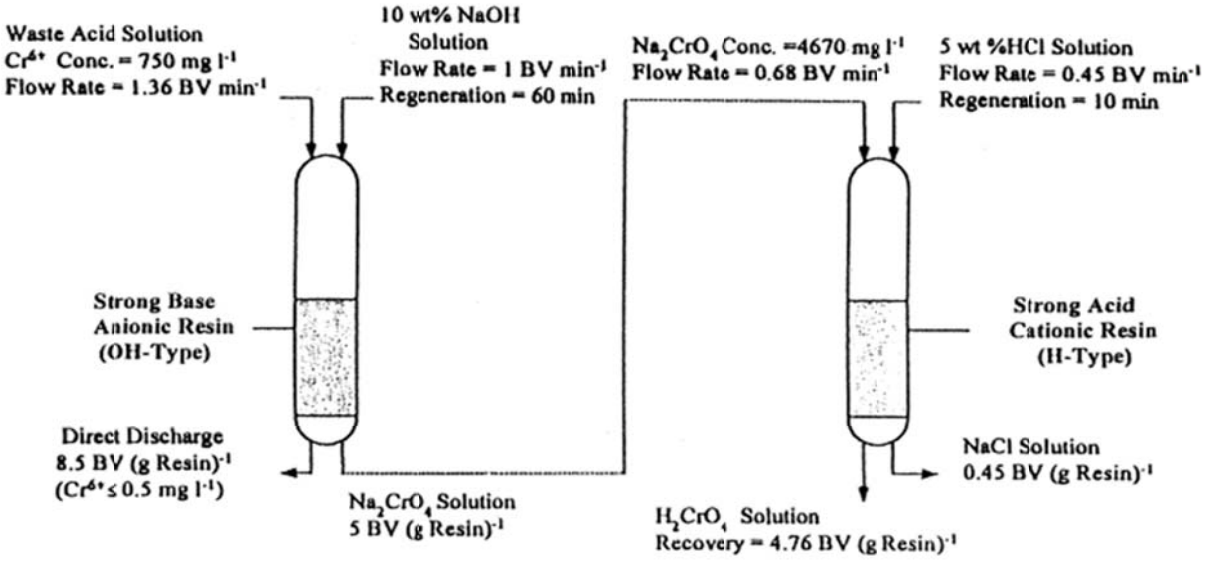

Fig. 5. Process flow chart of chromic acid recovery system [37].

The advantages of this system are summarized as follows [31-32]:

- high treatment capacity and removal efficiency for Cr (VI)
- fast kinetics
- Cr (VI) recovery for reuse
- applicability to highly concentrated Cr (VI) wastes
- higher selectivity for Cr (VI) as compared to SO_4^{2-}, NO_3^-, and Cl^-

Whereas the disadvantages include [31-32]:

- high capital and operational costs
- bench scale test requirements prior to implementation
- pretreatment requirements such as suspended solids removal
- large volumes of toxic brine produced
- not suitable for treating low Cr (VI) concentrations at large scale

1.3.3. Membrane filtration

Semi-permeable membranes are used to pass high-quality water while rejecting the passage of dissolved solids and are categorized by pore size. Reverse osmosis (RO) and nanofiltration (NF) are used to filter the small Cr (VI) anions from water. These are processes are pressure driven where the flux of water through the membrane is proportional to the pressure that is applied. RO membrane pore sizes are less than 0.002 µm can achieve the highest water effluent quality operating, however, at high pressures (15-50 bar). NF membrane pore sizes are typically between 0.001 and 0.01 µm also achieving high removal efficiencies while operating at lower pressures (about 5 bar) [33]. A study showed 99% rejection rate for an initial Cr (VI) of 1,000 mg/L using NF polyamide membranes [32]. Promising results were also found using a thin film negatively charged surface NF [1]. The rejection rate, which is equivalent to the removal rate had depended on ionic strength and pH. As the ionic strength of the water increased, Cr (VI) removal decreased and Cr (VI) removal improved with increasing pH as membrane surfaces were deprotonated increasing the electrostatic repulsion.

The advantages are as follows:

- high removal efficiency
- ease of operation
- less space requirement
- can remove Cr at wide range of operational conditions

Disadvantages that have limited use include:

- low chemical and thermal stability

- membrane fouling
- high cost operational costs
- low permeate flux

1.3.4. Activated carbon (AC) adsorption

Adsorption is a relatively new process for Cr (VI) removal that is simple, effective, and low in cost. The other advantages are design and operation flexibility, high efficiency, and possibility of regeneration [32]. Activated carbon (AC) has been the most studied and widely used adsorbent. It is a porous material with a surface area ranging from 500 to 1,500 m^2/g and is produced by the controlled thermalization of carbonaceous material from various sources [38]. Activated carbon is classified into four groups based on size and shape: powder activated carbon (PAC), granular-activated carbon (GAC), activated carbon fibrous (ACF), and activated carbon clothe (ACC) [1]. Numerous studies have found that adsorption processes depend on the source of raw material, extent of chemical activation, and physiochemical characteristics. GAC, for example, was found to remove Cr (VI) by two different mechanisms: electrostatic adsorption to GAC surfaces and reduction to Cr (III). The quantitative results had varied with the type of GAC used since the different types of GAC had different point of zero charge values. A different study found that oxidative treatment of GAC using nitric acid enhanced adsorption capacity by 300% [38]. Several commercial AC for Cr (VI) adsorption have also been extensively used. The depletion of commercial coal-based AC, however, has resulted in increased costs and a search for either alternative AC from abundant and inexpensive sources or additive and AC composites to improve removal performance [33]. Table 6 below reports some of the different adsorption capacities for different activated carbons determined from batch studies using synthetic wastewater.

Table 6. Various AC adsorption capacities [32].

Activated carbon	Adsorption capacity (mg/g)	Initial concentration (mg/L)	pH
PAC	390	-	2
GAC-Filtrasorb 400	53.19	-	2
Commercial, F-400	48.5	60	2
Commercial, fabric cloth	22.29	50	2

1.4. "Low-cost" adsorbents for chromium (VI)

Costly commercial AC has prompted interest in alternative adsorbents that are abundant and locally available for Cr (VI) removal worldwide. Several investigators have studied Cr (VI) adsorption using a variety of low-cost adsorbents such as chitosan, agricultural waste, peat moss, clay, zeolites, natural oxide, and industrial waste [39-41]. All these adsorbents cost much less than AC as shown in Table 7 below [39]. In Tables 8 to 14 the adsorption capacities and varying experimental conditions are also presented for reasonable comparison. It can be seen that many different alternative adsorbents particularly those chemically modified by contact with acids, alkalis, or organic acids are suitable for Cr (VI) removal. Numerous studies also highlight that adsorption depends mainly on the interaction of Cr (VI) with specific adsorbent surface groups and can be influenced by initial Cr (VI) concentration, medium pH, ionic strength, or the presence of competitive ions.

Table 7. Cost of adsorbents depending on quality, type, or process level [39].

Adsorbent	Cost (U.S. $/kg)
AC	20-22
Chitosan	15.43
Clay	0.04 - 0.12
Zeolite	0.03 – 0.12
Peat	0.024 – 0.052

1.4.1. Chitosan

Udaybhaskar et al. [42] studied the effect of pH, ionic strength, and kinetics of adsorption of Cr (VI) using chitosan, a linear polysaccharide composed of β-(1-4)-linked D-glucosamine, produced in the laboratory from chitin in fresh crab shells. It was found that at an initial Cr (VI) concentration of 5 mg/L, removal most effective at pH 3.0. As pH increased to 5.0, uptake decreased steadily whereas a sharp decrease observed from pH 5 to 6, and only 5 to 6% removal was observed at pH 7. It was found that at low pH, free amino groups are protonated and able to bind anions by electrostatic attraction. A higher correlation coefficient for the Langmuir model was obtained than for Freundlich. Thusly, a homogeneous distribution of sorption energies due to monolayer sorption on a limited number of surface sites is predicted. The rate of removal of Cr (VI) was determined using Lagergren's equation and the first order rate constant was calculated to be 1.92 hr^{-1} for an initial concentration of 5 mg/L. When ionic strength was increased from 10^{-5} to 10^{-3} M sodium perchlorate, there was an 18% decrease in adsorption

capacity, a steep decrease was observed beyond this point, and was reduced to negligible levels at 10^{-1} M. The changes in background electrolyte concentrations significantly affected sorbate-sorbent interactions as metal anion uptake is through electrostatic attraction. Increase in ionic strength not only decreases the ionic activity of dichromate ions, but also increases the concentration of competing perchlorate anions. It was found that regeneration of sorbent was not very effective after metal anion uptake when compared to metal cations. 57.8%, 56.2%, 63.5% desorption of Cr (VI) was observed with 0.01 M NaCl, 0.01 M $NaSO_4$, 0.01 M NaOH as opposed to 88% cadmium desorption with 0.01 M HCl.

Schmuhl el al. [43] agreed that Cr (VI) adsorption on chitosan was concentration driven, conformed to the Langmuir model, and that Cr (VI) uptake is through electrostatic attraction. In this study, chitosan of high, medium, and low molar mass was obtained from Aldrich Chemical Company, South Africa and batch studies were conducted using a higher initial Cr (VI) concentration of 100 mg/L. The maximum adsorption was obtained at pH 5. At lower and higher pH values, adsorption decreased. A low distribution ratio, k_d, was observed at pH 2 indicating instability of chitosan in dilute acidic solutions. Chitosan was cross-linked with epichlorohydrin to increase resistance to acid solutions. It was found that although the stability improved, cross-linked chitosan lost 30 mg/g of adsorption capacity. This lower capacity may be due to the loss of binding sites due to crosslinking.

1.4.2. Agricultural waste

Babel et al. [44] investigated coconut shell charcoal (CSC), an agricultural waste from the coconut industry, for Cr (VI) removal in batch studies. In this study, CSC type 12/40 from Carbokarn Co. Ltd in Bangkok, Thailand was used. The adsorbent is granular in as-received form and has a small surface area (5-10 m^2/g) with exchange/sorption properties due to the presence of functional groups, such as carboxylic, hydroxyl, and lactone. It was also found that CSC in as received form was highly efficient for Cr (VI) removal at lower concentrations (5 and 10 mg/L) with adsorption capacities of 4.30 and 3.74 mg/g and is comparable to as received commercial activated carbon (4.72 mg/g) at the same Cr (VI) concentration range. Furthermore, it was found that the adsorption capacity can be improved by increasing surface area through chemical/coating modification. Surface modifications with chitosan and/or strong oxidizing agents, such as nitric acid and sulfuric acid, had significantly improved Cr (VI) adsorption capacities. Oxidation of the unsaturated CSC carbon surface generated more oxygen-containing surface functional groups and yielded large amounts of surface area by improving pore structure. CSC oxidized with nitric acid required the least amount of dosage, lowest contact time, and lowest agitation speeds to achieve highest removal efficiency of Cr (VI). It can be seen from the Fig. 6 that only 12.0 g/L nitric oxidized CSC was required to achieve maximum removal as opposed to the 22.5 g/L of as-received CSC. It was also found that Langmuir isotherm is more applicable than Freundlich for Cr (VI) removal by for all concentrations studied. A complex physiochemical mechanism for Cr (VI) adsorption is assumed due to the presence of acidic surface functional groups. The Cr (VI) oxyanion is readily reduced to Cr (III) ions due to the presence of electron donors on CSC surface and Cr (III) adsorption through attractive columbic

interaction follows. An ion exchange mechanism of Cr (III) is also likely based on attractive electrostatic interaction between the electron-donating nature of the oxygen containing functional groups and the electron-accepting nature of heavy metal ions.

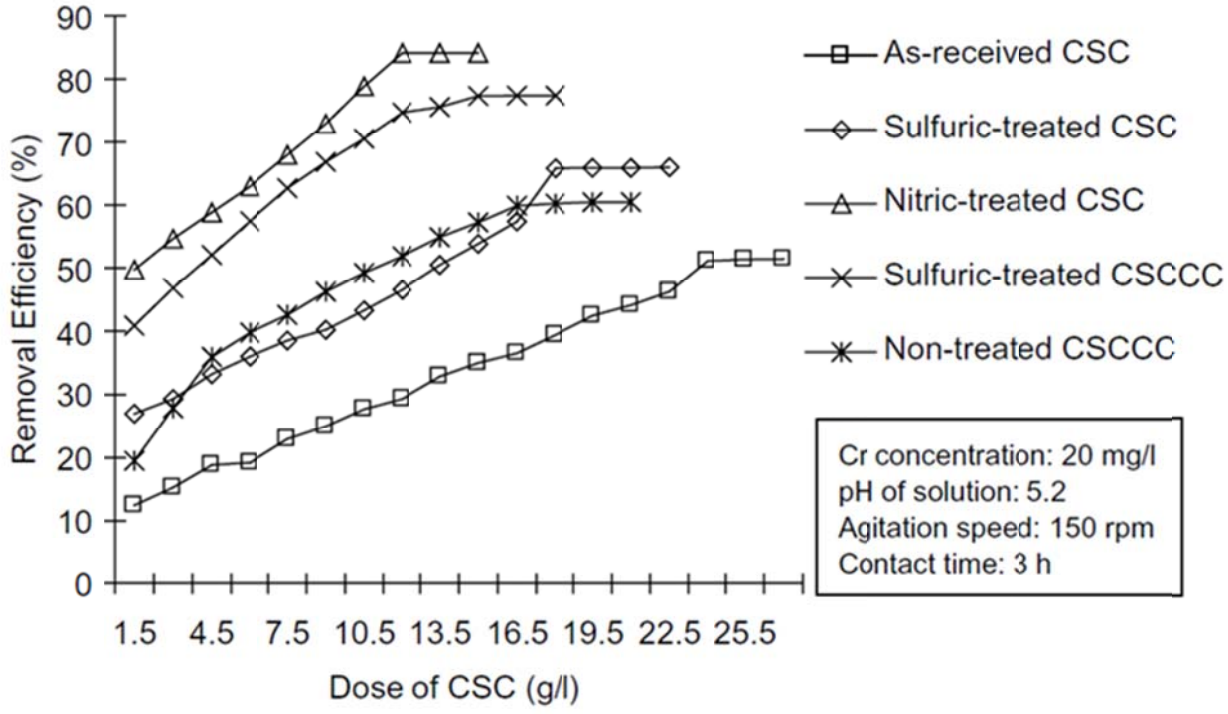

Fig. 6. Effect of dose on the removal efficiencies of all types of CSC.

Dakiky et al. [45] studied the following seven adsorbents from two different classes of fibers in batch adsorption technique at 30 °C to determine Cr (VI) removal: wool, pine needles, sawdust, olive cake, almond shells, cactus leaves and coal taken from local Palestinian natural resources. Natural wool from sheep is a protein-based animal fiber with amino and carboxylic groups to bind Cr (VI) whereas all other adsorbents are cellulose-based plant fibers with available hydroxyl groups for binding. The results showed that wool had the largest adsorption capacity for Cr (VI) and required the least contact time and amount of dose. At 8 g/L of adsorbent, 100

mg/L adsorbate, and pH 2.0 wool, sawdust, and olive cake showed 69.3, 53.5, and 47.1 % removal. The advantage of wool for the removal of Cr (VI) ions may arise from both the high concentration of sorption sites and the loose nature of the fiber allowing accessibility of these sites. For all adsorbents, the percentage Cr (VI) removal reached a maximum value at a pH of approximately 2.0 and showed little removal at pH 5.0. Similar experiments on Cr (III) showed no removal at pH 2.0 and maximum removal at pH 5.0. This suggests that the number of positively charged groups on the adsorbent matrix increases at a pH of 2.0 and enhances removal of Cr (VI) species by coulombic attraction. The kinetics of Cr (VI) adsorption on the all adsorbents was found to follow the first-order rate law derived by Lagergren. Wool had the highest rate constant (0.0396 min^{-1}) followed by olive cake (0.0899 min^{-1}) and sawdust (0.09 min^{-1}). This indicates that the compactness of the adsorbent affected the time needed to reach equilibrium. Wool was found to fit better to the Langmuir isotherm while all cellulose adsorbents fit better to the Freundlich isotherm as binding to adsorption sites is random due to slow diffusion steps. The Gibbs free energy obtained for wool (-2.26 kJ/mol) showed the largest capacity and affinity for the selective Cr (VI) removal followed by sawdust (-2.02 kJ/mol) and olive cake (-0.94 kJ/mol). A comparison of Cr (VI) removal by wool from synthetic 100 mg/L Cr(VI) solution and aluminum powder coating wastewater containing 100 mg/L Cr (VI), 19 mg/L Al, 30 mg/L Mg, 49 mg/L Ca, and 10 mg/L B, showed that adsorption is satisfactory and selective for Cr (VI). At 8 g/L wool, uptake in simulated solution was 8.5 mg/g and 7.0 mg/g in true wastewater.

Kobya [46] reported that hazelnut shell activated carbon (HSAC) obtained from species of *Corylus avellana* from Trabzon in Turkey is a highly effective adsorbent for the removal of

Cr(VI) from aqueous solutions in the pH range 1.0–2.0. Batch adsorption results show that as pH decreases from 8.0 to 1.0, the amount adsorbed increases from 8 to 38 mg/g. It was assumed that a high fraction of Cr (VI) reduces to Cr (III) form in the presence of carbon at low pH. It was observed that when changing the initial concentration from 50 to 300 mg/L, the amount adsorbed increased from 10.35 mg/g (99.99% removal) to 92 mg/g (92% removal) at 30 °C and a pH of 1.0. The Langmuir isotherm provided the best fit for Cr (VI) onto HSAC. The experimental data was also found to follow the pseudo first-order kinetic model. The adsorption constant values at different concentrations showed that Cr (VI) adsorbed rapidly when lower concentrations were used. It was also found that an increase in temperature from 20 to 50 °C doubled the maximum adsorption capacity indicating that adsorption is an endothermic process**.**

1.4.3. Peat

Sharma et al. [47] found that Irish sphagnum moss peat, a marketed horticultural soil conditioner, exhibited exceptionally high Cr (VI) adsorption capacities in batch adsorption and column studies. The cellulosic material having undergone humification reactions was found to be acidic in nature, effectively adsorb Cr (VI) ions through complexation and ion exchange in the pH range 1.5 to 3.0 depending on the initial Cr (VI) concentration, and poorly adsorb Cr (III) ions [47-48]. Kinetic batch reaction rates showed that Cr (VI) is rapidly absorbed and more efficiently at lower concentrations. Desorption studies show that only 51 % Cr (VI) had been eluted by 1 M NaOH indicating that Cr (VI) peat complex has a strong bond. Some Cr (III) ions were also eluted indicating chemical reduction of Cr (VI) to Cr (III). More Cr (VI) ions were reduced to Cr (III) at very low pH values. Fig. 7 shows that most Cr (III) ions were readily

desorbed suggesting that these ions exist at the outermost layers. Thus, in low Cr (VI) concentration ranges (< 20 mg/L) and low pH (below pH 3.0), chemical reduction of Cr (VI) to Cr (III) predominates and removal efficiency decreased. High concentrations (> 480 mg/L) in the other hand were best treated at pH 1.5 to counteract to significant increase of the pH in reaction mixtures. These findings were extended to column studies and regeneration data was also presented [49]. The influents were adjusted to pH 2.0 and 2.5 and contained 100 mg/L Cr (VI). The data obtained at pH 2.0 and a saturation level of 58% showed the higher capacities and a slightly higher regeneration efficiency of 39.4%. It was also observed that humic substances were leached during the alkaline regeneration phase and resistance to flow had increased after the regeneration. It was concluded that exhausted peat would require disposal through incineration.

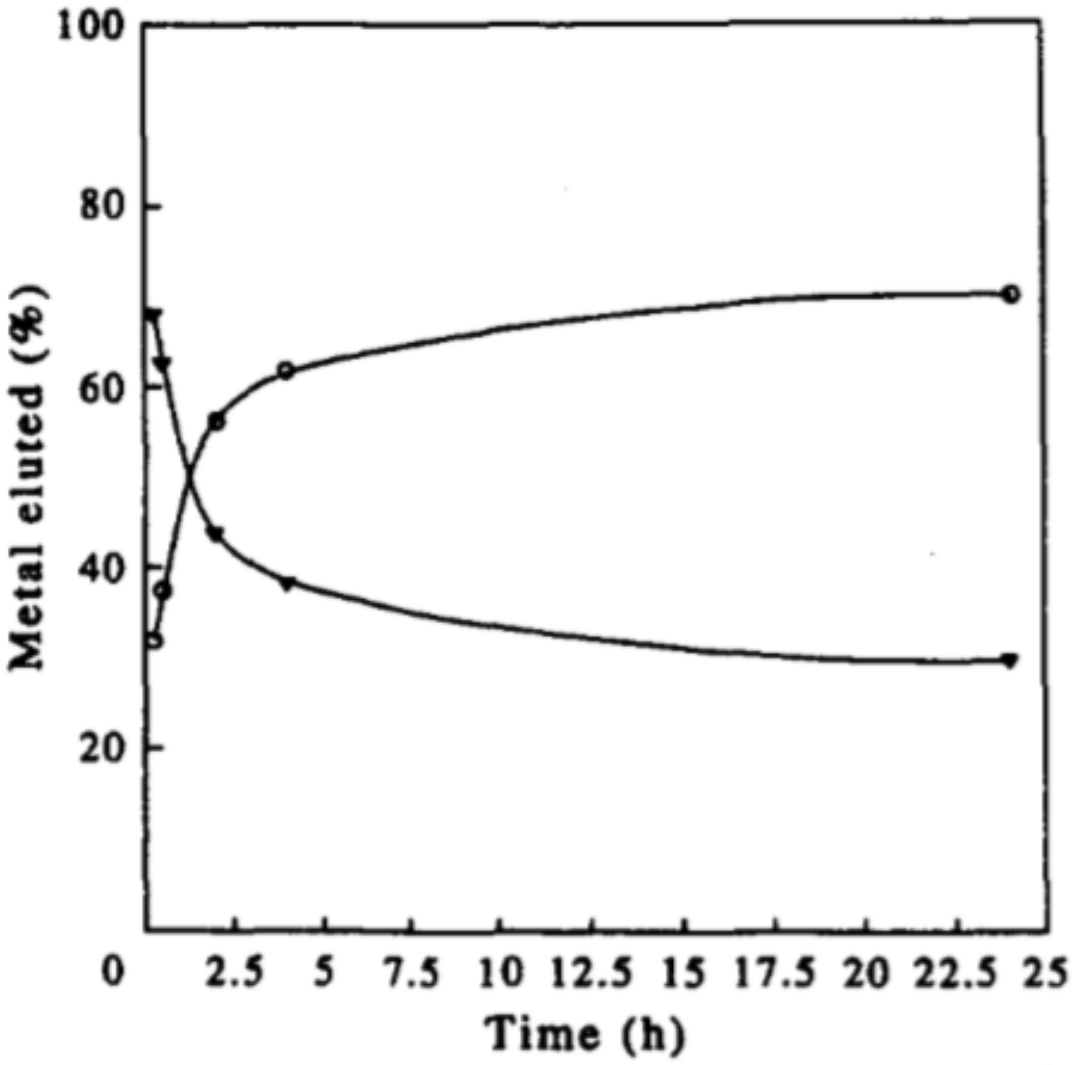

Fig. 7. The desorption of chromium by sodium hydroxide. Cr (III), ▼—▼; Cr (VI), ○—○.

1.4.4. Clay

Akar et al. [50] showed that natural, heat-activated, acid-activated, and hexadecyltrimethylammonium bromide (HDTMA) modified clays can be used as effective adsorbents for the removal of Cr (VI). The chemical analysis of Turkish natural clay showed montmorillonite as the major component along with some feldspar and analcime. It was observed

that an increase in initial metal ion concentration and contact time also increased Cr (VI) removal. It was found that the experimental data fit well with Langmuir, D–R isotherm, pseudo-second-order kinetics models. A mean free energy of 7.53 kJ/mol indicated a physical process for the Cr (VI) adsorption onto montmorillonite. The highest adsorption capacity was also found for HDTMA-modified clay

Khan et al. [51] reported that bentonite can effectively remove low concentrations of Cr (VI) with wastewater pH adjusted to 2.0. The bentonite samples from local clay contractors in Shina Bagh, Pakistan were used and found to contain both montmorillonite and quartz as the major mineral constituents (clay 24%, silt 74%, sand 2%). The sorption of Cr (VI) was studied by a batch technique in aqueous solutions and was found to fit the Freundlich isotherm instead. For a chromate concentration ranging from 5.2 to 52 mg/L, the mean free energy of sorption was found to be 10 kJ/mol. This indicated an ion-exchange process for Cr (VI) adsorption onto bentonite. While a $\Delta H°$ value of 5.619 kJ/mol at 20 °C and the increasing negative values of $\Delta G°$ for Cr (VI) with the rise in temperature also indicated an endothermic process.

1.4.5. Zeolites

Ramos et al. [52] reported significant Cr (VI) adsorption on a cationic surfactant-modified zeolite (SMZ) sieved to a particle diameter of 0.42 mm. The collected zeolite rock from the mineral deposit located in San Luis Potosi, Mexico was mostly composed of clinoptilolite. The SMZ was prepared using the HDTMA-bromide surfactant as in the previous modified-clay

study to improve its anion exchange capacity. The adsorption equilibrium data was determined in a batch experiments in aqueous solution. Maximum Cr (VI) adsorption capacity was observed at pH 6 and diminished when increasing pH increasing from 6 to 10 or decreasing pH from 6 to 4. An exothermic process for Cr (VI) adsorption was assumed due to a decrease in adsorption reduce capacity when temperature was increased from 15 to 25 °C. Desorption studies showing irreversible Cr (VI) adsorption onto SMZ and a ΔH_{ad} equal in magnitude to the heat of chemical reaction, confirmed a chemisorption process.

Li et al. [53] further conducted column tests using SMZ to study the effects of particle size on chromate transport and retardation. The smallest particle size resulted in higher amounts of HDTMA and bromide adsorption leading to a higher retardation factor for chromate transport. This indicates that SMZ is an effective absorbent for permeable barrier construction. The approximate 1:2 ratio of bromide to HDTMA sorption, revealed a bilayer configuration of surfactant. Furthermore, desorption of bromide with chromate sorption confirmed an anion exchange mechanism for chromate retention by SMZ and resulted the continuous deterioration of the surfactant bilayer. Therefore, restoration of bilayer or removal of the packed beds is required before reaching breakthrough. The breakthrough point was found to be 370-420 PVs for the □ 0.4 mm SMZ.

Silva 2008 et al. [54] found that Arthrobacter viscosus biofilm supported zeolite removes Cr (VI) from dilute solutions with no change in zeolite structure. Fig. 8 also shows that without bacteria, the zeolite achieves no Cr (VI) removal whereas Cr(III) is removed in either case. The batch

studies had been performed using 1 g of the zeolite, 15 mL of A. viscosus culture media, and varying concentrations of adsorbate. Cr (VI) uptake increase was observed with an increase in adsorbate. The obtained binding energies of biofilm-modified zeolites in 50 mg/L Cr (VI) and Cr (III) samples suggested that Cr (VI) was reduced to Cr (III) before the entrapment in the zeolite. Thusly, the assumed biofilm role is the reduction of Cr (VI) to the smaller Cr (III) cation for easy exchange in the zeolite internal surface.

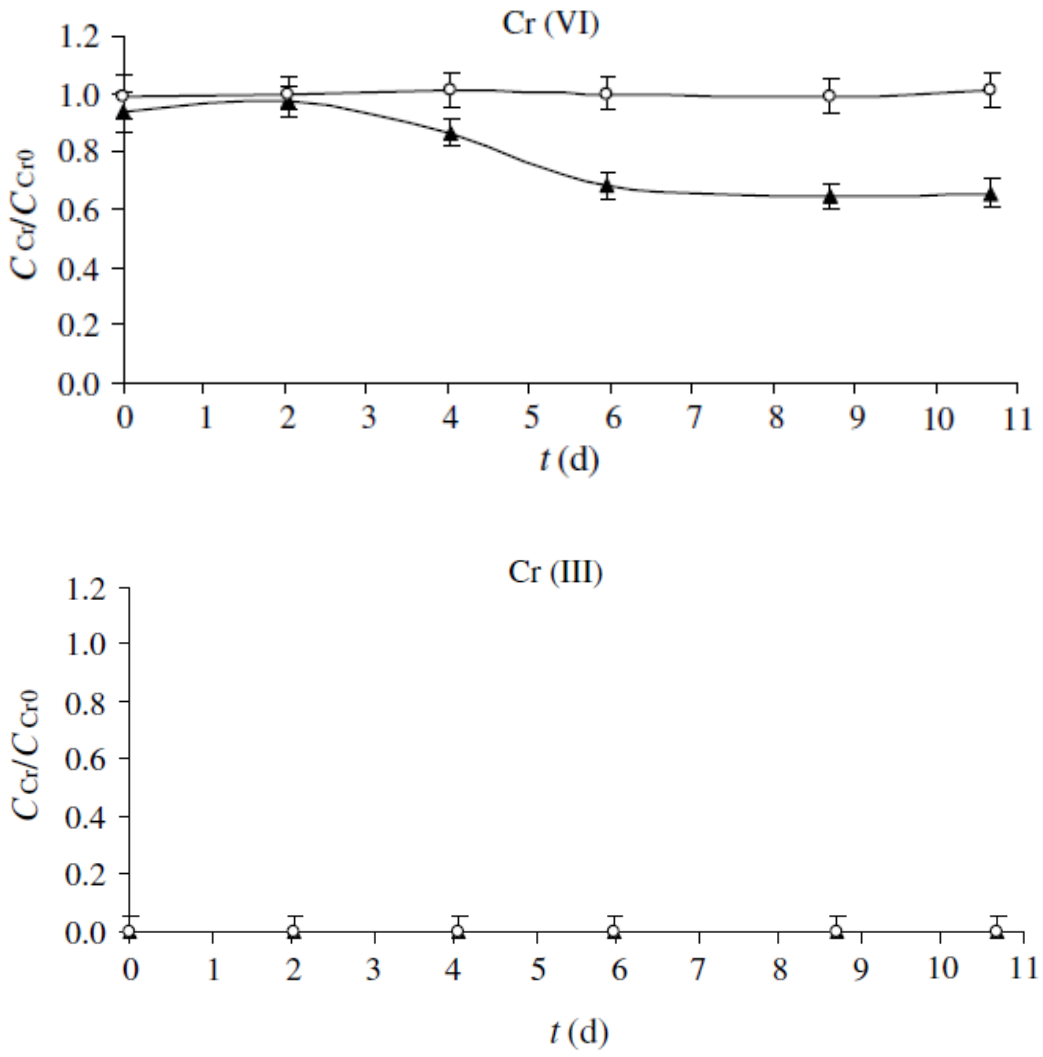

Fig. 8. Ratio between residual and initial chromium concentration (C_{Cr}/C_{Cr0}) as a function of contact time for 50 mg/L of Cr (VI) and Cr (III) in the presence of the zeolite with (▲) and without the bacteria (○).

1.4.6. Natural oxide

Weng et al. [55] evaluated Cr (VI) adsorption onto TiO_2 (anatase) particles by batch technique. It was observed that adsorption capacities decreased with increasing pH, temperature, and ionic strength. These results suggest that adsorption is favorable under acidic conditions (pH 2.5-5.0)

and exothermic in nature. The effect of ionic strength can be explained by a decrease in the electrostatic potential due to electric double compression. The experimental data fit well with Langmuir and surface complex formation models. It was shown that intrinsic stability constants for $TiOHCrO_4^{2-}$ and $TiOH_2CrO_4^-$ complexes decrease as the surface loading increases. The model was also used to determine adsorption free energy, $\Delta G°_{Ads}$. For a surface loading of 10^{-5} to 7.7×10^{-5} mol/g, the adsorption free energy of $HCrO_4^-$ and CrO_4^{2-} ranges from -0.52 to -2.26 kcal/mol and -0.34 to -2.13 kcal/mol. Comparing the magnitude of adsorption free energy, $HCrO_4^-$ is more favorably adsorbed. It was concluded that specific chemical interaction is the major mechanism for the adsorption process as the adsorption energy approximately equals the specific chemical energy. It was found that electrostatic energy contributed only 10 % for $HCrO_4^-$ and 33% for CrO_4^{2-} to the total free energy adsorption. Solvation energy was also found to have a relatively small contribution to total adsorption. The lateral interaction energy had been minimized by using Cr (VI) concentrations less than 10^{-4} M in the adsorption experiments as high surface loadings would result in adsorbate-adsorbate interactions.

Bhutani et al. [56] investigated the kinetics of radiometric adsorption/desorption of Cr (VI) using β-MnO2 as a carrier over a wide range of Cr (VI) concentration (5 - 500 mg/L) and temperature (30 – 50 °C). ^{51}Cr as $Na_2\ ^{51}CrO_4$ in dilute HCl solution used to prepare different concentration ranges. It was observed that the amount Cr (VI) adsorbed at equilibrium increases with an increase in adsorbate concentration. The adsorption dependence on the adsorbate concentration at equilibrium was described by Freundlich adsorption isotherm. This suggests that MnO_2 has a heterogeneous surface. It was also found that adsorption and desorption of Cr (VI) on MnO_2 follows the first order rate expression of Lagergren. It was also observed that rate constants for

adsorption are greater than those for desorption at all temperatures studied, indicating that the adsorption process is faster. Contrary to adsorption, the amount desorbed increases from 1.4 X 10^{-7} to 1.77 X 10^{-7}mol/g with a rise in temperature from 30 to 50 °C. Hence, a higher activation energy for desorption (30.025 kJ/mol) was calculated by Arrhenius equation than for adsorption (20.5 kJ/mol). Furthermore, it can be seen from Fig. 8 and 9 that the IR spectra of chromate adsorbed hydrated MnO_2 showed strong Cr-O bands at 950 and 890 cm^{-1} while hydrated MnO_2 only spectra show no band. This indicates chemical interaction between chromate and oxide surface. A ligand exchange mechanism was thus suggested for the adsorption of Cr (VI) to MnO_2.

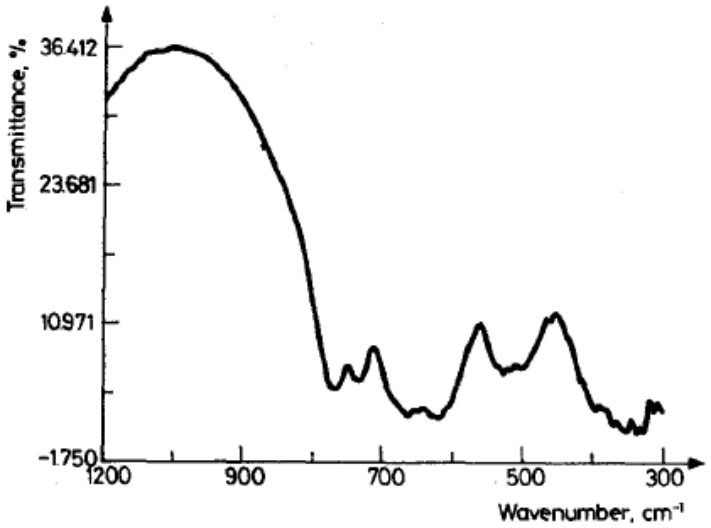

Fig.9. IR spectrum of hydrated MnO_2

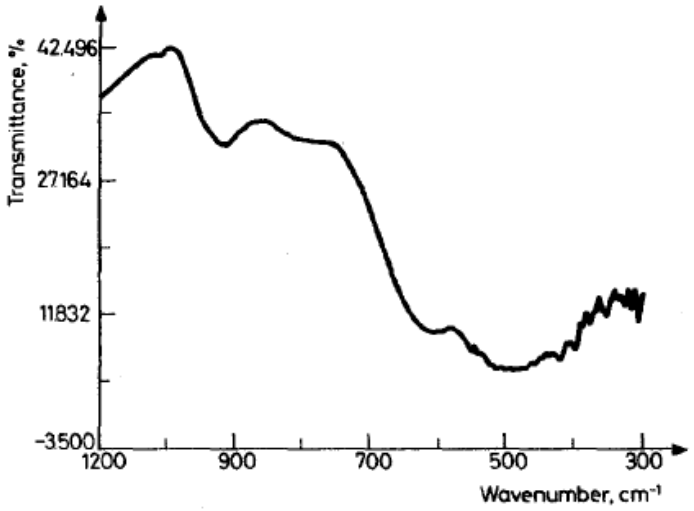

Fig.10. IR spectrum of chromate adsorbed hydrated MnO_2.

1.4.7. Industrial waste

Gupta et al. [57] reported that bagasse fly ash, a waste product from the sugar industry, is an economically feasible adsorbent for the removal of Cr (VI) from synthetic and natural

wastewater. The bagasse fly ash obtained from a local sugar refinery in Bijnor Uttar Pardesh India consists of carbon and oxides of silica, alumina, iron, calcium, and magnesium. It was treated with hydrogen peroxide to oxidize adhering organic matter. Batch adsorption studies were conducted to determine the effect of pH, temperature, initial Cr (VI) concentration, and competing ions. Results show an optimum pH of 1.0 for the adsorption of Cr (VI) and a sharp decrease in adsorption beyond pH 2.0. The same results were observed with blast furnace activated slag [58]. It was also found that Cr (VI) removal decreases with an increase in temperature, indicating that adsorption is an exothermic process. Furthermore, the removal of adsorbate decreases with increasing initial Cr (VI) concentration. Srivastava et al., Pradhan et al., and Mallick et al. [58-60] reported similar Cr (VI) adsorption behavior onto blast furnace slag, red mud, MnO_2 nodule residue. The presence of Na^+, Cd^{2+}, Zn^{2+}, Hg^{2+}, Al^{3+}, and an anionic detergent, Manoxol 1B showed interference with Cr (VI) uptake on bagasse fly ash and similarly on blast furnace slag. Sorption data followed both the Freundlich and Langmuir models. The Reichenberg (1953) model was also used to distinguish between film-diffusion-controlled and particle-diffusion controlled rates of adsorption. It was found that at low concentrations (500 mg/L), adsorption is film diffusion in nature while at concentrations greater than 500 mg/L, the overall rate of removal is governed by particle diffusion. Column studies were also performed using natural wastewater obtained from chrome tanning plant and 0.5 g bagasse fly ash. Adsorption of Cr (VI) was 100 percent at pH 1.8 – 2.0, SS 330 mg/L, TS 1200 mg/L, Cr 3700 mg/L. It was also found that 90 percent of Cr loaded can be desorbed with 3M NH_3 solution for reuse. It was advised that columns be regenerated after every 4 to 5 cycles and treated with 1 M HNO_3 after the first run to prevent loss of sorption capacity.

The blast furnace slag previously mentioned is a byproduct in steel plants that has been was activated in air in a Muffle furnace at 600 °C and can be used for the removal of Cr (VI) as well as Pb^{2+}. The waste material was obtained in the form of small, spherical, soft granules from the Tata Iron and Steel Company Limited, Jamshedpur, India. The different constituents of the activated slag as determined by chemical analysis were CaO-30.47, SiO_2-30.77, S-0.85, MgO-9.85, MnO-0.59, Al_2O_3 -23.30, FeO-0.54, LOI-6.23 percent by weight. SEM photographs in Fig. 10 show the very porous texture of activated slag. Adsorption kinetics were studied to find that the rate of Cr (VI) removal increases with a decrease in the size of adsorbent particles and with increase in temperature indicating that the adsorption of Cr (VI) on slag is an endothermic process. It was also found that Lagergren first-order rate expression is valid for chromium-slag system and the specific constant rate of adsorption, $K_{ad} = 0.0099\ min^{-1}$. At high adsorbate concentrations (> 12.5 mg/L) it was also found that particle diffusion mechanism is the rate-limiting step and that in the later course of process, electrokinetic interactions and molecular diffusion may also be effective. Lastly, desorption of Cr (VI) can be observed in a strongly alkaline medium (pH > 8).

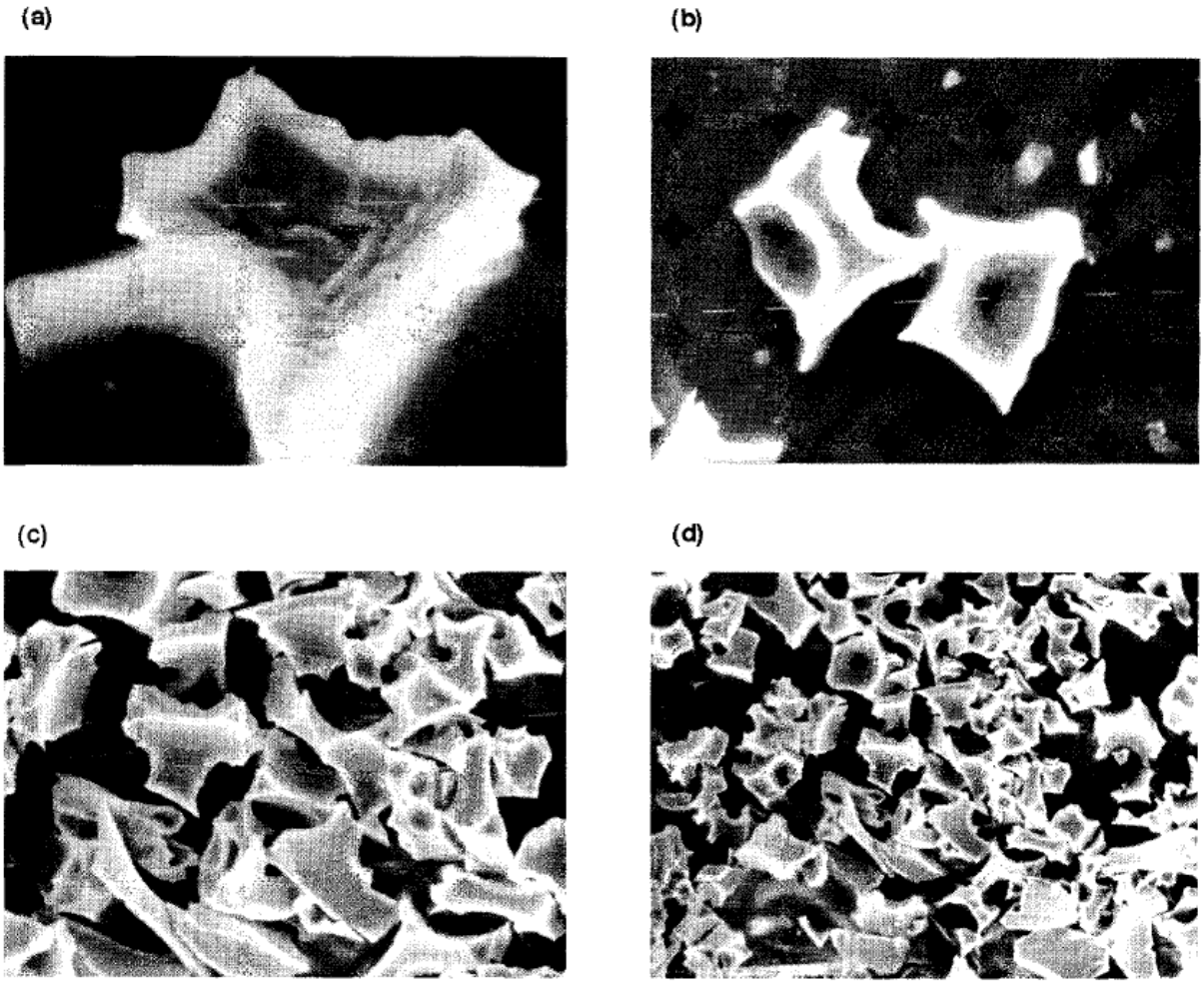

Fig.11. SEM photographs of activated slag at different magnifications: (a) 1 × 640; (b) 1 × 320; (c) 1 ×160; (d) 1 × 80.

Pradhan et al. [59] reported that red mud, a waste material formed during the production of alumina, is an excellent alternate adsorbent for Cr (VI) removal. Red mud was activated by acid dissolution and ammonia precipitation. Ionic strength in batch studies was maintained by adding 1 M KCl. Experimental data obeyed both Langmuir and Freundlich isotherms indicating that the adsorption is a surface phenomenon. Adsorption was observed to be maximum at pH 5.2, higher at lower pH, it is and almost negligible at pH 7.06. A heterogeneous nature of surface sites on the

activated red mud sample was deduced from isosteric heats of adsorption as a function of adsorption density. This may be due to adsorbing ions interacting or different types of adsorption sites on sorbent. The effect of different competitive ions like nitrate, sulfate, and phosphate on the adsorption of Cr (VI) was also studied. It was found that the activated red mud surface shows the higher selectivity for sulfate and phosphate ions and that nitrate had very little effect. Adsorption studies were also performed using natural effluents from the sodium dichromate and basic chromium sulfate industries containing high values of Cr (VI). More than 90% Cr (VI) removal was achieved in natural wastewaters.

Mallick et al. [60] found that water-washed manganese nodule leached residues (WMNLR) are a waste that can be used for the effective removal of Cr (VI). The waste is found in huge amounts after the recovery of metals such as copper, nickel, and cobalt. The manganese nodule leached residue (MNLR) sample was obtained from NH_3–SO_2 leaching of Indian Ocean manganese nodules in Bhubaneswar, India. The sorbent was stirred in water for 4 hours and washed thoroughly in distilled water. WMNLR shows higher surface area, surface oxygen, and surface hydroxyl groups than unwashed samples. The X-ray image map of WMNLR shows that Mn and Fe predominate in the leached residue. The X-ray map of WMNLR, after adsorption of Cr shows that Cr selectively adsorb within the Mn-rich phase. The pHpzc of WMNLR was found to be 4.5. It was observed that a significant amount of chromate adsorption occurs at pH > pHpzc (4.5) suggesting that inner-sphere complex formation is likely during the adsorption. It was also found that kinetic data follows a pseudo second-order rate model. It was concluded that adsorption of Cr (VI) is a reversible process as 99 percent desorption occurs using 0.04 M NaOH.

Table 8. Chitosan adsorption capacities and experimental conditions.

	pHpzc	Type of water	pH	Temp. (˚C)	Initial Cr (VI) conc. range (mg/L)	Sorbent dosage (g/L)	Contact time	Adsorption model	Adsorption capacity (mg/g)	Refs.
Chitosan	6.3	Aqueous solution	4	28	5	0.5	12 hr	Langmuir	27.3	[42]
Non-crosslinked	-	Aqueous solution	5	25	10-1000	3.3	160 min	Langmuir	78	[43]
Epichlorohydrin crosslinked	-	Aqueous solution	5	25	10-1000	3.3	160 min	Langmuir	50	[43]

Table 9. Agricultural waste adsorption capacities and experimental conditions.

	Surface area (m^2/g)	Type of water	pH	Temp. (˚C)	Initial conc. range Cr(VI) (mg/L)	Adsorbent dosage (g/L)	Contact time (hr)	Adsorption model	Adsorption capacity (mg/g)	Refs.
Coconut shell charcoal (CSC)	5-10	Synthetic electroplating water	6	20-25	5-25	1.5	3	Langmuir	2.18	[44]
Nitric-treated CSC	-	Synthetic electroplating water	4	20-25	5-25	1.5	3	Langmuir	10.88	[44]
Wool	-	Natural wastewater	2	30	100	8	2	Langmuir	41.15	[45]
Olive cake	-	Natural wastewater	2	30	100	8	2	Langmuir	33.44	[45]
Sawdust	-	Natural wastewater	2	30	100	8	2	Langmuir	15.82	[45]
Hazelnut shell activated carbon	-	Aqueous solution	1	30	1000	2.5	72	Langmuir	170	[46]

Table 10. Peat adsorption capacities and experimental conditions.

	pHpzc	Type of water	pH	Temp. (˚C)	Initial Cr (VI) conc. range (mg/L)	Dosage (g/L)	Contact time (hr)	Adsorption model	Adsorption capacity (mg/g)	Refs.
Sphagnum Moss	7.25	Aqueous solution	1.5 -3.0	25	10-1000	4	24	Langmuir	119	[47]
Sphagnum Moss	-	Aqueous solution	2	-	100	-	-	Breakthrough capacity	43.9	[49]

Table 11. Clays adsorption capacities and experimental conditions.

	Surface area (m^2/g)	Type of water	pH	Temp. (˚C)	Initial concentration range (mg/L)	Dosage (g/L)	Contact time	Adsorption model	Adsorption capacity (mg/g)	Refs.
Natural montmorillonite	-	Aqueous solution	1	20	250	10	7 hr	Langmuir	3.61	[50]
Heat activated montmorillonite (100˚C)	-	Aqueous solution	1	20	250	10	7 hr	Langmuir	4.2	[50]
Acid-activated montmorillonite	-	Aqueous solution	1	20	250	10	7 hr	Langmuir	4.51	[50]
HDTMA-modified montmorillonite	-	Aqueous solution	1	20	250	10	7hr	Langmuir	10.18	[50]
Bentonite	34	Aqueous solution	2	40	0.52-52	50	30 min	Freundlich	0.57	[51]

Table 12. Zeolites adsorption capacities and experimental conditions.

	Surface area (m^2/g)	pH_{PZC}	Type of water	pH	Temp. (˚C)	Initial Cr(VI) conc. range (mg/L)	Adsorbent dosage (g/L)	Contact time	Adsorption model	Adsorption capacity (mg/g)	Refs.
HDTMA bromide-modified	6.9	8.0	Aqueous solution	6	15	10-150	12.5-25	5 days	Langmuir	5.07	[52]
Natural zeolite	21.8	-	Aqueous solution	6	25	10-150	12.5-25	5 days	Langmuir	0.14	[52]
< 0.40 SMZ	-	-	Aqueous solution	8.1	-	15	-	520-630 PVs	Breakthrough capacity	3.17	[53]
Biofilm supported NaY zeolite	900	-	Aqueous solution	-	-	100	-	-	-	3	[54]

Table 13. Natural Oxides adsorption capacities and experimental conditions.

	Surface area (m^2/g)	pH_{PZC}	Type of water	pH	Temp. (˚C)	Initial conc. range Cr(VI) (mg/L)	Dosage (g/L)	Contact time	Adsorption model	Adsorption capacity (mg/g)	Refs.
Anatase (Ti02)	37.8	6.15	Aqueous solution	2.5-5.0	25	0.5-4	1	24 hr	Langmuir	7.38-14.56	[55]
Manganese dioxide (β-MnO2)	15.8	6.0	Aqueous solution	7.1	25-45	520	16.7	50 min	Freundlich	1.727	[56]

Table 14. Industrial wastes adsorption capacities and experimental conditions.

Adsorbent material	Surface area (m^2/g)	Type of water	pH	Temp. (˚C)	Initial conc. range Cr (VI) (mg/L)	Adsorbent dosage (g/L)	Contact time (hr)	Adsorption model	Adsorption capacity (mg/g)	Refs.
Bagasse Fly Ash	440	Aqueous solution	1	30	500	1	10	Langmuir	260	[57]
Activated Slag Blast Furnace	107	Electroplating wastewater	1	30	50	10	24	Langmuir	7.5	[58]
Red Mud	-	Aqueous solution	5.2	30	2-30	-	24	Langmuir	1.6	[59]
Mn Nodule Leached Residue	109.17	Aqueous solution	3	60	10	2	3	Langmuir	25.78	[60]

1.5 Why manganese oxides

Many studies including those above have found that manganese oxides can be used as alternate low-cost adsorbents for the removal of Cr (VI). Mn oxides have been studied because of their widespread natural distribution and their similarity to more complex aluminosilicates and other minerals [61]. Additionally, synthetic forms of this mineral have well-defined and reproducible physical and chemical properties. The objective of the present work is to evaluate a wider selection of Mn oxides including Mn_2O_3 as well as Mn-Al coated sands for adsorption and removal of Cr (VI) from water. The effect of dosage, contact time, pH, and coexisting ions on the removal of Cr (VI) will also be investigated. Recycling and regeneration studies and surface charge analysis of sorbents will also be conducted.

2. REFERENCES

[1] Guertin, Jacques, James A. Jacobs, and Cynthia P. Avakian. *Chromium (VI) Handbook*. Boca Raton, FL: CRC Press, 2005.

[2] Cieślak-Golonka, Maria, and Marek Daszkiewicz. "Coordination geometry of Cr (VI) species: Structural and spectroscopic characteristics." *Coordination Chemistry Reviews* 249.21 (2005): 2391-2407.

[3] Rai, D., L. E. Eary, and J. M. Zachara. "Environmental chemistry of chromium." *Science of the total environment* 86.1 (1989): 15-23.

[4] Kotaś, J., and Z. Stasicka. "Chromium occurrence in the environment and methods of its speciation." *Environmental pollution* 107.3 (2000): 263-283.

[5] Richard, Françoise C., and Alain CM Bourg. "Aqueous geochemistry of chromium: a review." *Water Research* 25.7 (1991): 807-816.

[6] Oze, Christopher, Dennis K. Bird, and Scott Fendorf. "Genesis of hexavalent chromium from natural sources in soil and groundwater." *Proceedings of the National Academy of Sciences* 104.16 (2007): 6544-6549.

[7] Mills, Christopher T., et al. "Chromium (VI) generation in vadose zone soils and alluvial sediments of the southwestern Sacramento Valley, California: a potential source of geogenic Cr (VI) to groundwater." *Applied Geochemistry* 26.8 (2011): 1488-1501.

[8] Robles-Camacho, J., and M. A. Armienta. "Natural chromium contamination of groundwater at Leon Valley, Mexico." *Journal of Geochemical Exploration* 68.3 (2000): 167-181.

[9] Cooper, G. R. C. "Oxidation and toxicity of chromium in ultramafic soils in Zimbabwe." *Applied Geochemistry* 17.8 (2002): 981-986.

[10] Garnier, J., et al. "Understanding the genesis of ultramafic soils and catena dynamics in Niquelândia, Brazil." *Geoderma* 151.3 (2009): 204-214.

[11] Lilli, Maria A., et al. "Characterization and mobility of geogenic chromium in soils and river bed sediments of Asopos basin." *Journal of hazardous materials* 281 (2015): 12-19.

[12] Kaprara, E., N. Kazakis, K. Simeonidis, S. Coles, A. I. Zouboulis, P. Samaras, and M. Mitrakas. "Occurrence of Cr (VI) in drinking water of Greece and relation to the geological background." *Journal of hazardous materials* 281 (2015): 2-11.

[13] Organization, World Health. 2013. *Inorganic Chromium(VI) Compounds*. Geneva: World Health Organization. http://public.eblib.com/choice/publicfullrecord.aspx?p=1681146.

[14] USEPA: Basic information about Chromium in Drinking Water (2013). http://water.epa.gov/drink/contaminants/basicinformation/chromium.cfm

[15] California EPA: Chromium-6 Drinking Water MCL (2014). http://www.waterboards.ca.gov/drinking_water/certlic/drinkingwater/Chromium6.shtml

[16] Guha, Hillol, et al. "Chromium transport, oxidation, and adsorption in manganese-coated sand." *Journal of contaminant hydrology* 49.3 (2001): 311-334.

[17] Barrera-Díaz, Carlos E., Violeta Lugo-Lugo, and Bryan Bilyeu. "A review of chemical, electrochemical and biological methods for aqueous Cr (VI) reduction." Journal of hazardous materials 223 (2012): 1-12.

[18] Guidelines for drinking-water quality, 2nd ed. Vol. 2. Health criteria and other supporting information. World Organization, Health Geneva, 1996.

[19] Tandon, R. K., P. T. Crisp, J. Ellis, and R. S. Baker. "Effect of pH on chromium (VI) species in solution." *Talanta* 31, no. 3 (1984): 227-228.

[20] Bailey, N.A.,Carrington, K.A., Lott, K.,Symons, M.C.R. “55.Structure and reactivity of the oxyanions of transition metals. Part VIII. Acidities and spectra of protonated oxyanions.” *Journal of the Chemical Society* (1960): 290-297.

[21] Bjerrum, Jannik, Gerold Schwarzenbach, Lars Gunnar Sillén, Clara Berecki-Biedermann, and Lorens Maltesen. 1958. *Stability constants of metal-ion complexes, with solubility products of inorganic substances*. London: Chemical Society.

[22] Haynes, W.M.,CRC *Handbook of Chemistry and Physics, 94th Edition.* CRC Press, 2013

[23] Alvarez-Ayuso, E., A. Garcia-Sanchez, and X. Querol. "Adsorption of Cr (VI) from synthetic solutions and electroplating wastewaters on amorphous aluminum oxide." *Journal of Hazardous Materials* 142, no. 1 (2007): 191-198.

[24] Brasch, Nicola E., David A. Buckingham, A. Bram Evans, and Charles R. Clark. "^{17}O NMR Study of Chromium(VI) Ions in Water." *Journal of the American Chemical Society* 118 (1996): 7969-7980

[25] Mandich, N. V. "Chemistry & theory of chromium deposition: part I-chemistry." *Plat. Surf. Finish* 84 (1997): 108-115.

[26] Weckhuysen, Bert M., Israel E. Wachs, and Robert A. Schoonheydt. "Surface chemistry and spectroscopy of chromium in inorganic oxides." *Chemical reviews* 96.8 (1996): 3327-3350.

[27] Fendorf, Scott E. "Surface reactions of chromium in soils and waters." *Geoderma* 67.1 (1995): 55-71.

[28] King, Larry D. "Retention of metals by several soils of the southeastern United States." *Journal of Environmental Quality* 17, no. 2 (1988): 239-246.

[29] Politzer, Peter, et al. "Electronegativity and the concept of charge capacity." *Journal of Molecular Structure: THEOCHEM* 259 (1992): 99-120.

[30] Calder, L.M., "Chromium contamination of groundwater." *Advances in Environmental Science and Technology* 20 (1988): 215-229.

[31] Fu, Fenglian, and Qi Wang. "Removal of heavy metal ions from wastewaters: a review." *Journal of Environmental Management* 92.3 (2011): 407-418.

[32] Owlad, Mojdeh, et al. "Removal of hexavalent chromium-contaminated water and wastewater: a review." *Water, air, and soil pollution* 200.1-4 (2009): 59-77.

[33] World Health Organization. *Guidelines for drinking-water quality: recommendations*. Vol. 1. World Health Organization, 2004. www.who.int/water_sanitation_health/dwq/gdwq3_8.pdf

[34] Ramakrishnaiah, C.R., B. Prathima. "Hexavalent Chromium Removal from Industrial Watsewater By Chemical Precipitation Method." *International Journal of Engineering Research and Applications* 2, no. 2 (2012): 599-603.

[35] Chen, Shiao-Shing, Chih-Yu Cheng, Chi-Wang Li, Pao-Hsuan Chai, and Yu-Min Chang. "Reduction of chromate from electroplating wastewater from pH 1 to 2 using fluidized zero valent iron process." *Journal of Hazardous materials* 142, no. 1 (2007): 362-367.

[36] Sapari, Nasiman, Azni Idris, and Noor Hisham Ab Hamid. "Total removal of heavy metal from mixed plating rinse wastewater." *Desalination* 106, no. 1 (1996): 419-422.

[37] Lin, S. H., and C. D. Kiang. "Chromic acid recovery from waste acid solution by an ion exchange process: equilibrium and column ion exchange modeling." *Chemical Engineering Journal* 92, no. 1 (2003): 193-199.

[38] Selvi, K., S. Pattabhi, and K. Kadirvelu. "Removal of Cr (VI) from aqueous solution by adsorption onto activated carbon." *Bioresource Technology* 80.1 (2001): 87-89.

[39] Babel, Sandhya, and Tonni Agustiono Kurniawan. "Low-cost adsorbents for heavy metals uptake from contaminated water: a review." *Journal of hazardous materials* 97.1 (2003): 219-243.

[40] Bailey, Susan E., et al. "A review of potentially low-cost sorbents for heavy metals." *Water research* 33.11 (1999): 2469-2479.

[41] Kurniawan, Tonni Agustiono, et al. "Comparisons of low-cost adsorbents for treating wastewaters laden with heavy metals." *Science of the Total Environment* 366.2 (2006): 409-426.

[42] Udaybhaskar, P., Leela Iyengar, and A. V. S. Rao. "Hexavalent chromium interaction with chitosan." *Journal of Applied Polymer Science* 39.3 (1990): 739-747.

[43] Schmuhl, R., H. M. Krieg, and K. Keizer. "Adsorption of Cu (II) and Cr (VI) ions by chitosan: Kinetics and equilibrium studies." *Water Sa* 27.1 (2004): 1-8.

[44] Babel, Sandhya, and Tonni Agustiono Kurniawan. "Cr (VI) removal from synthetic wastewater using coconut shell charcoal and commercial activated carbon modified with oxidizing agents and/or chitosan." *Chemosphere* 54.7 (2004): 951-967.

[45] Dakiky, M., et al. "Selective adsorption of chromium (VI) in industrial wastewater using low-cost abundantly available adsorbents." *Advances in environmental research* 6.4 (2002): 533-540.

[46] Kobya, M. "Removal of Cr (VI) from aqueous solutions by adsorption onto hazelnut shell activated carbon: kinetic and equilibrium studies." *Bioresource technology* 91, no. 3 (2004): 317-321.

[47] Sharma, D. C., and C. F. Forster. "Removal of hexavalent chromium using sphagnum moss peat." *Water Research* 27.7 (1993): 1201-1208.

[48] Sharma, D. C., and C. F. Forster. "A preliminary examination into the adsorption of hexavalent chromium using low-cost adsorbents." *Bioresource Technology* 47.3 (1994): 257-264.

[49] Sharma, D. C., and C. F. Forster. "Continuous adsorption and desorption of chromium ions by sphagnum moss peat." *Process Biochemistry* 30.4 (1995): 293-298.

[50] Akar, Sibel Tunali, Yasemin Yetimoglu, and Tevfik Gedikbey. "Removal of chromium (VI) ions from aqueous solutions by using Turkish montmorillonite clay: effect of activation and modification." *Desalination* 244.1 (2009): 97-108.

[51] Khan, Saad Ali, and M. Ali Khan. "Adsorption of chromium (III), chromium (VI) and silver (I) on bentonite." *Waste Management* 15.4 (1995): 271-282.

[52] Leyva-Ramos, Roberto, et al. "Adsorption of chromium (VI) from an aqueous solution on a surfactant-modified zeolite." *Colloids and Surfaces A: Physicochemical and Engineering Aspects* 330.1 (2008): 35-41.

[53] Li, Zhaohui, and Hanlie Hong. "Retardation of chromate through packed columns of surfactant-modified zeolite." *Journal of hazardous materials* 162.2 (2009): 1487-1493.

[54] Silva, Bruna, et al. "Zeolites as supports for the biorecovery of hexavalent and trivalent chromium." *Microporous and Mesoporous Materials* 116.1 (2008): 555-560.

[55] Weng, C. H., J. H. Wang, and C. P. Huang. "Adsorption of Cr (VI) onto TiO_2 from dilute aqueous solutions." *Water science and technology* 35.7 (1997): 55-62.

[56] Bhutani, M. M., A. K. Mitra, and Ramesh Kumari. "Kinetic study of Cr (VI) sorption on MnO_2." *Journal of radioanalytical and nuclear chemistry* 157.1 (1992): 75-86.

[57] Gupta, Vinod K., et al. "Removal of chromium (VI) from electroplating industry wastewater using bagasse fly ash—a sugar industry waste material." *Environmentalist* 19.2 (1998): 129-136.

[58] Srivastava, S. K., V. K. Gupta, and Dinesh Mohan. "Removal of lead and chromium by activated slag-A blast-furnace waste." *Journal of Environmental Engineering* 123.5 (1997): 461-468.

[59] Pradhan, Jyotsnamayee, Surendra Nath Das, and Ravindra Singh Thakur. "Adsorption of hexavalent chromium from aqueous solution by using activated red mud." *Journal of Colloid and Interface Science* 217.1 (1999): 137-141.

[60] Mallick, Sujata, S. S. Dash, and K. M. Parida. "Adsorption of hexavalent chromium on manganese nodule leached residue obtained from NH_3–SO_2 leaching." *Journal of colloid and interface science* 297.2 (2006): 419-425.

[61] Deng, Baolin, and Alan T. Stone. "Surface-Catalyzed Chromium(VI) Reduction: Reactivity Comparisons of Different Organic Reductants and Different Oxide Surfaces." *Environmental Science and Technology* 30 (1996): 2484–2494

Chapter II

II. ISOTHERM AND KINETIC STUDIES

2.1. Introduction

The need for cost-effective adsorbents to remove Cr (VI) from industrial waters particularly has prompted this investigation of different manganese oxide types as potential adsorbents. Crystalline aggregates and coatings of manganese oxide minerals are ubiquitous in soil and stream sediments and have been recently found to act as natural traps for heavy metal contaminates migrating from mining and other industrialized sites [1]. Manganese nodule leached residues were reported to specifically adsorb Cr (VI) species within the Mn-rich phase [2]. Bhutani et al. and Chang et al. [3, 4] additionally demonstrated that natural MnO_2 minerals and developed iron and manganese coated sands are effective in adsorbing Cr (VI) species. There remains ample opportunity to discovery other more effective manganese oxide types considering that more than thirty manganese oxide minerals are known to occur and to synthetize a more sustainable mixed manganese coated sand mixture.

Pure crystalline manganese (III) oxide (Mn_2O_3) powder and two prepared manganese-aluminum mixed coated sands (MCS) were selected for continued study based on a wide range of preliminary batch adsorption tests. The Mn_2O_3 powder had proved to be the best adsorbent of both pure and mixed manganese oxides tested including MnO_2, which has typically been investigated based on its structure. The mixed manganese coating on the low-cost matrix was developed to be the preferable adsorbent as the manganese requirement and overall material cost

SUMMARY

The increasing occurrence of hexavalent chromium [Cr (VI)] in water resources worldwide and recent evidence for genotoxic and carcinogenic effects of Cr (VI) by ingestion have heightened concern for this contaminant in drinking water. The current U.S. EPA maximum contaminant level (MCL) is 0.1 mg/L for total chromium. In contaminated water, Cr (VI) levels are typically three to five times the U.S. EPA limit and have been mainly traced to the leaking of industrial waste products such as stainless steel, electroplating, pigments, dyes, and leather tanning. The health concerns have not only led to a global trend towards more stringent regulations, but to the subsequent need for more effective and less expensive technologies for removal of Cr (VI).

The conventional methods for Cr (VI) removal, which include Cr (VI) reduction and precipitation, ion exchange, and membrane filtration, have several drawbacks such as high capital and operational cost, production of chemical sludge and sludge disposal problems. Adsorption has been considered as an effective but less expensive and simpler technology for the removal of Cr(VI) from water. Manganese oxide based sorbents have shown promise as low-cost adsorbents. In this study, the feasibility and application of manganese (III) oxide (Mn_2O_3) powder and two manganese-aluminum coated sands (New MCS and X MCS) were evaluated as potential sorbents for the removal of Cr (VI) from water. The processes were investigated by batch technique at room temperature and the adsorption data were analyzed using adsorption equilibrium equations and adsorption kinetic models. The Cr (VI) adsorption capacities and reaction rates were determined. The effect of pH and co- existing ions on adsorption of Cr(VI) was investigated. The reuse and regeneration of sorbent was also evaluated.

The Cr (VI) adsorption characteristics were best described using the Freundlich adsorption equation. The Dubinin-Radushkevich adsorption equation parameters showed that the Cr (VI) adsorption was predominately physical and reversible in nature. The mainly physical nature of adsorption also correlated with the rapid kinetics of Cr (VI) adsorption, particularly in case of the MCS adsorbents. Both Mn_2O_3 and MCS sorbents effectively adsorbed Cr (VI) within the pH range of 2 to 10. The adsorption of Cr (VI) was found to be slightly enhanced in the presence of Ca^{2+} and was suppressed in the presence of 0.1 mM PO_4^{3-}, 0.5 mM HCO_3^- , or 1 mM SO_4^{2-} concentrations. The reuse potential of the MCS adsorbents was greater than that of Mn_2O_3; New MCS showed potential for further reuse and Cr (VI) removal after regeneration using 0.001 N NaOH. The analysis of the point of zero charge (PZC) of Mn_2O_3 indicated that Cr (VI) anions were most likely adsorbed as inner-sphere complexes, while the more alkaline PZC of the MCS sorbents supported the formation of weakly bound Cr (VI) in outer-sphere complexes.

The adsorption capacity and kinetics were favorable for using Mn_2O_3 and MCS as sorbents for the removal of Cr (VI) from water. The application of MCS sorbents for Cr (VI) removal can offer the following advantages: lower cost, faster kinetics, wider effective pH range, greater stability under competing ion conditions and sorbent reuse potential. It is recommended that the MCS sorbents be developed further to improve the Cr (VI) adsorption capacity. The surface complex structures can be confirmed from spectroscopic studies in future work, and the sand coating mixture and consistency can be optimized for future preparations of the MCS sorbents.

is reduced. However, the adsorption properties and structure of the adsorbed species on these materials can vary due to varying laboratory conditions. To determine the repeatability of the coating procedure and consistency in surface properties, two manganese coated sands of slightly varying composition (denoted New and X MCS) were studied in parallel to pure Mn_2O_3. From acid digestion results, the manganese content of New and X MCS was found to be 10.54 mg/g and 13.4 mg/g, respectively and the New and X MCS aluminum content was 14.18 mg/g and 12.64 mg/g, respectively.

In this chapter, the adsorption equilibria and kinetics of Cr (VI) adsorption onto these three manganese oxide sorbents were studied to evaluate sorbent quality. Adsorption capacities, Cr (VI) affinities, and equilibrium times were specifically determined for this purpose. These parameters also provided some understanding as to the mechanism of adsorption. The capacities and rate constants were also compared to other sorbents examined under similar conditions to justify application of treatment processes.

2.2. Materials and methods

2.2.1. Chemicals and reagents

All chemicals were of analytical reagent grade and no further purification was carried out. All solutions were prepared with de-ionized (DI) water made in the laboratory with a resistance

greater than 18 MΩ. The manganese (III) oxide powder (Mn_2O_3, 98 % purity, density of 4.5 g/mL at 25 °C) with an average particle size less than 325 U.S. mesh (44 μm) was obtained from Alfa Aesar (Ward Hill, MA). The sand was coated using manganese (II) chloride tetrahydrate ($MnCl_2 \cdot 4H_2O$, 99% purity) and aluminum chloride hexahydrate ($AlCl_3 \cdot 6H_2O$, 99% purity) obtained from Acros. Potassium dichromate ($K_2Cr_2O_7$, ACS grade, crystals) was also obtained from Acros and used to prepare stock solutions of Cr (VI) in DI water.

2.2.2. Manganese- aluminum-coated sand (MCS) sorbent preparation

First, the sand was washed and soaked in 0.1 M HCl solution for 3 hours, then rinsed with de-ionized water, and dried in an oven at 110 ºC. The coating solution was prepared next by mixing 50 mL solutions of 1 M $MnCl_2$ with 50 mL of 1 M $AlCl_3$ and slowly adjusting the mixture pH to approximately 6.5 using 6 N NaOH, which results in a slurry of manganese and aluminum hydroxide precipitates. The coating solution was then combined with 80 g of the washed sand in a flask and mixed for 24 hours. This sand mixture was air dried for 12 hours, heated in an oven at 110 ºC for 4 hours, and finally introduced into a furnace at 550 ºC for 5 hours to complete coating metal oxides on sand.

2.2.3. Batch adsorption isotherm experiments

Batch sorption studies were mainly performed to obtain data on the extent and rate of adsorption. The adsorption equilibrium and kinetics of 1 mg/L Cr (VI) concentrations were studied in batch

experiments with Mn_2O_3 powder and two batches of manganese oxide coated sands (abbreviated New 5hr MCS and X 5hr MCS) as the adsorbents. The three adsorption equilibrium experiments were conducted using different concentrations of dry sorbent suspension at room temperature. Each solid sorbent sample was first immersed in 50 mL of Cr (VI) solution in high density polyethylene (HDPE) tube that was next shaken in a tumbler at 16 rpm and for 24 hours and finally centrifuged at 9,500 rpm to separate aqueous phase for Cr (VI) analysis. The equilibrium studies were conducted at pH 5.901 for Mn_2O_3 and New 5hr MCS and 6.09 for X 5hr MCS. The final solution pH after adsorption was also measured. Based on the results of this study, an optimum sorbent dosage of 20 g/L was selected for all remaining experiments as it was found that doubling this dosage only slightly increased Cr (VI) adsorption capacity.

2.2.4. Batch adsorption kinetics experiments

The adsorption kinetic experiments were also carried out at room temperature using instead a fixed sorbent dosage (20 g/L) and by varying sample shaking times in the tumbler between 10 minutes and 24 hours. The kinetic experiments were conducted at pH 6.09 for all Mn sorbents studied. The batch kinetics experiments were performed in triplicate and the averages of the results were presented.

2.2.5. Analytical methods

The chromium concentration in aqueous solution was determined by flame atomic absorption spectroscopy. The analysis for chromium was carried out using a Hollow Cathode Lamp (HCL) at wavelength 357.9 nm and silt setting 0.7 nm with a lean blue air-acetylene flame at about 2300 °C. An air flow of 17.0 L/min and acetylene flow of 2.5 L/min was used. The lower limit of quantitation for Cr analysis is 0.05 mg/L. The uptake of Cr (VI) on each sorbent was then calculated using the following equation:

$$q = \frac{(C_0 - C_e)}{m} \times A \qquad (1)$$

where C_0 and C_e are the initial and equilibrium concentration of Cr (VI) in the solution(mg/L), q is the adsorbed Cr (VI) (mg/kg), m is the adsorbent dosage (kg) and A is the solution volume (L).

2.3. Results and discussion

2.3.1. Adsorption isotherms

An adsorption isotherm is a graph that shows the resulting equilibria between the adsorbate in solution and the amount adsorbed at a constant temperature for a wide range of batch adsorption data. The adsorption isotherms obtained at 25 ºC with initial 1- 2 mg/L Cr (VI) solutions at pH 5.9 -6.0 are given in Figures 1, 2, and 3 for Mn_2O_3, New MCS, and X MCS, respectively. In each graph, a concave curve without a strict plateau was observed. This is a common isotherm shape

that can be classified as a high affinity L-type curve based on the initial slope [5,6]. The decrease in slope and plateau at higher Cr (VI) concentration can be attributed to the decrease in available surface sites on the adsorbent and a limited number of sites. Thus, the plateau marks the adsorbent saturation capacity and was roughly observed at 108 mg/kg, 96 mg/kg, and 90 mg/kg for Mn_2O_3, New 5hr MCS, and X 5hr MCS respectively.

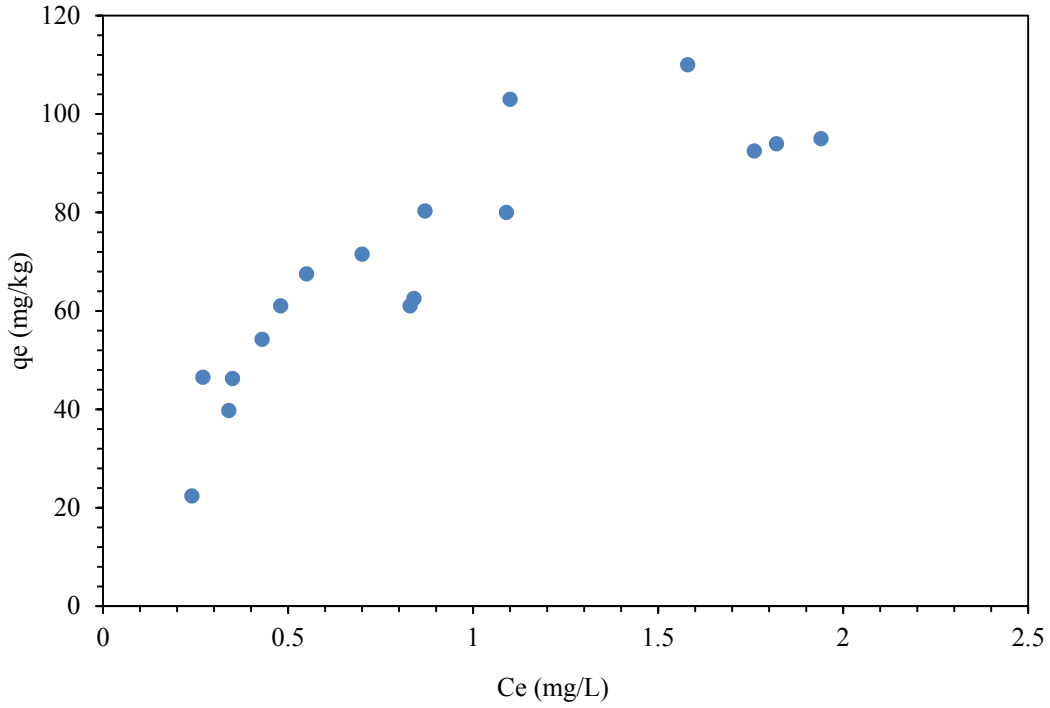

Fig. 1. Mn_2O_3 adsorption equilibrium isotherm data

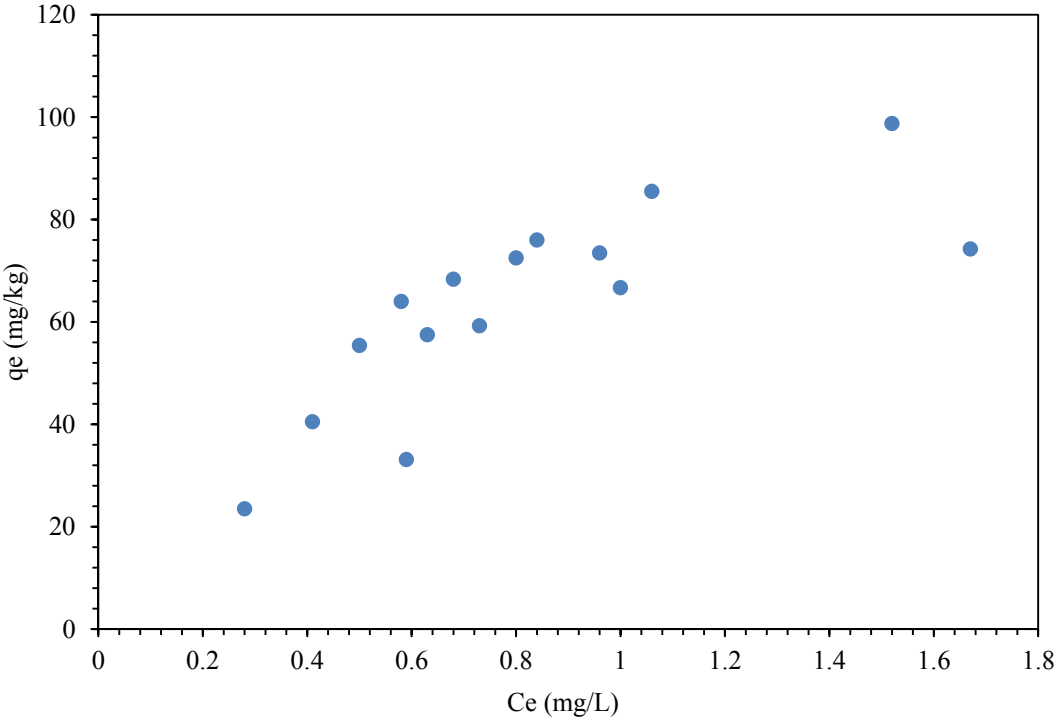

Fig. 2. New 5hr MCS adsorption equilibrium isotherm data.

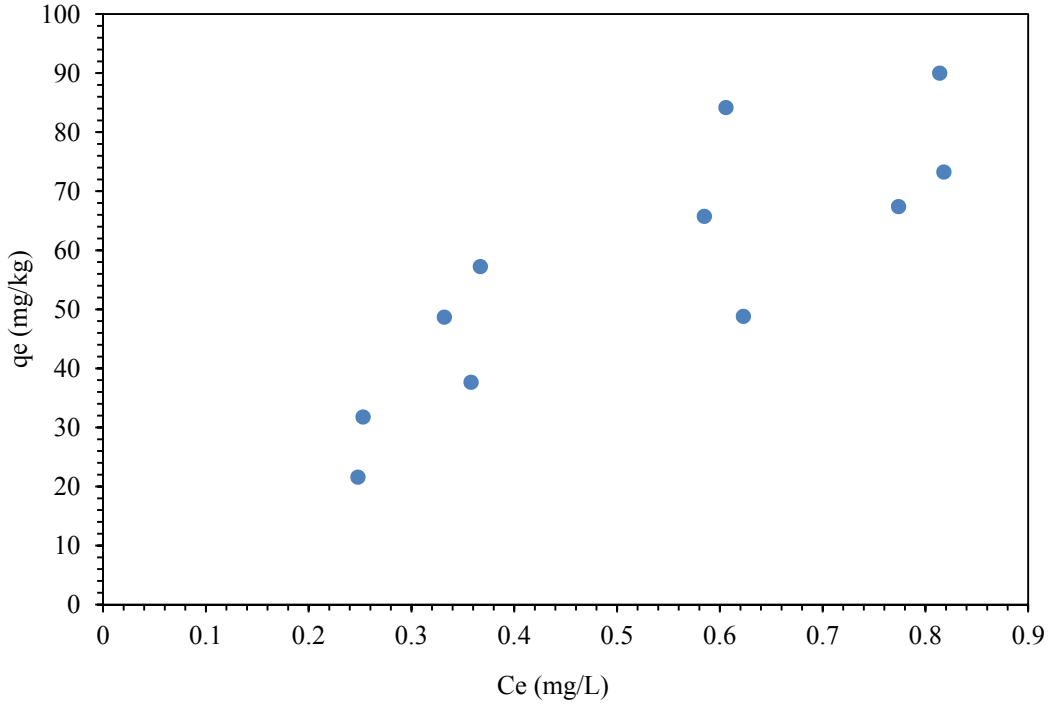

Fig. 3. X 5hr MCS adsorption equilibrium isotherm data.

To better understand adsorption behavior, the change in initial solution pH with adsorption was also monitored for the 1 mg/L Cr (VI) stock solution samples. The solution pH readings following adsorption are presented in Tables 1, 2, and 3 along with the initial stock solution pH. From these tables, it can be seen that the initial solution pH generally increased following Cr (VI) adsorption onto New and X MCS and in the case of Mn_2O_3 generally decreased indicating the slightly acidic nature of the surface and an adsorption mechanism that is different from MCS. The dependence of adsorption behavior on initial solution pH will be discussed in detail in the next chapter.

Table 1. Isotherm pH readings for Mn_2O_3

Mass (g)	pH
2	5.638
1	5.591
0.8	6.02
0.65	5.624
0.5	6.166
0.4	6.223
0.25	5.781
0.2	5.802
0.165	5.758
STOCK	5.901

Table 2. Isotherm pH readings for New 5hr MCS

Mass (g)	pH
2	7.45
1	7.26
0.65	6.275
0.5	6.11
0.4	6.14
0.3	5.829
0.25	6.12
0.2	6.586
0.165	6.346
STOCK	5.901

Table 3. Isotherm pH readings for X 5hr MCS

Mass (g)	pH
2	7.257
1	6.401
0.8	6.676
0.65	6.301
0.5	6.569
0.4	6.332
0.3	6.267
0.2	6.518
0.165	6.507
0.1	6.616
STOCK	6.09

The adsorption data were next fitted to the following isotherm models for a more accurate quantitative description of the observed adsorption behavior: Langmuir, Freundlich, and Dubinin–Radushkevich (D-R). These models are common and have been successfully used by numerous authors to quantify and contrast the performance of different adsorbents. The most appropriate model was then selected for comparison of the adsorption systems as there are differences in the physical interpretation of the model parameters.

2.3.1.1. Langmuir adsorption isotherm

A good fit to the Langmuir model would signify that adsorption occurs through monolayer formation. It could then be assumed that the activity of surface species is proportional to their concentrations and that energy of adsorption is constant. This model is usually applicable at low concentrations so that lateral interaction insignificant [7]. The Langmuir isotherm can be described as the following equation [8,9,10].

$$q_e = \frac{q_m K_L C_e}{1 + K_L C_e} \qquad (2)$$

where q_e is the amount of Cr (VI) adsorbed per unit weight of adsorbent (mg/kg), q_m is maximum Cr (VI) adsorbed (mg/kg) corresponding to complete coverage of available sites, K_L is Langmuir constant related to the free energy or net enthalpy of adsorption and C_e is the concentration of Cr (VI) in solution at equilibrium (μg/L).

The linear form of Langmuir model is as:

$$\frac{C_e}{q_e} = \frac{C_e}{q_m} + \frac{1}{K_L q_m} \quad (3)$$

where of q_m and K_L can be calculated from the slope and intercept of the plot of C_e/q_e versus C_e. The feasibility of Langmuir isotherm criterion can be resolved from the dimensionless constant separation (R_L), which is computed as [11]:

$$R_L = \frac{1}{1 + K_L C_0} \quad (4)$$

where K_L is the Langmuir constant (L/mg) and C_0 is the initial Cr (VI) concentration (mg/L). A value of R_L between 0 and 1 indicates the favorable adsorption. The resulting Langmuir plots for the Mn_2O_3, New MCS, and X MCS adsorption data are presented in Figures 4, 5, and 6, respectively.

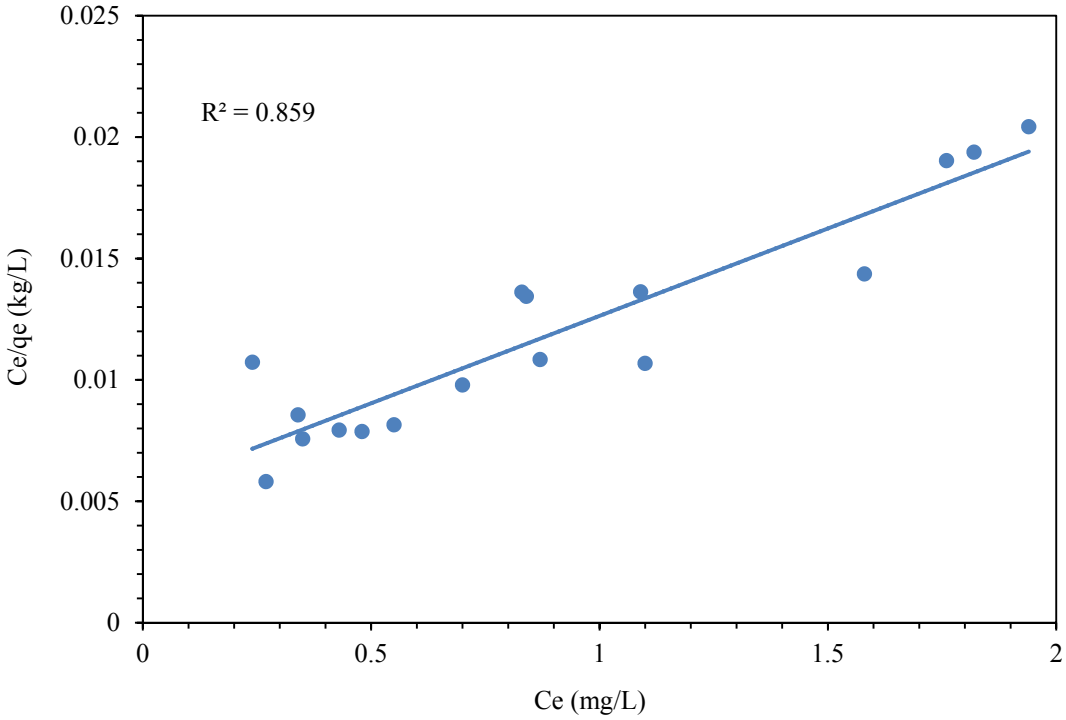

Fig. 4. The Langmuir plot for Mn_2O_3.

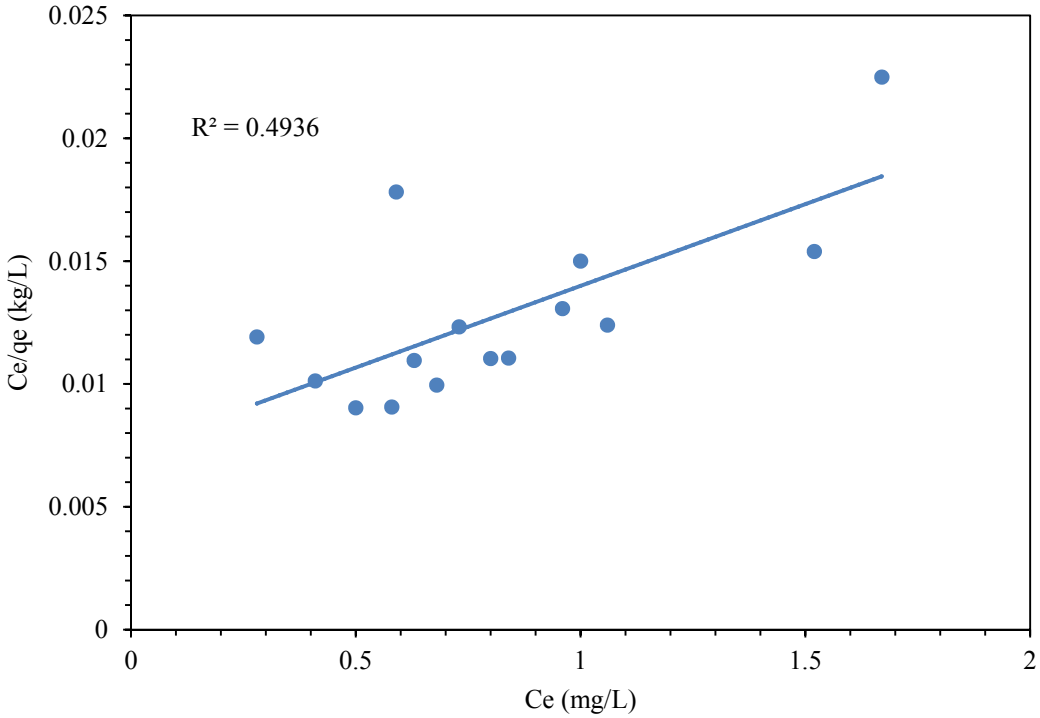

Fig. 5. The Langmuir plot for New 5hr MCS.

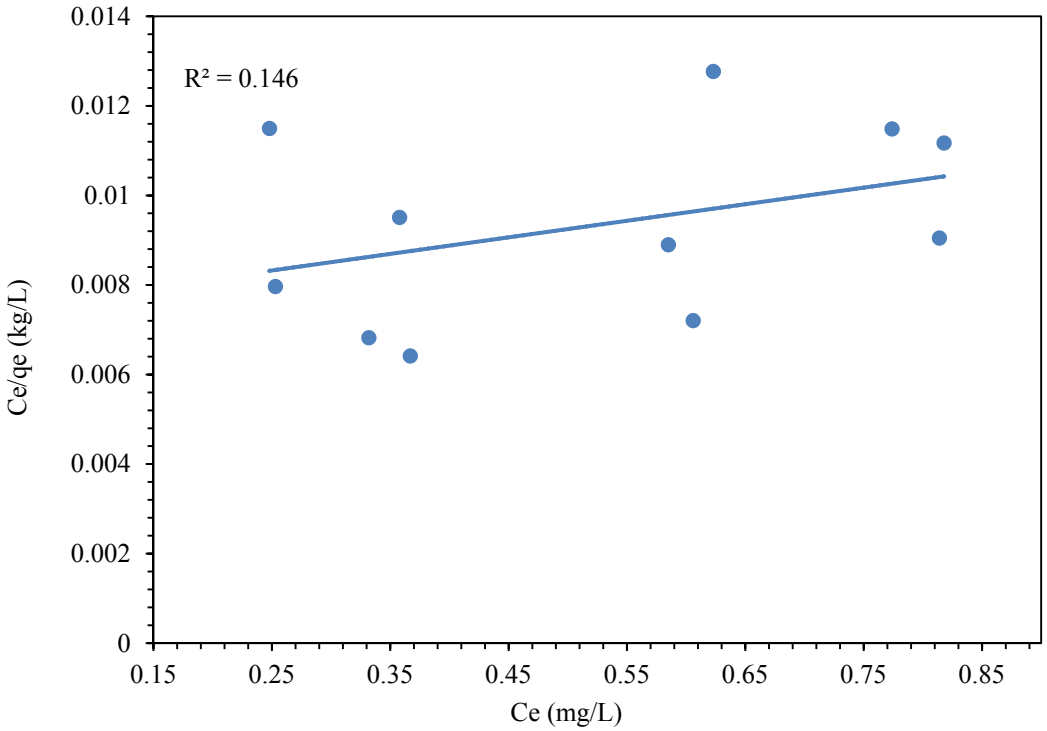

Fig. 6. The Langmuir plot for X 5hr MCS.

The Langmuir model was found to be suitable for the Mn_2O_3 and New 5hr MCS adsorption data based on the correlation coefficients. This suggests that monolayer formation is likely in these cases and that these surfaces are homogenous. It should be noted that a homogenous surface is more suggestive for the Mn_2O_3 sorbent due to the higher R^2 value. Hence, these two sorbents can be compared using the Langmuir parameters obtained from the above adsorption isotherm plots, which are given in Table 4. The estimated maximum adsorption capacities of 139 mg Cr (VI) adsorbed per kg Mn_2O_3 with a R^2 value of 0.859 and 149 mg Cr (VI) adsorbed per kg New 5hr MCS with a R^2 value of 0.497 were found to be similar and comparable to that of other "low cost" adsorbents such as chitosan, hazelnut shell AC, and sphagnum moss [12,13,14].

The Langmuir constants related to free energy (K_L) were found to be 1.3 L/mg for the Mn_2O_3 adsorption data and 0.918 L/mg for the New 5hr MCS adsorption data; the greater K_L value for Mn_2O_3 implies that stronger binding occurs on this surface. Also, the separation factor (R_L) values, calculated from the K_L values, were found to be 0.43 for Mn_2O_3 and 0.52 for New 5hr MCS indicating that adsorption of Cr (VI) is favorable in each case with Cr (VI) adsorption onto Mn_2O_3 being the more favorable case as its the R_L value is closer to zero. In conclusion, Mn_2O_3 is postulated to be the better adsorbent based on the R^2 and R_L values, which are more reliable indices than the obtained q_m values. The better Langmuir fit, stronger binding, and greater favorability for the Mn_2O_3 sorbent can be explained by its pure and crystalline surface facilitating the necessary contact for strong binding and monolayer formation.

Table 4. Langmuir parameters for adsorption of Cr (VI) onto Mn_2O_3, New and X 5hr MCS.

	Mn_2O_3	**New 5hr MCS**	**X 5hr MCS**
q_m (mg/kg)	138.89	149.25	270.27
K_L (L/mg)	1.333	0.918	0.5
R_2	0.859	0.497	0.146

2.3.1.2. Freundlich adsorption isotherm

The Freundlich model accounts for lateral interactions between adsorbed molecules, energetic surface heterogeneity, and describes non-ideal adsorption that is not limited to monolayer formation [15,16]. The model has been widely applied to multilayer adsorption [17]. In many of

these cases, the magnitude of heat of adsorption decreases logarithmically with increasing extent of adsorption; the assumption thus is that the adsorption sites are exponentially distributed with respect to adsorption energy. The Freundlich empirical equation and its linearized form are expressed as follow:

$$q_e = K_F C_e^{1/n} \tag{5}$$

$$\log q_e = \log K_F + (1/n) \log C_e \tag{6}$$

where K_F is the Freundlich constant indicating the adsorption capacity and 1/n is a measure for the adsorption intensity or surface heterogeneity [18]. In this context, a 1/n value of less than one would imply favorable adsorption. In a deeper explanation, the closer this value gets to zero, the more favorable the adsorption, the more heterogeneous surface, and the greater the extent of adsorption [19]. A limitation in this approach, however, is that a maximum adsorption limit is not indicated. The Freundlich plots of log q_e against log C_e for Mn_2O_3, New MCS, and X MCS are shown in Figures 7, 8, and 9, respectively. The K_F and 1/n values are determined from the intercept and slope of the plots and are displayed in Table 5.

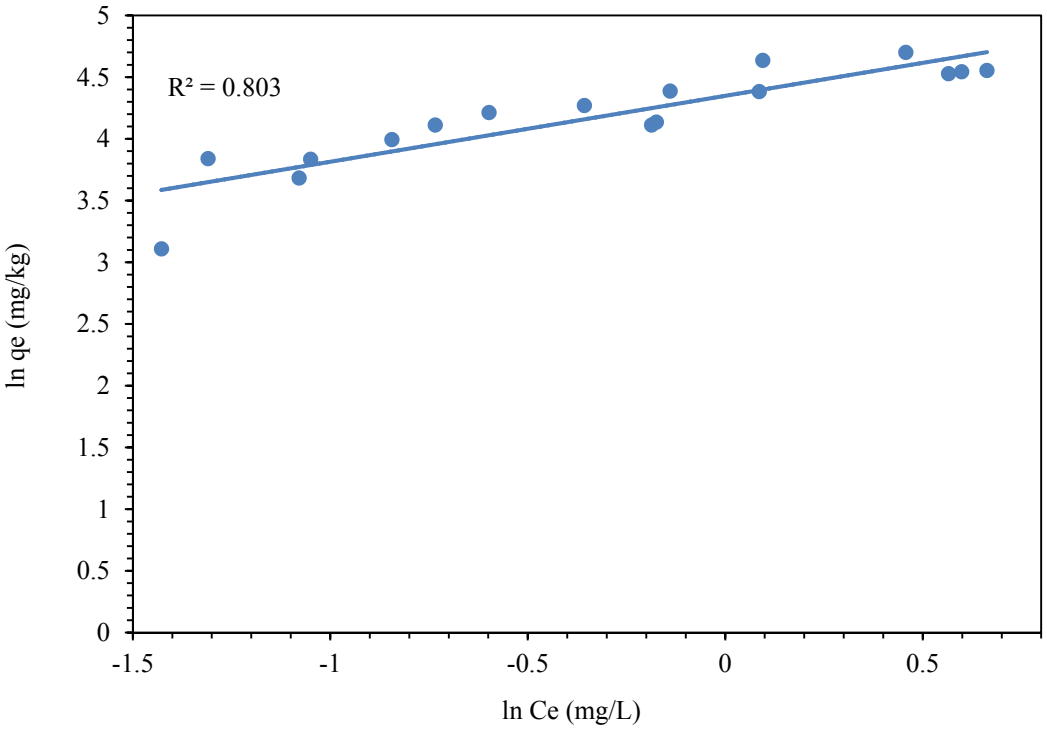

Fig. 7. The Freundlich plot for Mn_2O_3.

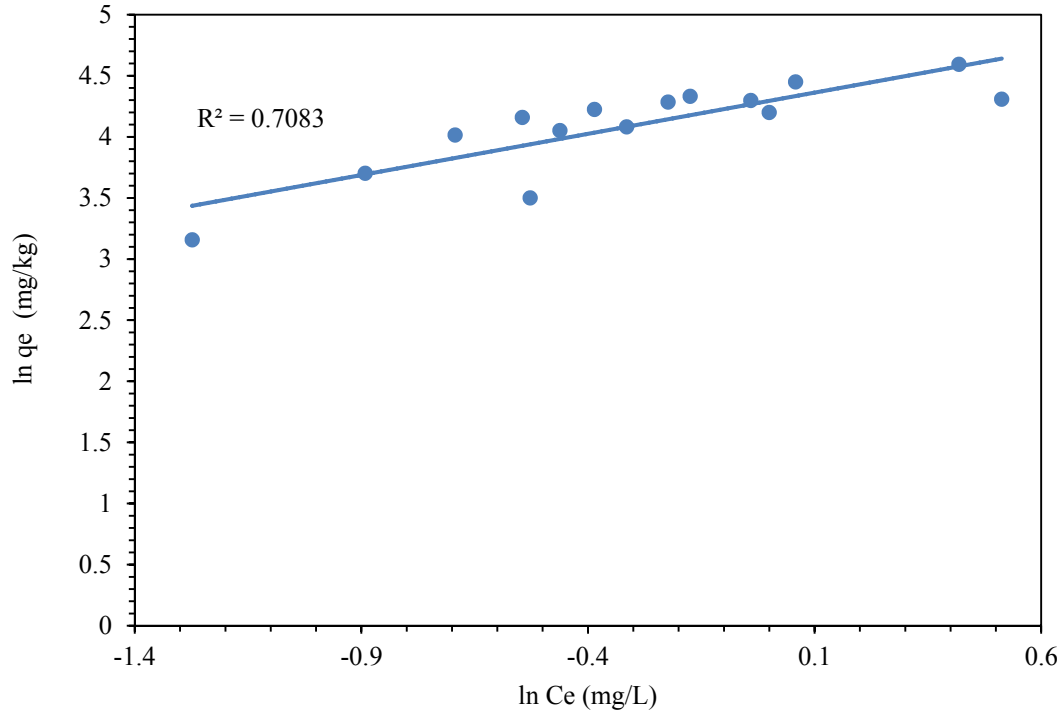

Fig. 8. The Freundlich plot for New 5hr MCS.

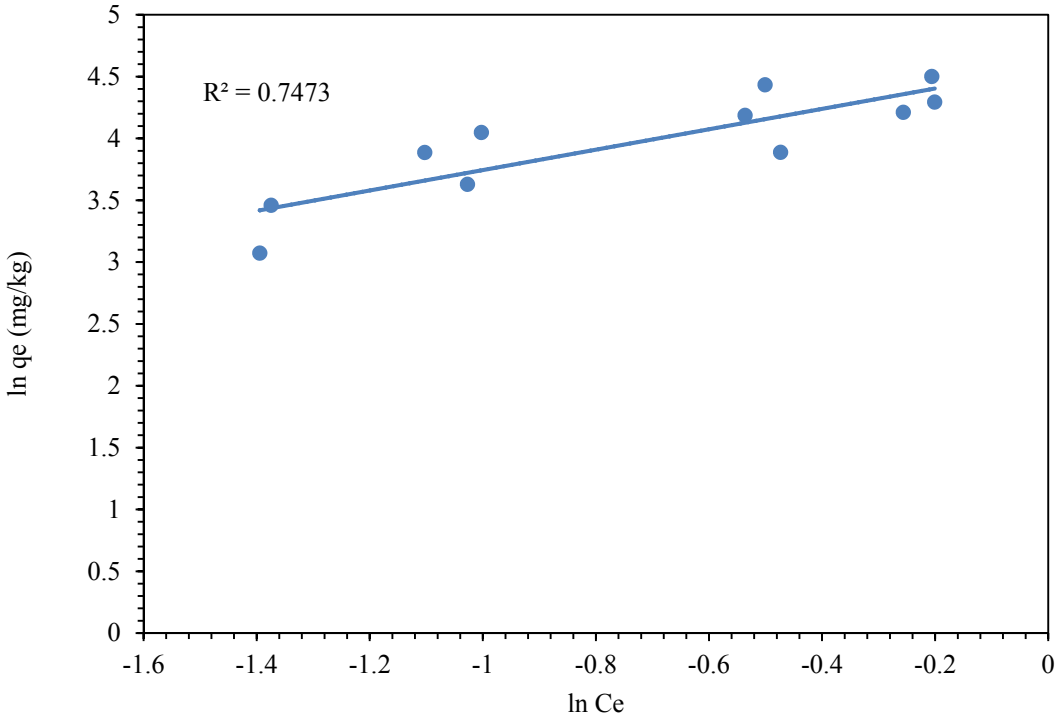

Fig. 9. The Freundlich plot for X 5hr MCS.

The adsorption data of Mn_2O_3, New 5hr MCS, as well as X 5hr MCS were found to fit the Freundlich model with obtained R^2 values of 0.803, 0.708, and 0.747, respectively. The New MCS and X MCS adsorption data shows far more compatibility with the Freundlich isotherm than the Langmuir isotherm as a significantly higher R^2 value was obtained. This suggests that the MCS surfaces are more likely heterogeneous. The three sorbents can be more accurately compared using Freundlich parameters shown in Table 5 as the R^2 values are more similar. It was found that X 5hr MCS sorbent showed the highest adsorption capacity (96.5 mg/kg) followed by Mn_2O_3 (77.4 mg/kg) and New 5hr MCS was the lowest (73.3 mg/kg). These Freundlich adsorption capacities are higher than that of bentonite and manganese dioxide and the costlier adsorbents such as GAC and commercial AC [20,3]. It should also be noted that the K_F

values for Mn_2O_3 and New MCS were nearly equal and that the K_F value for X MCS may have been overestimated and may be less reliable for comparison purposes.

Also, the Freundlich 1/n values for the Mn_2O_3, New 5hr MCS, and X 5hr MCS data, respectively, are 0.534, 0.674, and 0.826 indicating the favorable adsorption in each case with all fractional values less than one. Mn_2O_3 shows the most favorable adsorption with a 1/n value closest to zero and the Mn_2O_3 data, therefore, shows the highest R^2 value. This also implies that the extent of adsorption is greater on Mn_2O_3 and that the K_F value or adsorption capacity in turn should also have been much higher. This discrepancy can be explained by a limitation in the number of available surface sites for Cr (VI) adsorption onto Mn_2O_3 because of steric hindrance and/or lateral interaction with increasing monolayer coverage. In contrast, the less favorable adsorption of Cr (VI) onto the MCS surfaces may be attributed to weaker binding due to cluster or multilayer formation. Overall, it can be concluded that Mn_2O_3 is the best adsorbent based on the favorability of the adsorption reaction and the highest R^2 value.

Table 5. Freundlich parameters for adsorption of Cr (VI) onto Mn_2O_3, New and X 5hr MCS.

	Mn_2O_3	**New 5hr MCS**	**X 5hr MCS**
K_F(mg/kg) $(L/mg)^{1/n}$	77.35	73.27	96.53
1/n	0.534	0.674	0.826
R^2	0.803	0.7083	0.7473

2.3.1.3. Dubinin–Radushkevich (D-R) isotherm model

The Dubinin–Radushkevich (D-R) model does not assume a homogenous surface or a uniform energy distribution and is considered the more general isotherm than the Langmuir and Freundlich models [15]. It has been shown to successfully fit a high to intermediate concentration range, but without satisfactory asymptotic properties. This approach is typically applied to evaluate the nature of adsorption by determining the mean free energy of the sorption, which is defined as the free energy change for removing a molecule from its location in the sorption space to the infinity [21]. The D-R adsorption isotherm can be expressed as:

$$q_e = q_m \exp(-K_{DR}\varepsilon^2) \tag{7}$$

and linearized as:

$$\ln q_e = \ln q_m - K_{DR}E^2 \tag{8}$$

where q_m is the D–R constant, ε (Polanyi potential) is RT ln (1 + 1/C_e) and K_{DR} is a constant related to adsorption energy (mol^2. kJ^2)$^{-1}$. The q_m and K_{DR} can be determined from the intercept and slope of the plot ln q_e versus ε^2. The mean free energy (E) in the system is computed using the following equation [22]:

$$E = \frac{1}{\sqrt{(2K_{DR})}} \tag{9}$$

A mean free energy (E) value of less than 8 kJ/mol would be characteristic of physisorption and an E value in the range of 8 to 16 kJ /mol would be indicative of chemisorption. The D-R plots for Mn_2O_3, New MCS, and X MCS are presented Figures 10, 11, and 12, respectively.

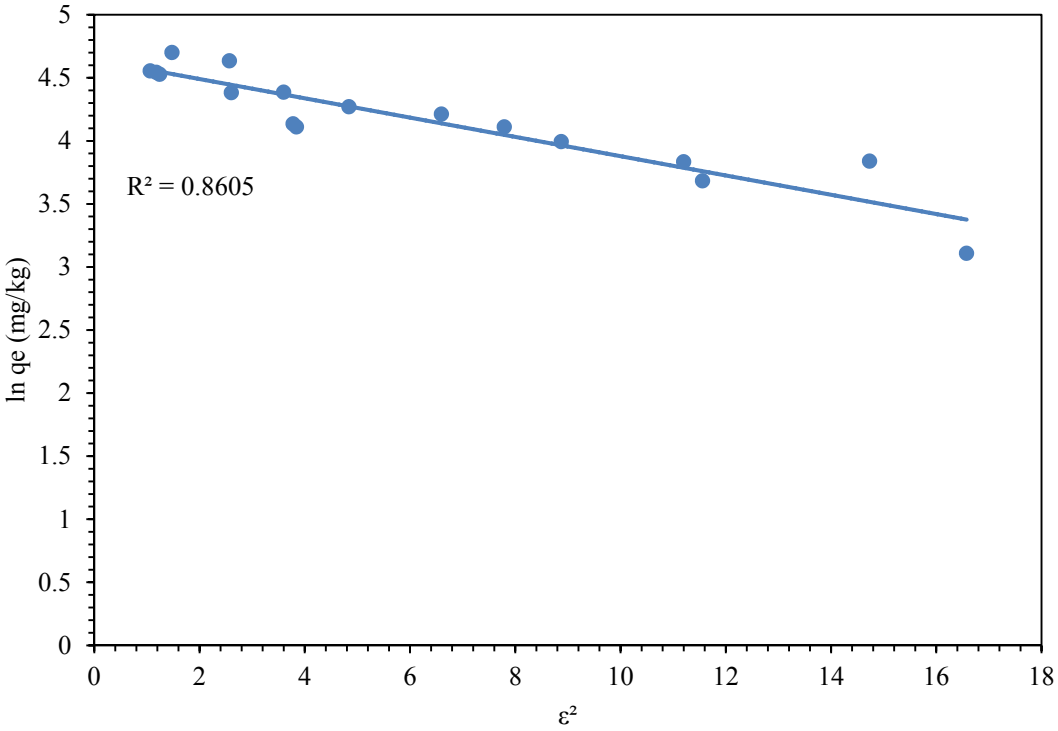

Fig. 10. The D-R plot for Mn_2O_3.

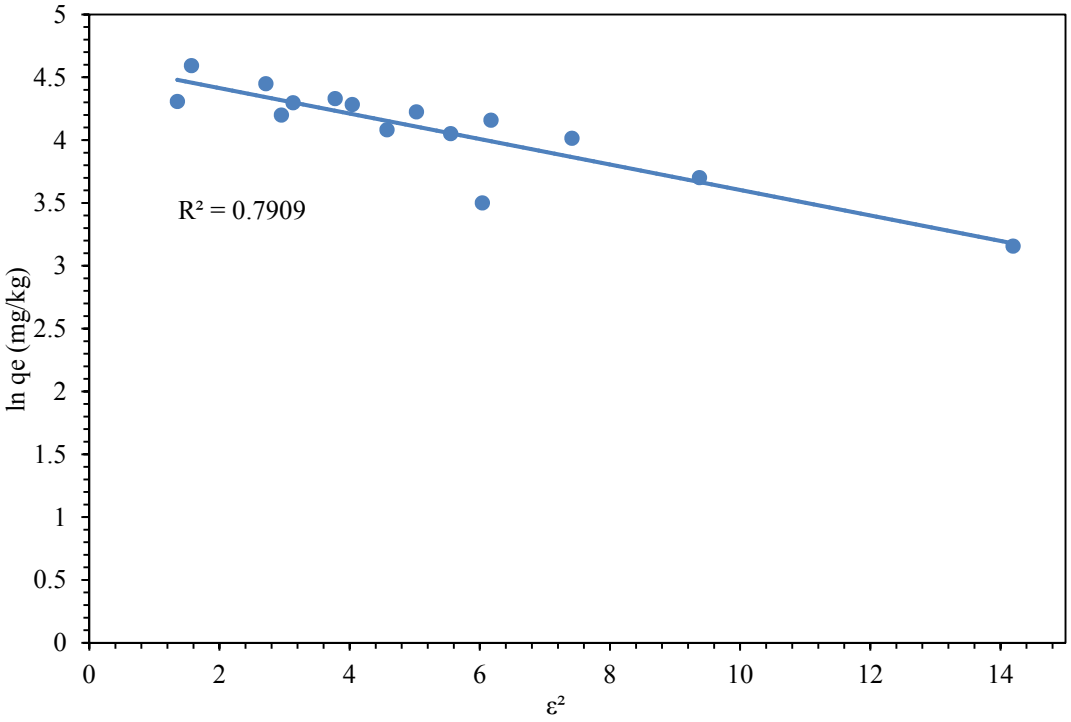

Fig. 11. The D-R plot for New 5hr MCS.

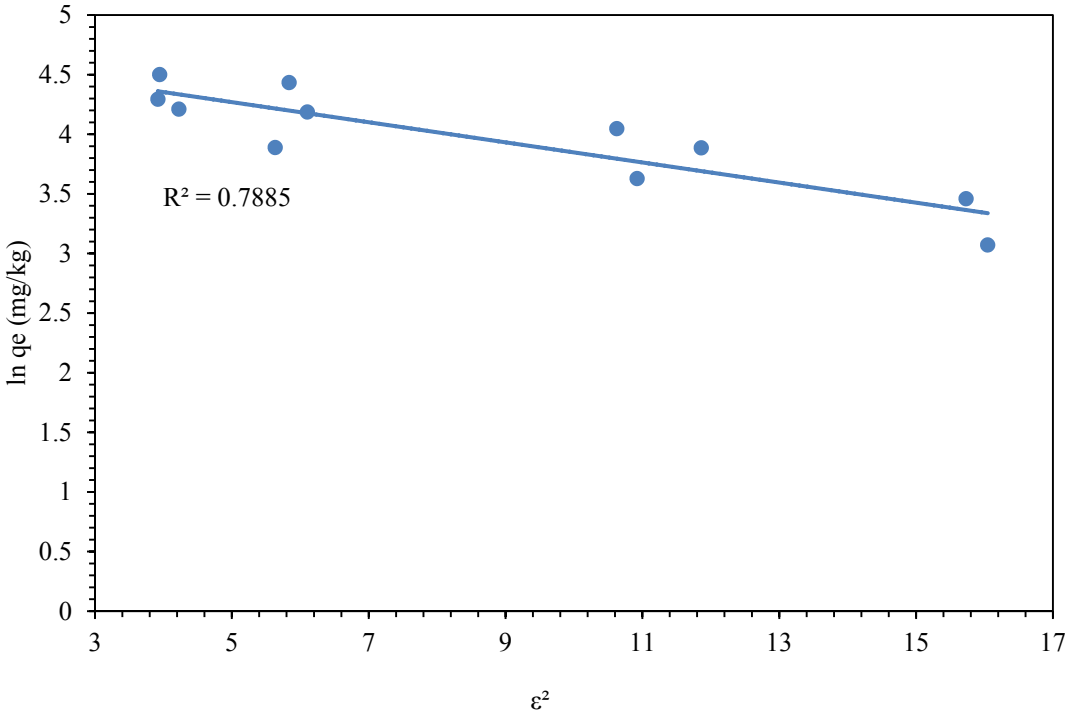

Fig. 12. The D-R plot for X 5hr MCS.

The D-R model was found to describe all adsorption data reasonably well with R^2 values ranging from 0.786 to 0.861. The R^2 value for Mn_2O_3 adsorption is again the highest. Both the obtained adsorption capacities and mean free energy values, given in Table 6, were found to be similar in the study of all three adsorbents. This is suggestive of a similar mechanism of adsorption. The calculated mean free energy values of 2.56 kJ/mol, 2.22 kJ/mol, and 2.44 kJ/mol for the Mn_2O_3, New 5hr MCS, and X 5hr MCS adsorbents, respectively, indicate that physical forces predominate in the adsorption of Cr (VI) ions. The mean free energy for Mn_2O_3 is greatest and in agreement with the previous finding that binding is strongest with Mn_2O_3; however, this value is lower than expected suggesting that very little chemical interaction occurs. The mechanism of physical adsorption was similarly found to be valid for montmorillonite clay, manganese dioxide, and nitric-treated coconut shell charcoal "low cost" adsorbents [23,13,3]. Since physical

adsorption is prevailing phenomena, it also indicates possibility of better regeneration of the used sorbents.

Table 6. D-R parameters for adsorption of Cr (VI) onto Mn_2O_3, New and X 5hr MCS.

	Mn_2O_3	**New 5hr MCS**	**X 5hr MCS**
q_m (mg/kg)	103.92	101.11	108.95
K_{DR}	0.0765	0.1013	0.0843
E(kJ/mol)	2.56	2.22	2.44
R^2	0.861	0.791	0.7885

2.3.2. Adsorption kinetics

The kinetics of adsorption describes the rate of adsorption of Cr (VI) onto the adsorbents; this rate controls the equilibrium time. The kinetics of Cr (VI) adsorption for an initial Cr (VI) concentration of 1 mg/L and a fixed sorbent dosage of 20 g/L were studies in batch experiments at 25 °C by taking samples at different time intervals over a 48-hour period and measuring the residual Cr (VI) concentration. The residual concentration data of each sorbent were plotted as a function of time and are shown in Figures 13 to 15.

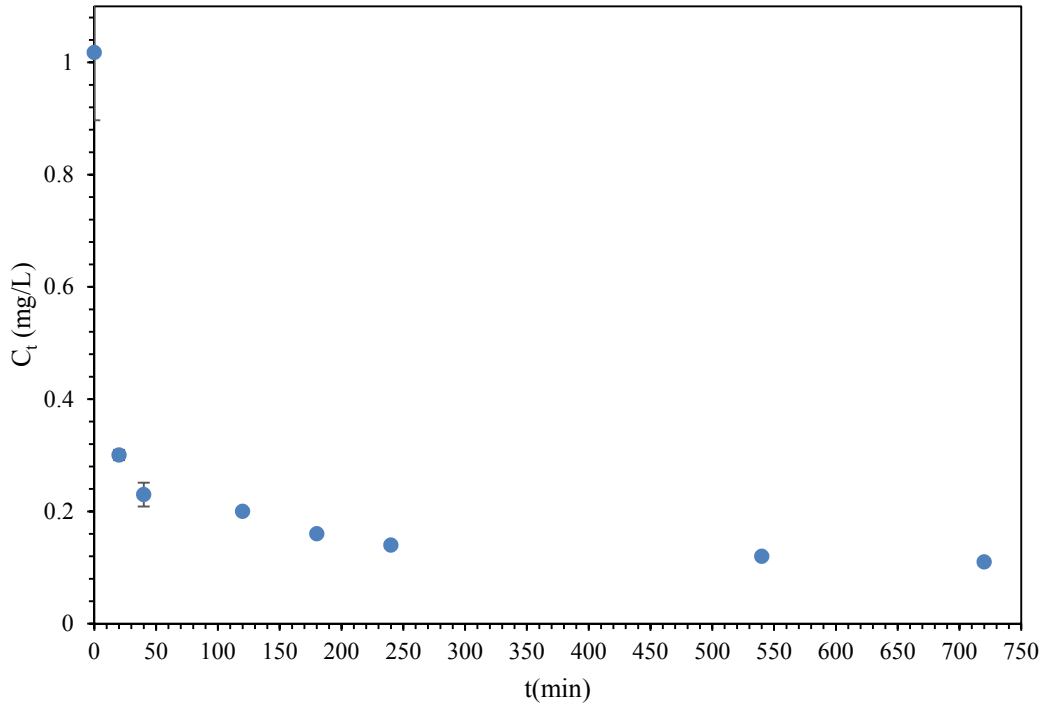

Fig. 13. Effect of contact time on adsorption of Cr (VI) onto Mn_2O_3.

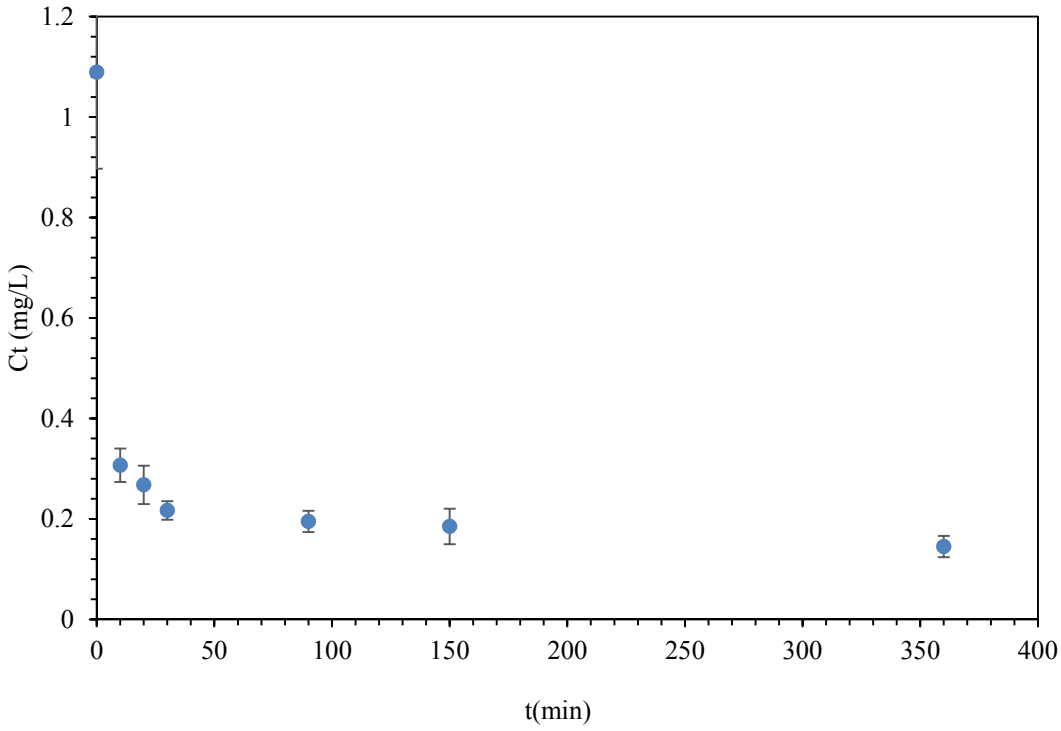

Fig. 14. Effect of contact time on adsorption of Cr (VI) onto New 5hr MCS.

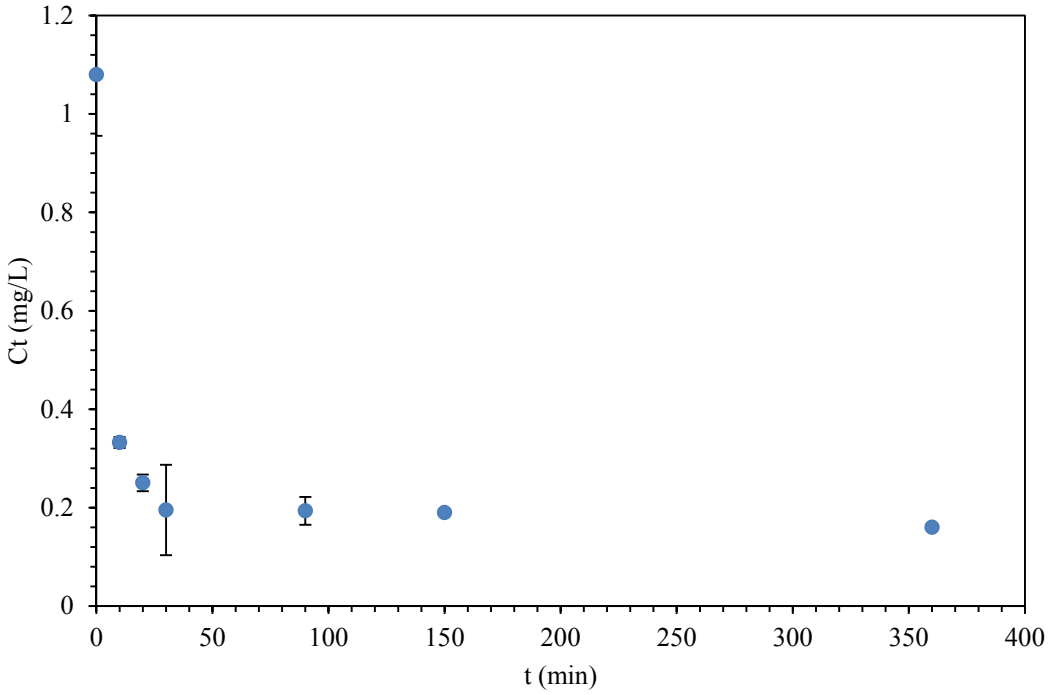

Fig. 15. Effect of contact time on adsorption of Cr (VI) onto X 5hr MCS.

The plots reveal rapid adsorption kinetics in each case. The data points show that uptake is initially fast and later slows to ultimately reach equilibrium after 360 to 720 minutes; within the first 60 minutes of contact, about 89%, 82%, and 81% removal of Cr (VI) was achieved for Mn_2O_3, New 5hr MCS, and X 5hr MCS, respectively and the percent increase in removal is relatively minute thereafter (4-5%). The slower adsorption can be due to the decrease in the driving concentration difference between the surface and the bulk solution, which slows the transport of the Cr (VI) species to the surface of Mn_2O_3 and New 5hr MCS or due to the decrease in positive surface charge density with Cr (VI) adsorption. Similar behavior is noted for "low cost" adsorbents such as chitosan and hazelnut shell activated carbon [12,13]. The declining adsorption rates of Cr (VI) onto the Mn_2O_3, New 5hr MCS, and X 5hr sorbents, particularly

towards the end of the experiments can be indicative of possible monolayer formation of Cr (VI) ions sorbent surfaces.

The change in initial solution pH was again monitored with adsorption as it is the most important parameter in adsorption studies. The final solution pH readings for all samples are given in Tables 7, 8, and 9. It appears that the solution pH stabilized near equilibrium contact time in case of all three adsorbents. This confirms that no further adsorption can occur.

Table 7. Kinetics pH readings for Mn_2O_3

Time (min)	pH
20 #1	6.559
20 #2	6.382
20 #3	6.446
40 #1	6.391
40 #2	6.425
40 #3	6.456
60 #1	6.287
60 #2	6.221
60 #3	5.649
120 #1	5.397
240 #2	5.71
540 #3	5.877
720 #4	5.811
STOCK	6.09

Table 8. Kinetics pH readings for New 5hr MCS

Time (min)	pH
10 #1	6.243
10 #2	6.542
10 #3	6.715
20 #1	6.547
20 #2	6.259
20 #3	6.54
30 #1	6.533
30 #2	6.612
30 #3	6.18
45 #1	6.3732
45 #2	6.312
45 #3	6.305
60 #1	6.269
60 #2	6.638
60 #3	6.59
90 #1	5.743
90 #2	5.666
90 #3	5.792
150 #1	6.232
150 #2	6.107
150 #3	5.948
360 #1	5.882
360 #2	5.87
360 #3	5.999
STOCK	6.09

Table 9. Kinetics pH readings for X 5hr MCS

Time (min)	pH
10 #1	6.525
10 #2	6.655
10 #3	6.501
20 #1	6.616
20 #2	6.422
20 #3	6.486
30 #1	6.164
30 #2	6.722
45 #1	6.212
45 #2	6.785
45 #3	6.266
60 #1	6.24
60 #2	6.325
60 #3	6.375
90 #1	6.082
90 #2	5.994
90 #3	6.105
150 #1	6.112
150 #2	5.875
150 #3	6.183
360 #1	5.928
360 #2	5.99
360 #3	5.935
STOCK	6.09

The experimental kinetics data are interpreted next in terms of Lagergren pseudo-first order, pseudo-second order, and intra-particle diffusion models to determine rate constants and characteristics of the sorption process. These models are based on the decrease of available active sites to interact with solute (adsorption capacity) and the term "pseudo" is used to distinguish the use of solid concentrations from solute concentrations; the rate depends on adsorbed amount rather than concentration or pressure [24].

2.3.2.1. Lagergren pseudo-first order model

The reaction kinetics of Lagergren pseudo-first order model [25] was studied using the results of the uptake of Cr (VI) onto the sorbents at different time interval to understand the dynamics of the adsorption process and evaluate the performance of the sorbent with the time. It is assumed that reaction rates are chemically equivalent for all sites. The pseudo-first order model is given as:

$$\frac{dq_t}{dt} = k_1(q_e - q_t) \tag{10}$$

where q_e and q_t are the adsorption capacities (mg/kg) at equilibrium and at time t, respectively and k_1 is the adsorption rate constant (min^{-1}) of pseudo-first order adsorption. The integrated form of the Lagergren pseudo-first order is as follow:

$$\ln(q_e - q_t) = \ln q_e - k_1 t \tag{11}$$

The adsorption rate constant (k_1) and the theoretical value of the equilibrium adsorption capacity (q_e) can be obtained from the slope and the intercept of the linear plot of $\ln(q_e-q_t)$ versus t,

respectively. The resulting plots for Mn_2O_3, New MCS, and X MCS are given in Figures 16, 17, and 18, respectively.

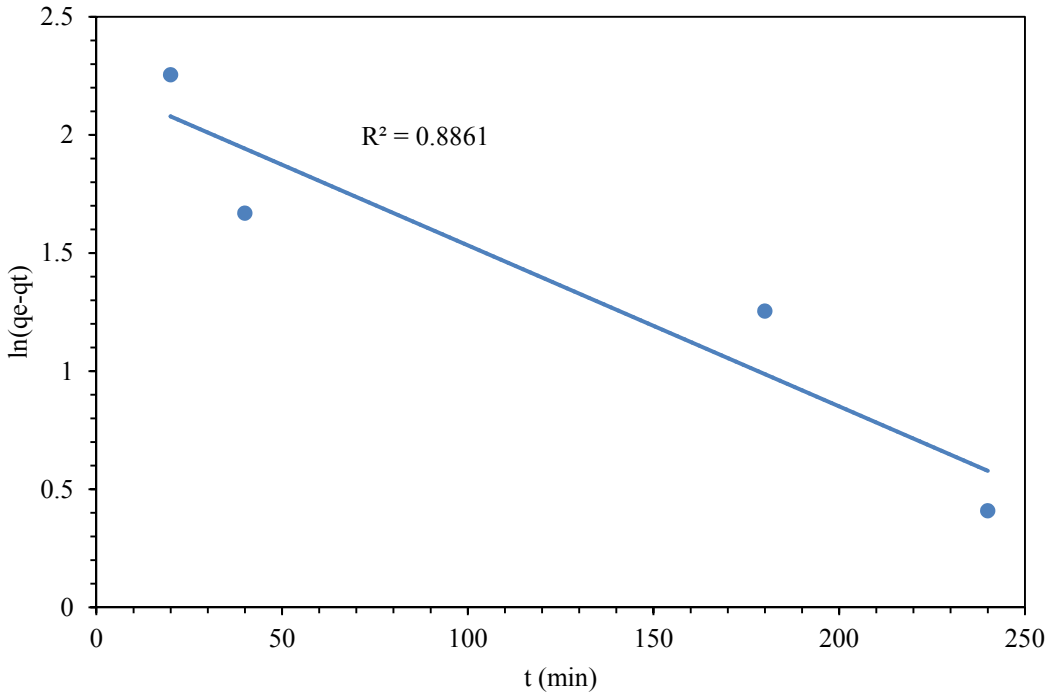

Fig. 16. Pseudo-first order kinetics model for Mn_2O_3.

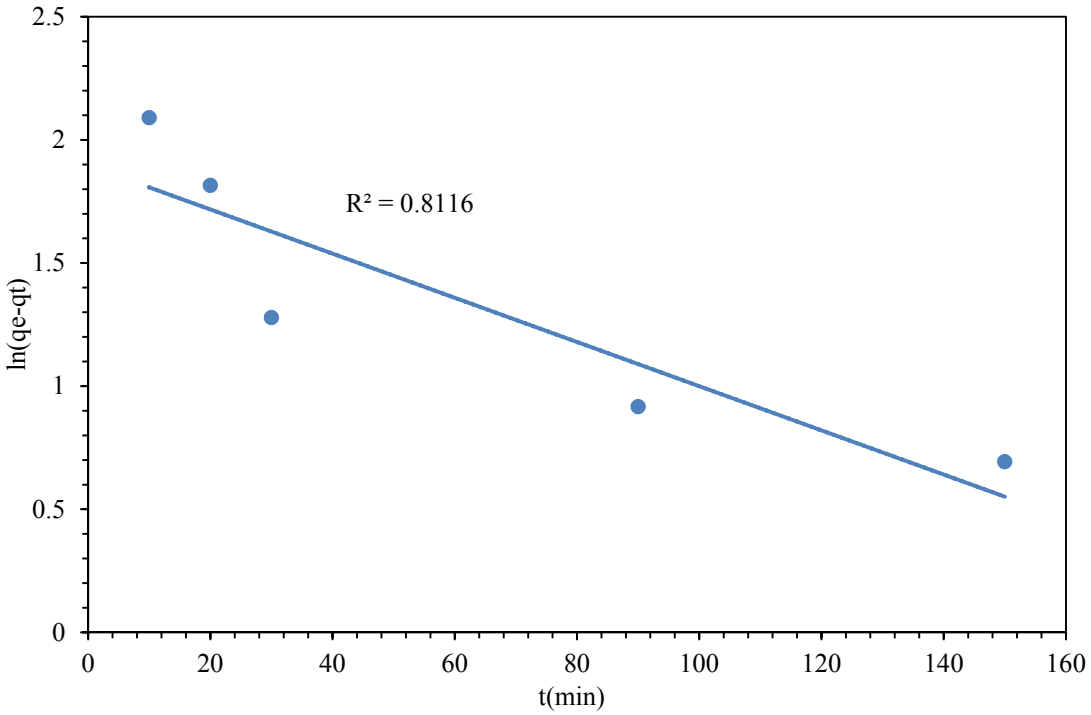

Fig. 17. Pseudo-first order kinetics model for New 5hr MCS.

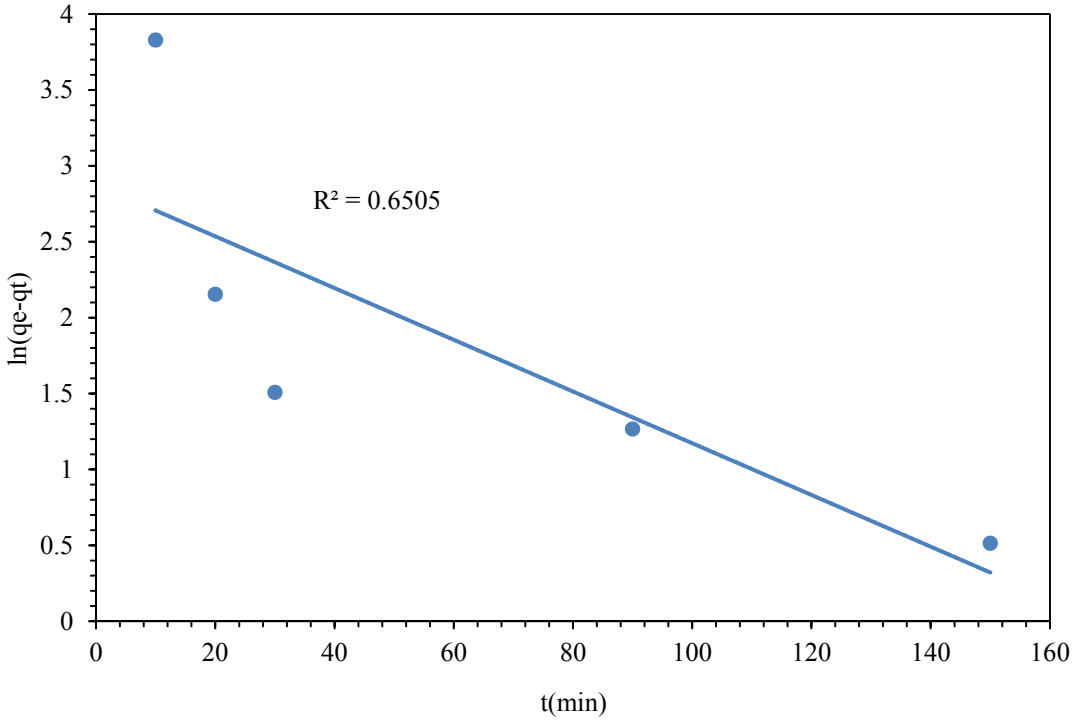

Fig. 18. Pseudo-first order kinetics model for X 5hr MCS.

In the figures above, a poor correlation was observed between the experimental data and the pseudo-first order model, particularly for the MCS adsorbents in comparison to the pseudo-second order model results shown next. Also, the calculated adsorption capacities, q_e, in Table 10, are significantly different from the experimental q_e for any of the three studied sorbents. Therefore, these kinetic parameters cannot be used for comparison to other adsorbents or for design purposes.

Table 10. Pseudo-first order kinetic parameters.

	Mn_2O_3	**NEW 5 hr MCS**	**X 5 hr MCS**
Experimental q_e (mg/kg)	45.4	43.2	46
k_1 (min^{-1})	0.0068	0.009	0.017
q_e (mg/kg)	9.16	6.67	17.75
R^2	0.886	0.812	0.651

2.3.2.2. Pseudo-second order model

The pseudo-second order model has been widely applied recently and has been successfully applied to the adsorption of metal ions from aqueous solutions [26]. It is assumed that chemical adsorption is the overall rate-limiting step and once again that the reaction rates are chemically equivalent for all sites. The pseudo-second order model [27] and its linearized form are given below:

$$\frac{dq_t}{dt} = k_2(q_e - q_t)^2 \tag{12}$$

$$\frac{t}{q_t} = \left(\frac{1}{k_2}\right)\left(\frac{1}{q_e^2}\right) + \frac{t}{q_e} \tag{13}$$

where k_2 is the adsorption rate constant ($g.mg^{-1}.min^{-1}$) of pseudo-second order adsorption and can be obtained from the intercept of a linear plot of t/qt against t. These plots for Mn_2O_3 are presented in Fig. 19, 20, and 21, respectively.

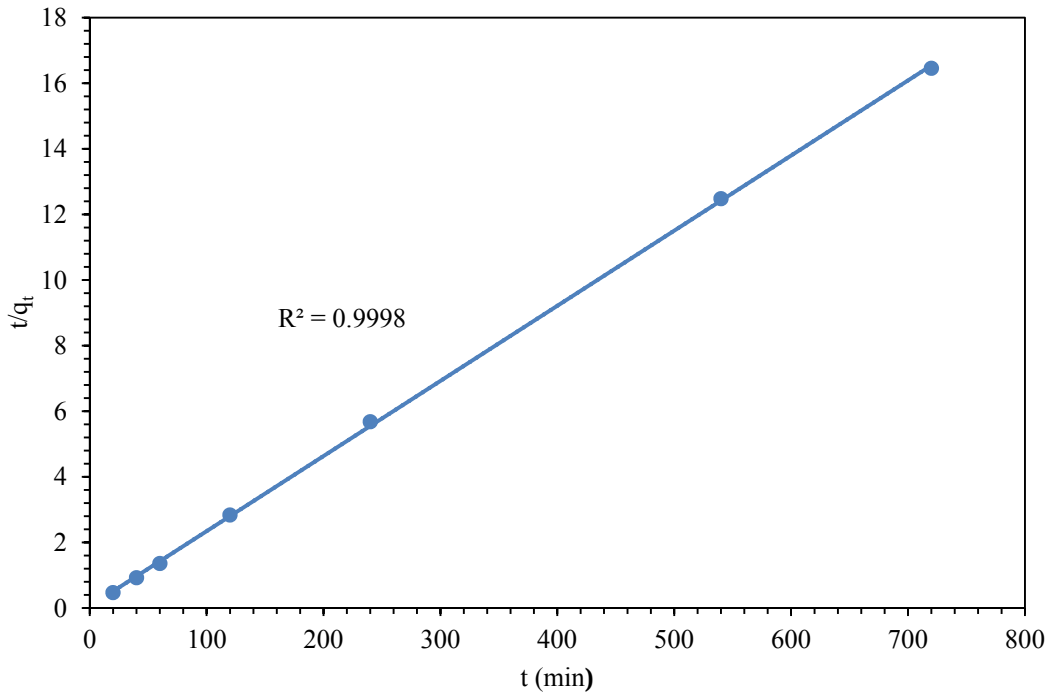

Fig. 19. Pseudo-second order kinetics model for Mn_2O_3.

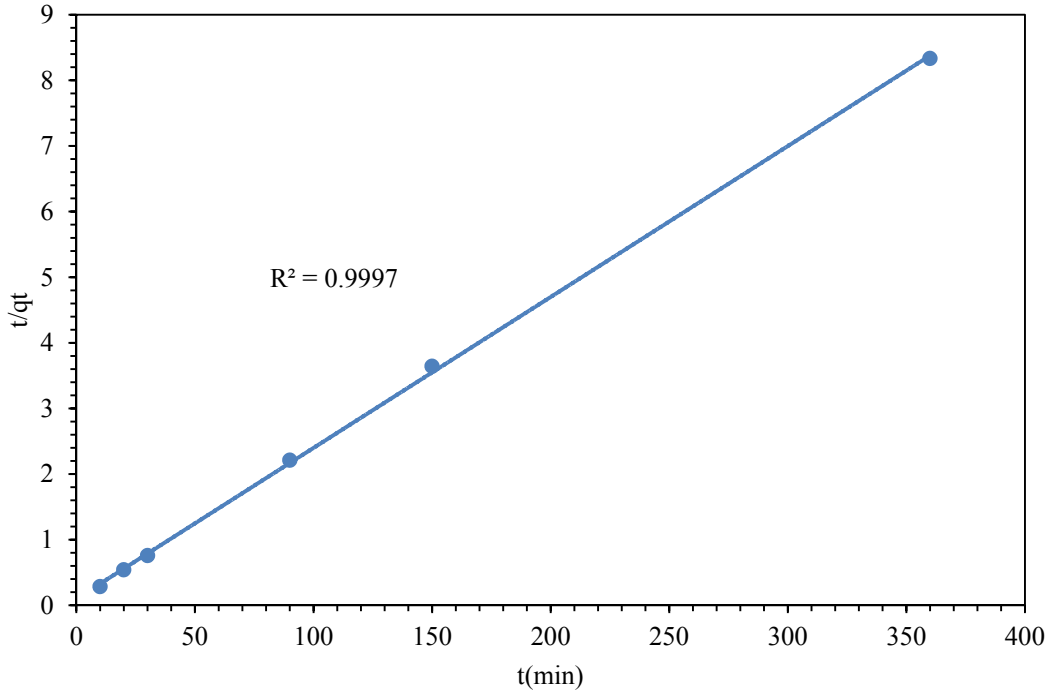

Fig. 20. Pseudo- second order kinetics model for New 5hr MCS.

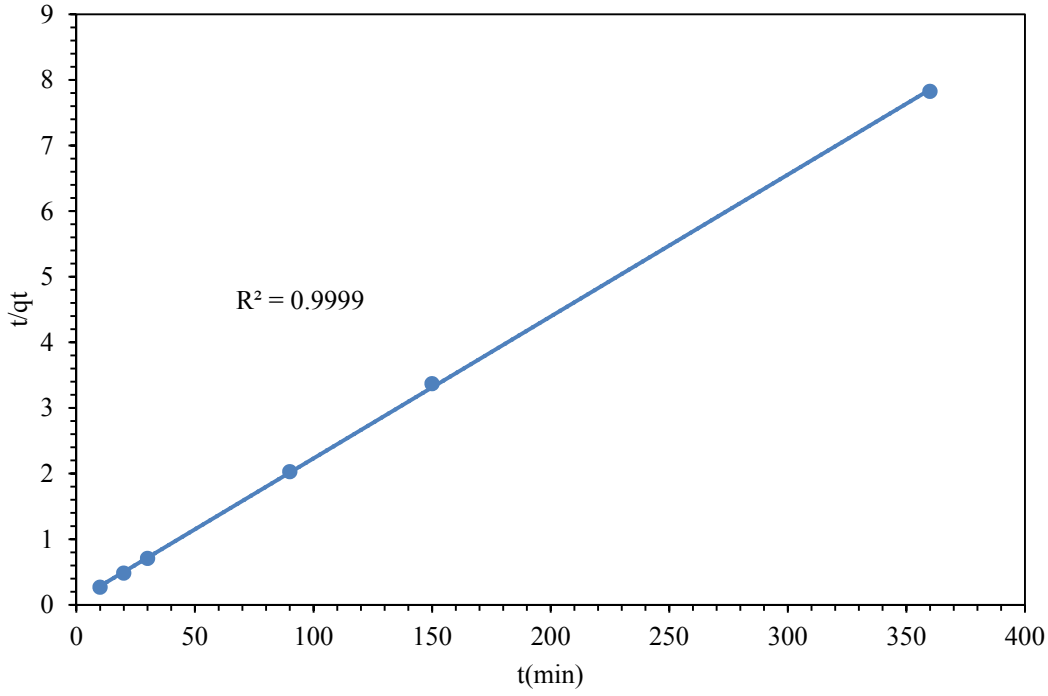

Fig. 21. Pseudo- second order kinetics model for X 5hr MCS

In terms of the second order rate equation, all obtained R^2 values are above 0.999 and calculated q_e values and experimental values given in Table 11 are nearly the same. The calculated adsorption capacities were found to be 45.7, 43.5, and 46.3 mg/kg for Mn_2O_3, New MCS, and X MCS, respectively. The adsorption phenomena for the three studied adsorbents, therefore, appear to follow a second order rate law; that is, the rate is proportional to the concentration of available surface sites raised to the second power. Numerous other adsorption kinetic studies have likewise shown that the removal of Cr (VI) from aqueous solution using various adsorbents including tyres, sawdust, amine-modified polyacrylamide-grafted coconut coir pith, calcined Mg–Al–CO 3 hydrotalcite, grape stalks wastes encapsulated in calcium alginate beads, and Aeromonas caviae also followed the pseudo-second order model [28,29,30,31,32].

Also, given in Table 11 are the rates of reactions, which were found to be 0.0067 kg/mg·min^{-1}, 0.0054 kg/mg·min^{-1}, and 0.0024 kg/mg·min^{-1} for X 5hr MCS, New 5hr MCS, and Mn_2O_3, respectively. It can be seen that X 5hr MCS showed the fastest kinetics and highest adsorption capacity of the three Mn sorbents studied suggesting that X 5 hr MCS surface possesses highest affinity to Cr (VI) ions. The better application of pseudo-second order model to the kinetic data also suggests that chemisorption is a possible alternative mechanism for adsorption, a two-step reaction mechanism occurs, and more than one rate-controlling step may exist [33]. However, the integration method may not be precise enough to determine reaction order because of uncertainty in measurement of small concentration changes and the complexity of the reactions [34].

Table 11. Pseudo-second order kinetic parameters.

	Mn_2O_3	NEW 5 hr MCS	X 5 hr MCS
Experimental q_e (mg/kg)	45.4	43.2	46
k_2 ($kg \cdot mg^{-1} \cdot min^{-1}$)	0.0024	0.0054	0.0067
q_e (mg/kg)	45.7	43.5	46.3
R^2	0.999	0.999	0.999

A similar adsorption kinetics behavior was observed for Mn nodule leached residue waste, montmorillonite clay, and iron coated sand [2,23,4]. The reported rate constants for these alternative sorbents shown in Table 12 are also comparable to those found in this study. From this table, it is observed that that only montmorillonite clay had a higher rate constant than MCS in the present work. It can also be noted that the rate constants for MCS are much higher than that found for iron coated sand.

Table 12. Comparison of pseudo-second order rate constants of various adsorbents for Cr (VI).

	k_2 ($kg/mg \cdot min^{-1}$)	q_e (mg/kg)	Reference
Mn nodule leached residue	0.00386	19.41	[2]
Montmorillonite clay	0.0092	2.8	[23]
Iron coated sand (IMCS)	0.001	36.1	[4]
Mn_2O_3	0.0024	45.66	Present study
New 5 hr MCS	0.0054	43.5	Present study
X 5hr MCS	0.0067	46.3	Present study

2.3.2.3. Intraparticle diffusion model

The intraparticle diffusion model gives a more comprehensive view of adsorption as a series of distinct steps and can be used to better understand the mechanism of Cr(VI) adsorption onto each sorbent and determine the rate limiting step in each adsorption process. More specifically, the three main steps that could occur in the process of Cr (VI) adsorption onto the Mn sorbents are:

1. Transport of adsorbate molecules from bulk solution to the external surface of the sorbent by diffusion through the boundary layer (film diffusion).

2. Diffusion of the adsorbate from the external surface into the pores of the adsorbent (pore diffusion)

3. Adsorption of the adsorbate on the active sites on the internal surface of the pores.

Typically, the adsorption reaction itself is very rapid and usually does not represent the rate-controlling step in the adsorption process [35]. Therefore, the diffusion steps are considered to most likely control the adsorption rate. It should be noted that, however, the mechanism of adsorption, particularly onto a heterogeneous sorbent may be far more complex.

To determine if intraparticle diffusion is the overall rate controlling step in the adsorption process the experimental data can be modeled based on by Fick's 2nd law (Eq. 14) [36]:

$$q_t = k_{id} t^{1/2} + c \qquad (14)$$

where q_t (mg/kg) is the adsorption capacities (mg/kg) at time t(min), k_{id} ($mg.kg^{-1}.min^{-1/2}$) is the rate constant of intraparticle diffusion, and C represents the boundary layer effect. The value of k_{id} and C can be determined from the slope and intercept in q_t versus $t^{1/2}$ plots. In this context, a greater C value signifies a greater boundary layer thickness and a greater degree of external mass transfer [37] whereas a C=0 would indicate that intraparticle diffusion is the sole rate controlling step in the adsorption process [38]. Multi-linearity in the plot would suggest that a more complex adsorption process occurs. The intraparticle diffusion model plots for Mn_2O_3, New MCS, and X MCS are presented in Fig. 22, 23, and 24, respectively.

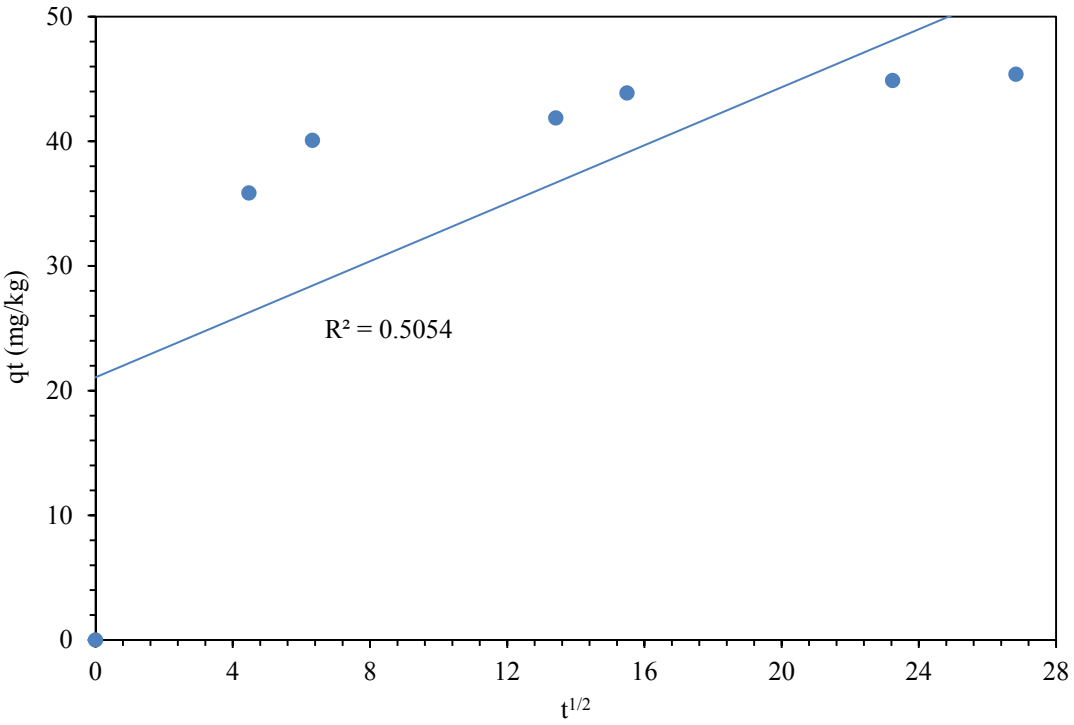

Fig. 22. Intraparticle diffusion model for Mn_2O_3.

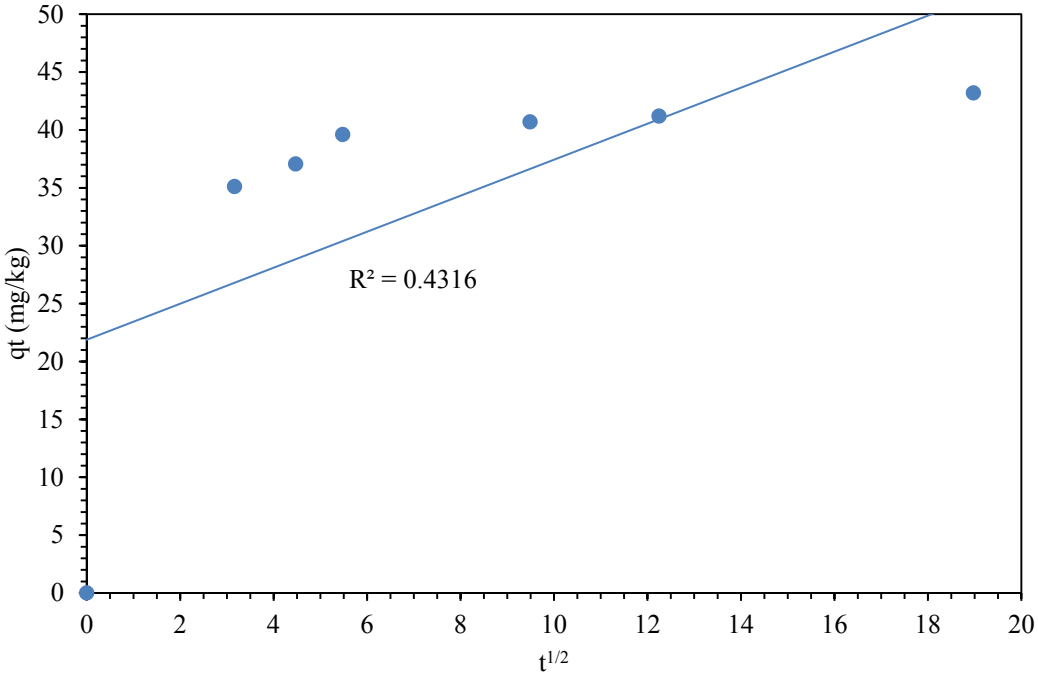

Fig. 23. Intraparticle diffusion model for New 5hr MCS.

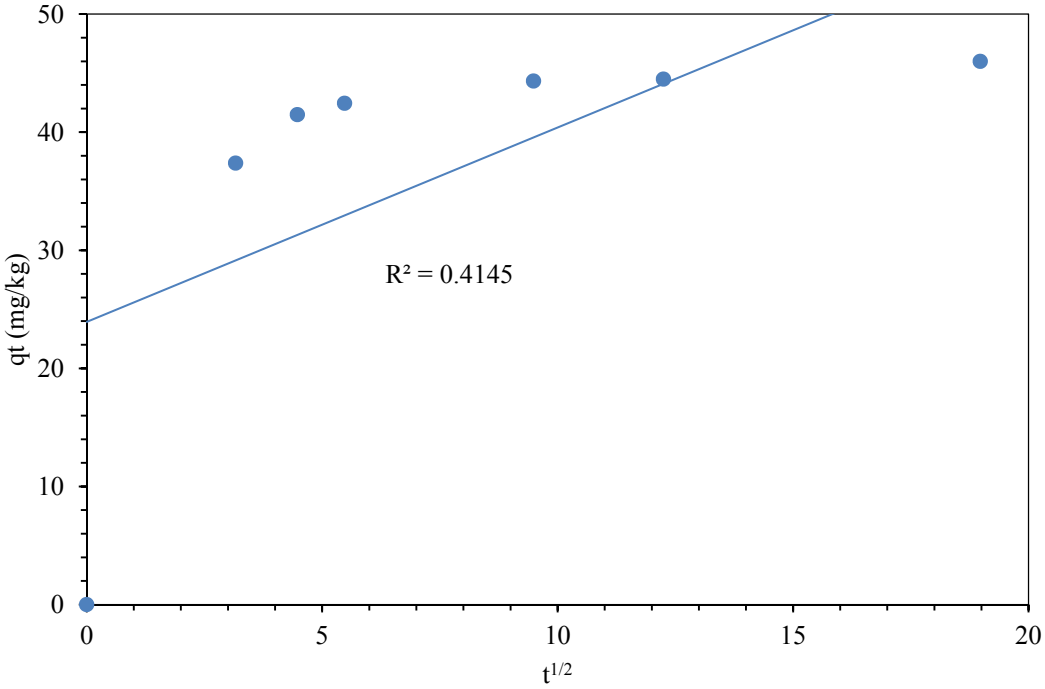

Fig. 24. Intraparticle diffusion model for X 5hr MCS.

The low R^2 values and the vastly different theoretical and experimental q_e values shown in Table 13 suggest that intraparticle diffusion does not occur in the process of Cr (VI) adsorption onto Mn_2O_3, New MCS, or X MCS. However, the plots can be divided into two distinct linear regions and then interpreted: the initially very steep slope would be indicative of rapid film diffusion (external mass transfer) including chemisorption and the second nearly horizontal segment that does not pass through the origin would indicate some degree of boundary layer effect and slow chemisorption due to fewer available sites and lower affinity rather than gradual intraparticle diffusion. These results instead support a two-step reaction governing the process of Cr (VI) adsorption onto the Mn sorbents and show that external mass transfer may be a rate controlling step. It was similarly found that the Cr (VI) adsorption rate on a fly ash-wollastonite mixture was governed first by diffusion and followed by surface complex formation [39].

Table 13. Intraparticle diffusion parameters.

	Mn_2O_3	**NEW 5 hr MCS**	**X 5 hr MCS**
Experimental q_e (mg/kg)	45.4	43.2	46
k_{id} (mg/kg/min0.5)	1.16	1.56	1.65
C	21.07	21.9	23.9
R^2	0.505	0.432	0.415

2.4. Conclusion

It was found that a Freundlich type adsorption reaction was favorable for Cr (VI) adsorption onto each studied Mn adsorbent with heterogeneity and affinity constants in the order of Mn_2O_3 □ New MCS □ X MCS and X MCS □ Mn_2O_3 □ New MCS, respectively. The adsorption data for Mn_2O_3 also conformed to a Langmuir type reaction since the crystalline and smooth surface allows close contact for stronger binding and monolayer formation whereas the irregular & multi-phase MCS surface results in weak binding and multi-layer adsorption. The highest heterogeneity and lower affinity results for Mn_2O_3 can then be explained by lateral interaction of adsorbed Cr (VI) at medium to high surface coverage, steric hindrance, or surface defects such as steps or corners, all of which may reduce the active surface area. Additionally, all three adsorbents displayed similar and low mean free energy indicative of predominating physical adsorption in the order of Mn_2O_3 □ X MCS □ New MCS. The Freundlich model also correlates with a physical adsorption process. Researchers have also reported that sorption characteristics on fly-ash, bentonite, sawdust, b-MnO2, & Mn leached nodule are suitably described by Freundlich with adsorption capacities comparable to those found in the current study.

The fast sorption kinetics of MCS and Mn_2O_3 for Cr (VI) removal were also favorable and best described by a simple pseudo-second order rate expression. The sorption rate was found to be in the order of X MCS □ New MCS □ Mn_2O_3. The much slower second-order constant and initial velocity for Mn_2O_3 in comparison to MCS supports a difference in the surface properties. It is likely that the rapid adsorption on MCS is physical and reversible whereas slow chemisorption is occurring on Mn_2O_3. The pseudo-second order rate constants for Mn oxides adsorbents are

similar to those reported for Mn nodule leached residue, montmorillonite, & iron-manganese coated sand. Also, a two-step mechanism is postulated for all three sorbents with either external mass transfer as rate-limiting step or chemisorption or both.

REFERENCES

[1] Post, Jeffrey E. "Manganese oxide minerals: Crystal structures and economic and environmental significance." *Proceedings of the National Academy of Sciences* 96, no. 7 (1999): 3447-3454. http://www.pnas.org/content/96/7/3447.full.pdf

[2] Mallick, Sujata, S. S. Dash, and K. M. Parida. "Adsorption of hexavalent chromium on manganese nodule leached residue obtained from NH_3–SO_2 leaching." *Journal of colloid and interface science* 297.2 (2006): 419-425.

[3] Bhutani, M. M., A. K. Mitra, and Ramesh Kumari. "Kinetic study of Cr (VI) sorption on MnO_2." *Journal of radioanalytical and nuclear chemistry* 157.1 (1992): 75-86.

[4] Chang, Yoon-Young, Jae-Woo Lim, and Jae-Kyu Yang. "Removal of As (V) and Cr (VI) in aqueous solution by sand media simultaneously coated with Fe and Mn oxides." *Journal of Industrial and Engineering Chemistry* 18.1 (2012): 188-192.

[5] Giles, Charles H., David Smith, and Alan Huitson. "A general treatment and classification of the solute adsorption isotherm. I. Theoretical." *Journal of Colloid and Interface Science* 47.3 (1974): 755-765.

[6] Osman, Khan Towhid. *Soils: principles, properties and management*. Springer Science & Business Media, 2012.

[7] Bradl, Heike B. "Adsorption of heavy metal ions on soils and soils constituents." *Journal of Colloid and Interface Science* 277.1 (2004): 1-18.

[8] Langmuir,I.,The constitution and fundamental properties of solids and liquids,I.Solids. , J.Am.Chem.Soc.38 (1916) 2221-2295.

[9] Goldberg, Sabine, Louise J. Criscenti, David R. Turner, James A. Davis, and Kirk J. Cantrell. "Adsorption–desorption processes in subsurface reactive transport modeling." *Vadose Zone Journal* 6, no. 3 (2007): 407-435.

[10] Weber, Walter J., Paul M. McGinley, and Lynn E. Katz. "Sorption phenomena in subsurface systems: concepts, models and effects on contaminant fate and transport." *Water Research* 25, no. 5 (1991): 499-528.

[11] Foo, [5.5] KY, and B. H. Hameed. "Insights into the modeling of adsorption isotherm systems." *Chemical Engineering Journal* 156.1 (2010): 2-10.

[12] Yang, Chung-hai. "Statistical mechanical study on the Freundlich isotherm equation." *Journal of Colloid and Interface science* 208.2 (1998): 379-387.

[13] I.A.W.Tan;A.L.Ahmad;B.H.Hameed. Adsorption isotherms, kinetics, thermodynamics and desorption studies of 2, 4, 6-trichlorophenol on oil palm empty fruit bunch-based activated carbon. J.Hazard.Mater. 164 (2009) 473–482.

[14] Udaybhaskar, P., Leela Iyengar, and A. V. S. Rao. "Hexavalent chromium interaction with chitosan." *Journal of Applied Polymer Science* 39.3 (1990): 739-747.

[15] Kobya, M. "Removal of Cr (VI) from aqueous solutions by adsorption onto hazelnut shell activated carbon: kinetic and equilibrium studies." *Bioresource technology* 91.3 (2004): 317-321.

[16] Sharma, D. C., and C. F. Forster. "Removal of hexavalent chromium using sphagnum moss peat." *Water Research* 27.7 (1993): 1201-1208.

[17] Ho, Y.S., Porter, J.F., McKay, G., Equilibrium isotherm studies for the sorption of divalent metal ions onto peat:copper,nickel and lead single component systems.,Water Air Soil Pollut. 141(2002), 1–33.

[18] Freundlich HMF. Uber die adsorption in losungen. Z Phys Chem. 57(A) (1906)385–470.

[19] C. Raji, T.S. Anirudhan, Batch Cr (VI) removal by polyacrylamide-grafted sawdust: Kinetics and thermodynamics ,Water Res. 32 (1998) 3772–3780.

[20] Khan, Saad Ali, and M. Ali Khan. "Adsorption of chromium (III), chromium (VI) and silver (I) on bentonite." *Waste Management* 15.4 (1995): 271-282.

[21] M.M. Dubinin, L.V. Radushkevich, Equation of the characteristic curve of activated charcoal, Chem. Zentr. 1 (1947) 875-889.

[22] Mahamudur Islam,Prakash Chandra Mishra,Rajkishore Patel, Fluoride adsorption from aqueous solution by a hybrid thorium phosphate composite,Chemical Engineering Journal .166 (2011) 978–985.

[23] Akar, Sibel Tunali, Yasemin Yetimoglu, and Tevfik Gedikbey. "Removal of chromium (VI) ions from aqueous solutions by using Turkish montmorillonite clay: effect of activation and modification." *Desalination* 244.1 (2009): 97-108.

[24] Ho,Y.S. and McKay, G.: Pseudo-second order model for sorption processes. Process Biochem, 34 (1999) 451–465.

[25] Lagergren, S., Zur theorie der sogenannten adsorption gelöster stoffe. Kungliga Svenska Vetenskapsakademiens. Handlingar, Band 24.4 (1898) 1-39.

[26] Ho, Yuh-Shan. "Review of second-order models for adsorption systems."*Journal of hazardous materials* 136.3 (2006): 681-689.

[27] G. Blanchard, M. Maunaye and G. Martin, Removal of heavy metals from waters by means of natural zeolites, Water Res.18 (1984) 1501-1507.

[28] Hamadi, Nadhem K., et al. "Adsorption kinetics for the removal of chromium (VI) from aqueous solution by adsorbents derived from used tyres and sawdust." *Chemical Engineering Journal* 84.2 (2001): 95-105.

[29] Unnithan, Maya R., V. P. Vinod, and T. S. Anirudhan. "Synthesis, characterization, and application as a chromium (VI) adsorbent of amine-modified polyacrylamide-grafted coconut coir pith." *Industrial & engineering chemistry research* 43.9 (2004): 2247-2255.

[30] Lazaridis, N. K., and D. D. Asouhidou. "Kinetics of sorptive removal of chromium (VI) from aqueous solutions by calcined Mg–Al–CO 3 hydrotalcite." *Water research* 37.12 (2003): 2875-2882.

[31] Fiol, Núria, Jordi Poch, and Isabel Villaescusa. "Chromium (VI) uptake by grape stalks wastes encapsulated in calcium alginate beads: equilibrium and kinetics studies." *Chemical Speciation & Bioavailability* 16.1-2 (2004): 25-33.

[32] Loukidou, Maria X., et al. "Equilibrium and kinetic modeling of chromium (VI) biosorption by Aeromonas caviae." *Colloids and Surfaces A: Physicochemical and Engineering Aspects* 242.1 (2004): 93-104.

[33] Sen, T.K., and Sarzali, M.V., Removal of cadmium metal ion (Cd^{2+}) from its aqueous solution by aluminum oxide (Al_2O_3): a kinetic and equilibrium study, Chem. Eng. J. 142 (2008), 256.

[34] Chang, R., "Physical Chemistry for the Biosciences." University Science Books. 2005.

[35] Singh,T.S and Pant,K.K.: Kinetics and Mass Transfer Studies on the Adsorption of Arsenic onto Activated Alumina and Iron Oxide Impregnated Activated Alumina.Water Qual. Res. J. Canada., 41:147,2006.

[36] M. Alkane, O. Demirbas, S. Celikcapa, M. Dogan, Sorption of acid red 57 from aqueous solution onto sepiolite, J. Hazard. Mater. B116 (2004) 135– 145.

[37] Z. Bekci, C. Ozveri, Y. Seki, K. Yurdakoc, Sorption of malachite green on chitosan bead, J. Hazard. Mater. 154 (2008) 254–261.

[38] Y.S. Ho, Removal of copper ions from aqueous solution by tree fern, Water Res. 37 (2003) 2323–2330.

[39] Panday KK, Prasad G, Singh VN. Removal of Cr(VI) from aqueous solution by adsorption on fly ash wollastonite. J Chem Techol Biotechnol A—Chemical Technology 1984; 34:367–74.

Chapter III

III. pH, CO-EXISTING IONS, ZETA POTENTIAL, AND REGENERATION STUDIES

3.1. Introduction

In the previous chapter, the adsorption capacities, favorability constants, and removal rates of Cr (VI) adsorption onto the three Mn oxide sorbents were determined under very specific conditions. In this chapter, the feasibility of using Mn oxide adsorbents for Cr (VI) removal under a variety of conditions has been explored and the optimal conditions for maximum Cr (VI) adsorption were determined. The effect of pH, sorbent surface charge, and presence of co-existing ions on the adsorption capacities were specifically investigated. The results of these studies were then used to gain insight on the adsorption mechanisms and provide recommendations to improve the Cr (VI) adsorption capacities and further develop the MCS adsorbent.

For a more comprehensive evaluation of the best Mn sorbent for Cr (VI) removal in the present work, the regeneration and reuse of adsorbents including recovery of the adsorbate material were also studied as these are important processes in wastewater treatment. The advantage of sorbent reuse with little or no loss in Cr (VI) adsorption capacity would be further reductions in cost while the recovery and recycling of chromium would also be economically beneficial for certain industries such as tanneries [1]. The reuse capacities and the regeneration efficiency for New MCS were therefore determined and compared to those reported for other alternative sorbents.

3.2. Materials and methods

3.2.1. Chemicals and reagents

All chemicals were of analytical reagent grade and no further purification was carried out. All solutions were prepared with de-ionized (DI) water made in the laboratory with a resistance greater than 18 MΩ. The manganese (III) oxide powder (Mn_2O_3, 98 % purity, density of 4.5 g/mL at 25 °C) with an average particle size less than 325 U.S. mesh (44 μm) was obtained from Alfa Aesar (Ward Hill, MA). The sand was coated using manganese (II) chloride tetrahydrate ($MnCl_2{\cdot}4H_2O$, 99% purity) and aluminum chloride hexahydrate ($AlCl_3{\cdot}6H_2O$, 99% purity) obtained from Acros. Potassium dichromate ($K_2Cr_2O_7$, ACS grade, crystals) was also obtained from Acros and used to prepare stock solutions of Cr (VI) in DI water. Hydrochloric acid (HCl, ACS plus grade) and sodium hydroxide (NaOH 10 N solution, 30% w/w certified) were to adjust solution pH. The calcium chloride ($CaCl_2$, 98.8% purity, ACS grade), sodium sulfate (Na_2SO_4, 99.3% purity, ACS grade) and sodium bicarbonate ($NaHCO_3$, 100% purity, ACS grade) obtained from Fisher scientific were used to prepare different co-existing ions solutions.

3.2.2. Manganese- aluminum-coated sand (MCS) sorbent preparation

First, the sand was washed and soaked in 0.1 M HCl solution for 3 hours, then rinsed with de-ionized water, and dried in an oven at 110 ºC. The coating solution was prepared next by mixing 50 mL solutions of 1 M $MnCl_2$ with 50 mL of 1 M $AlCl_3$ and slowly adjusting the mixture pH to approximately 6.5 using 6 N NaOH, which results in a slurry of manganese and aluminum hydroxide precipitates. The coating solution was then combined with 80 g of the washed sand in

a flask and mixed for 24 hours. This sand mixture was air dried for 12 hours, heated in an oven at 110 ºC for 4 hours, and finally introduced into a furnace at 550 ºC for 5 hours to complete coating metal oxides on sand.

3.2.3. Batch studies

The effects of pH, ionic strength and co-existing ions, and recycling and regeneration on the removal of Cr (VI) by the different manganese oxide sorbents were also studied by batch technique. For all batch experiments, 1 g of sorbent was mixed in High Density Polyethylene centrifuge tubes with 50 mL of the different Cr (VI) solutions. All samples were shaken at room temperature in a tumbler at 16 rpm for a period 24 hours, then centrifuged at 9,500 rpm, and lastly analyzed for Cr. The initial stock solution and solution pH after adsorption were also measured. The nuances of each experiment are described in sub-sections below.

3.2.4. pH experiments

The effect of solution pH on Cr (VI) removal from DI water was investigated over a broad range of solution pH. For the experiment, the pH of the 1 mg/L Cr (VI) stock solution was adjusted from 2 to 11 using 0.1 M HCl and 0.1 M NaOH solutions.

3.2.5. Co-existing ions experiments

To determine the effects of ionic strength and co-existing ions on Cr (VI) adsorption on the three different sorbents, the uptake of Cr (VI) from binary systems containing different concentrations of either calcium, sulfate, bicarbonate, or phosphate added to the 1 mg/L Cr (VI) DI solution was studied. The sources of calcium, sulfate, bicarbonate, and phosphate used were $CaCl_2$, Na_2SO_4, $NaHCO_3$, and Na_2PO_4, respectively. The studies were conducted at pH values ranging from 5.48 to 5.73 for the Ca^{2+} ion concentrations, 5.62 to 5.70 for the SO_4^{2-} concentrations, 7.57 to 8.78 for HCO_3^- ions, and 5.37 to 5.65 for PO_4^{3-} ion concentrations.

3.2.6. Zeta potential measurements

To determine the net effective charge on each adsorbent surface, the zeta potential of the different sorbent suspensions was measured by a Zeta-meter system 3.0 (Zeta meter Inc.; VA) at pH range of 2 to 12. The following suspensions were prepared with and without 1 mg/L of Cr (VI) in 1 mM NaCl solutions: 0.2 g/L of Mn_2O_3, 5 g/L of New 5hr MCS, and 5 g/L X 5hr MCS. A high concentration of MCS sorbents were applied due to the settling problems of MCS particles and the Zeta-meter cell limitation. The pH of each sample was adjusted using 0.1 M HCl and 0.1 M NaOH solutions.

3.2.7. Sorbent recycling experiments

To evaluate the reuse of the different Mn sorbents, the adsorption experiments were carried out in three consecutive adsorption cycles. For the subsequent adsorption cycles, the 1 g mass of the used sorbent in the previous adsorption cycle was again exposed to a fresh batch of Cr (VI) solution. The experiments were performed in triplicates and the averages of the results for each adsorption cycle are presented.

3.2.8. MCS regeneration experiment

The regeneration of New 5hr MCS (20 g/L) in 0.001, 0.01, and 0.1 N NaOH was studied at initial Cr (VI) concentrations of 1, 3, and 5 mg/L. In this experiment, one adsorption cycle proceeds and follows the regeneration cycle for a total of three cycles. For the regeneration cycle, the Cr (VI)-loaded sorbent was first gently washed with DI water to remove any Cr (VI) ions that were not adsorbed, then mixed with 50 ml of aqueous NaOH solution, shaken at room temperature in a tumbler at 16 rpm for 24 hours, and finally the solids were separated for reuse. The regeneration efficiency was determined using the following equation:

$$Regeneration\ efficiency\ (RE\%) = \left(\frac{A_r}{A_o}\right) \times 100 \qquad (1)$$

where the A□ is the mass of chromium ions adsorbed from solution per unit mass of sorbent (assuming that exhaustion had occurred) and A□ is the mass of chromium ions adsorbed from solution per unit mass of regenerated sorbent (assuming that exhaustion had occurred).

3.2.9. Analytical methods

The chromium concentration in aqueous solution was determined by flame atomic absorption spectroscopy. The analysis for chromium was carried out using a Hollow Cathode Lamp (HCL) at wavelength 357.9 nm and silt setting 0.7 nm with a lean blue air-acetylene flame at about 2300 °C. An air flow of 17.0 L/min and acetylene flow of 2.5 L/min was used. The lower limit of quantitation for Cr analysis is 0.05 mg/L. The uptake of Cr (VI) on each sorbent was then calculated using the following equation:

$$q = \frac{(C_0 - C_e)}{m} \times A \qquad (2)$$

where C_0 and C_e are the initial and equilibrium concentration of Cr (VI) in the solution(mg/L), q is the adsorbed Cr (VI) (mg/kg), m is the adsorbent dosage (kg) and A is the solution volume (L). The removal percent (%) was calculated using the following equation:

$$\mathrm{Re}moval(\%) = \frac{(C_0 - C_e)}{C_0} \times 100 \qquad (3)$$

3.3. Results and discussion

3.3.1. Effect of pH on adsorption of Cr (VI)

The pH dependence of Cr (VI) adsorption has been indicated for several sorbents [2,3,4]. In one case, the solution pH effects adsorption if the stability of product is Cr (VI) species dependent as the stability of speciation is pH dependent; the corresponding stability of Cr (VI) species to pH values are: H_2CrO_4 below pH 0.9, $HCrO_4^-$ from pH 0.9 to 6.4, and CrO_4^{2-} above pH 6.4 [5]. Also for the Cr (VI) concentration studied, the suggested $HCrO_4^-$ species abundance between pH

6.0 to 5.0 is 75 to 96% and the suggested CrO_4^{2-} species abundance between pH 7.0 to 8.0 is 76 to 97% [6]. Hence, higher adsorption under acidic conditions would indicate that the $HCrO_4^-$ is the more favorable species, which has been found for many adsorbents [7]. Figures 1, 2, and 3 respectively show the Cr (VI) uptake by Mn_2O_3, New 5 hr MCS, and X 5 hr MCS as a function of pH to determine effect of pH on the Cr (VI) adsorption capacities and optimum pH for each adsorption system.

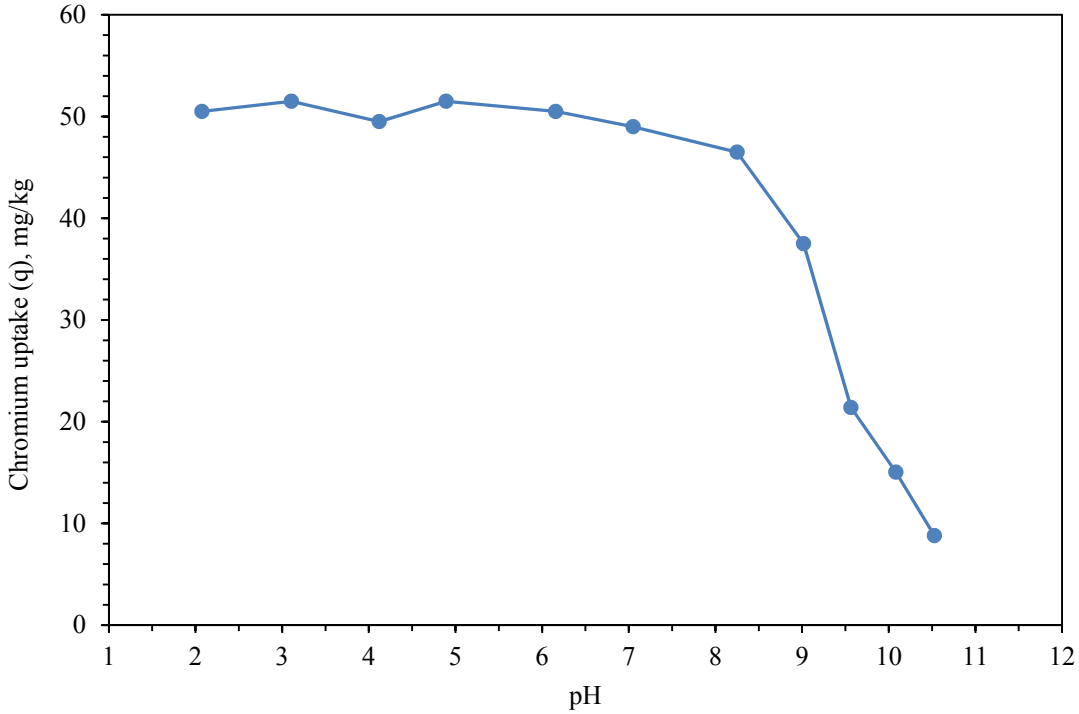

Fig. 1. Effect of pH on adsorption of Cr (VI) onto Mn_2O_3 (20 g/L sorbent dosage) from a 1 mg/L solution.

In the above figure, Mn_2O_3 most effectively adsorbed Cr (VI) in the pH interval of 2.0 to 6.0 with nearly 83 to 86 % Cr (VI) removal and a maximum adsorbed Cr (VI) of 51.5 mg/g achieved at pH 3.0 and 5.0. The adsorption of Cr (VI) onto Mn_2O_3 decreased only slightly in the pH range

of 6.0 to 8.0, while decreasing sharply at solution pH greater than 8.0. Cr (VI) removal was only 60% at pH 9 and only 14% at pH 10.5. Also, the significant Cr (VI) uptake at solution pH as high as 8.0 indicates that both $HCrO_4^-$ and CrO_4^{2-} species are adsorbed and that Cr (VI) speciation has no influence on adsorption. The adsorption reaction condition becomes unfavorable at pH above 8.0 instead because of increased OH^- competition. Namasivayam et al. found a similar trend for the Cr (VI) adsorption onto waste Fe (III)/Cr (III) hydroxide where a decrease in Cr (VI) uptake had been observed with the gradual increase in pH of the system because of deprotonation [2].

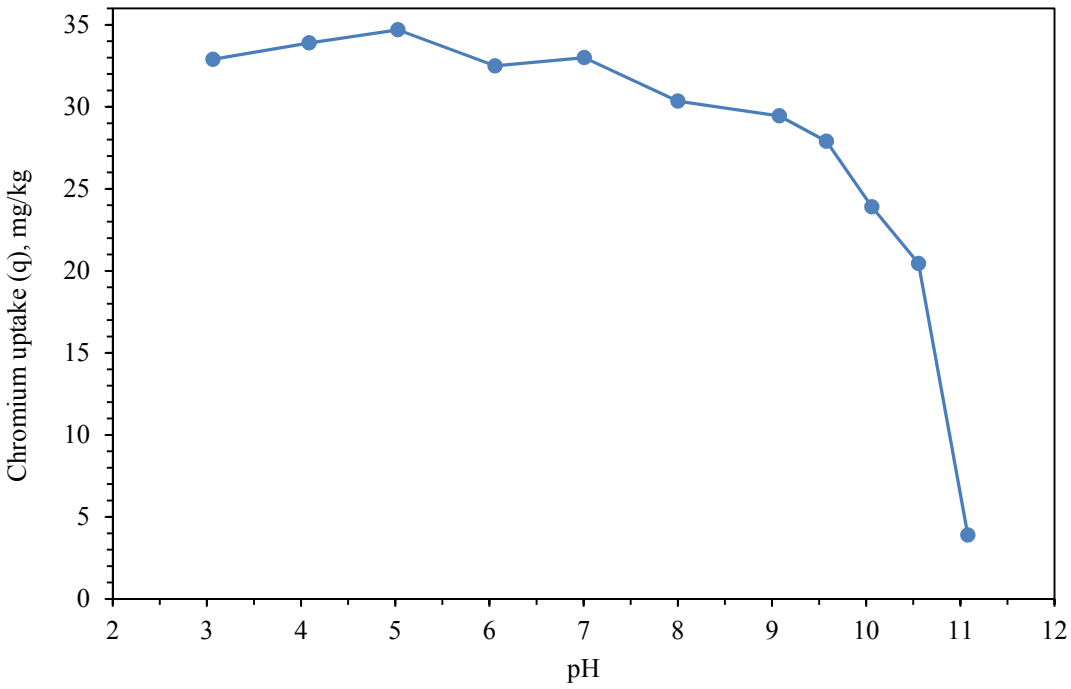

Fig. 2. Effect of pH on adsorption of Cr (VI) onto NEW 5 hr MCS (20 g/L sorbent dosage) from a 1 mg/L solution.

New 5 hr MCS was observed to most effectively adsorb Cr (VI) in the pH interval of 3.0 to 7.0 with approximately 62 to 66 % Cr (VI) removal and a maximum adsorbed Cr (VI) of 34.7 mg/g at pH 5.0. The adsorption of Cr (VI) onto New 5 hr MCS decreased slightly in the pH range of 7.0 to 9.5 and sharply decreased thereafter. Cr (VI) removal reduced to 45% at pH 10.0 and only 7% at pH 11.0. The behavior of Cr (VI) adsorption onto New 5 hr MCS was like Mn_2O_3 in that adsorption generally decreased with increasing pH and differed in that New 5 hr MCS displayed weaker adsorption yet had a wider pH range. The weaker adsorption may be attributed to the higher adsorption on lower affinity sites of aluminum. A similar type of behavior is also reported for the adsorption of Cr (VI) anions on activated red mud and fly ash [3,4].

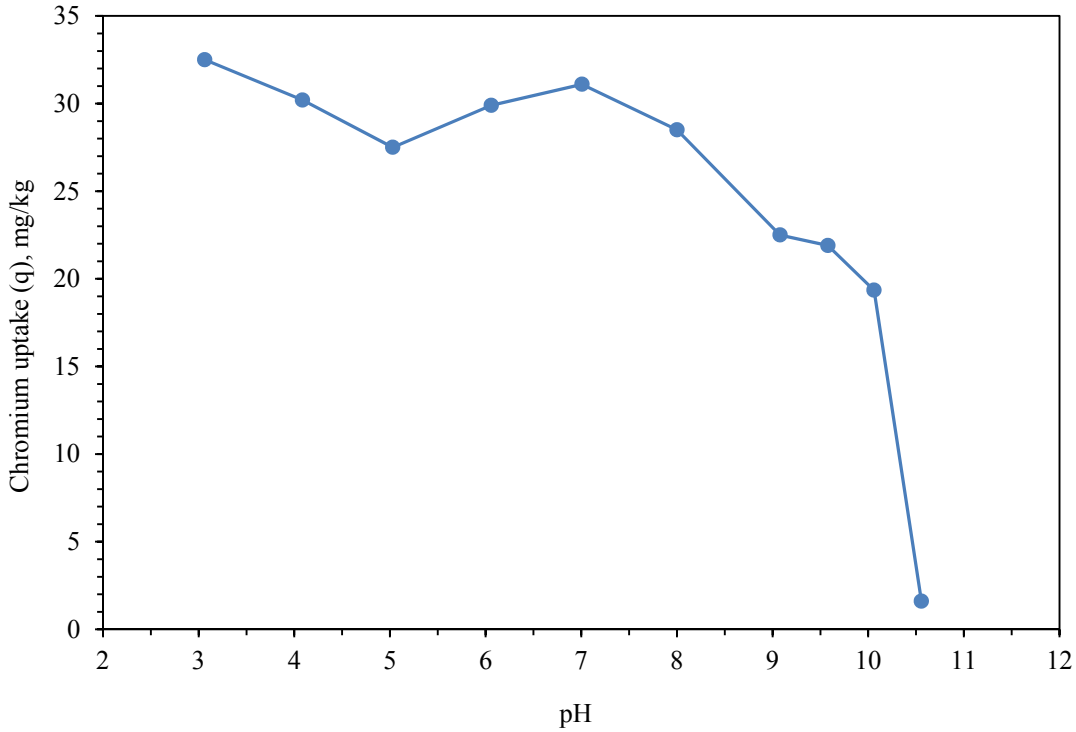

Fig. 3. Effect of pH on adsorption of Cr (VI) onto X 5 hr MCS (20 g/L sorbent dosage) from a 1 mg/L solution.

The effect of pH on adsorption of Cr (VI) onto X 5 hr MCS observed in Figure 3 was very like that of New MCS with Cr (VI) adsorbed most effectively in the pH interval of 3.0–7.0 (excluding pH 5.0) with about 59-64 % Cr (VI) removal and a maximum adsorbed Cr (VI) of 32.5 mg/g at an optimum pH of 3.0. The Cr (VI) removal by X MCS was only slightly lower than New MCS and can be explained by the slightly lower Al content or less aging. The similar capacities of MCS indicate that the adsorption mechanism is the same and that a small variation in adsorbent Mn and Al content will not significantly change the Cr (VI) adsorption capacity. However, there was a decline observed in adsorption capacity between pH 5.0 to 7.0 that differed from Mn_2O_3 and New 5hr MCS. The adsorption capacity then increased back to a high value at pH 7.0 to nearly equal to the maximum obtained at pH 3.0. The kink in the curve may be attributed to Si or Al impurities on X MCS [8]. Again, similarly to New MCS, Cr (VI) adsorption onto X 5hr MCS decreased continually from pH 7.0 to 11.0 and then sharply from pH 10.0 to 10.5 with 38 to 3% Cr (VI) removal illustrating the applicability in a wide pH range.

To better understand the adsorption mechanism, the equilibrium pH was also measured and are presented in Tables 1, 2, and 3 with the initial solution pH. From these tables, the equilibrium pH increased under acidic conditions and decreased at initial solution pH values above 7.0 suggesting that adsorption mechanism may differ by pH range. The increase in equilibrium pH is likely due to ligand exchange while the decrease in equilibrium pH is associated with competitive OH^- adsorption. A second observation was that within a certain initial pH range, the equilibrium pH values were stable and adsorption capacities were different. The equilibrium pH values for Mn_2O_3 were also lower than MCS with higher capacities indicating more stable adsorption.

Table 1. Initial and final pH readings from pH study Mn_2O_3.

Initial pH	Final pH
2.075	2.757
3.106	4.249
4.121	5.292
4.892	5.574
6.157	5.615
7.05	5.681
8.25	5.813
9.017	6.734
9.564	7.132
10.082	7.195
10.527	8.583

Table 2. Initial and final pH readings from pH study for NEW 5 hr MCS.

Initial pH	Final pH
3.064	4.672
4.086	6.313
5.029	6.393
6.06	6.515
7.007	6.415
8.001	6.258
9.078	6.542
9.578	6.672
10.061	6.761
11.079	9.513

Table 3. Initial and final pH reading from pH study for X 5 hr MCS.

Initial pH	Final pH
3.064	5.002
4.086	6.595
5.029	6.564
6.06	6.581
7.007	6.668
8.001	6.612
9.078	6.597
9.578	6.735
10.061	6.964
10.556	7.725
11.079	9.332

In summary, all three adsorbents show a similar effective pH range of adsorption that is wider than those reported for other adsorbents. The results also follow typical anion adsorption since Cr (VI) removal was found to generally decrease with increasing pH. Mn_2O_3 showed by far the highest adsorption capacities between pH 2 and 9 while New 5hr MCS showed the highest adsorption capacities at pH 9.5, 10, and 10.5. Lastly, some variation of Mn and Al content and sorbent aging did not significantly affect the adsorption capacity of MCS.

In the second case, the solution pH determines the surface charge of the sorbent as the charge develops from the protonation and deprotonation of the oxide surface. The sorbent surfaces are reported to be positively charged at a solution pH value below its point zero charge (PZC) and

negatively charged at solution pH above its PZC. A surface that is positively charged would favor anion adsorption because of electrostatic attraction. Thus, the drastic decrease in adsorption of Cr (VI) shown in the figures above may be attributed to the rapid deprotonation of the sites at the pH above sorbent PZC and the resulting electrostatic repulsion between the Cr (VI) anions and the negatively charged sorbent. For solution pH at the PZC, both cations and anions may adsorb onto the surface through the formation of outer-sphere complexes via van der Waals forces. The next section therefore discusses sorbent point of zero charge and surface charge.

3.3.2. Sorbent surface charge and pH

To understand the interactions at solid/solution interfaces, the sorbent point of zero surface charge was determined from measured zeta potential values of sorbent against pH values of sorbent suspensions. Figures 4 to 12 show the zeta potentials (ZP) plotted against the pH values of sorbent suspensions in DI water and 1 mM NaCl with and without 1 mg/L Cr (VI). The point of zero charge (PZC or pH_{pzc}), for Mn_2O_3 was determined as 6.56 (Figure 4). The PZC for New 5hr MCS and X 5hr MCS were determined as 9.72 and 10, respectively (Figures 5 and 6). The higher PZC values for MCS can be attributed to the aluminum content.

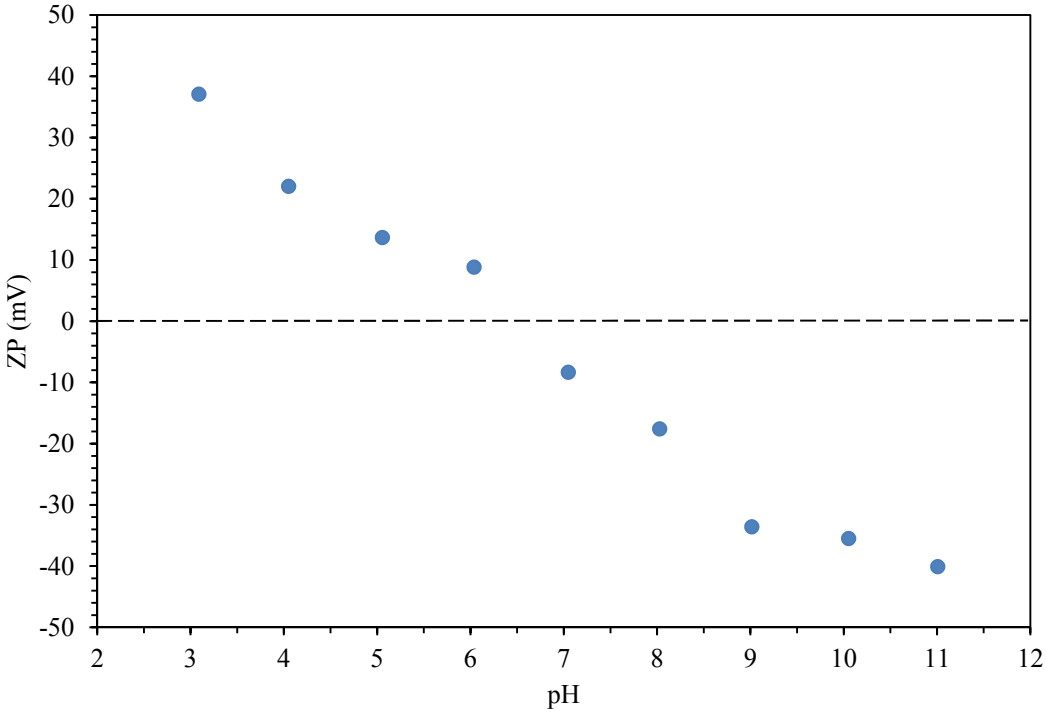

Fig. 4. ZP of 0.2 g/L Mn_2O_3 as a function of pH in DI water and 1 mM NaCl.

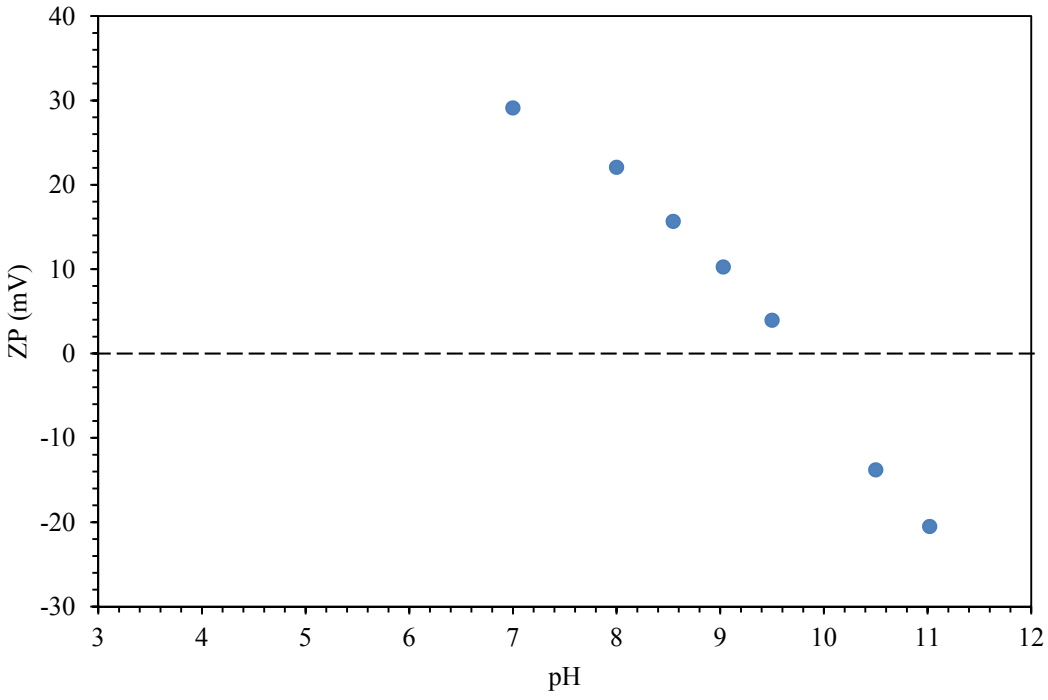

Fig. 5. ZP of 5 g/L NEW 5 hr MCS as a function of pH in DI water and 1 mM NaCl.

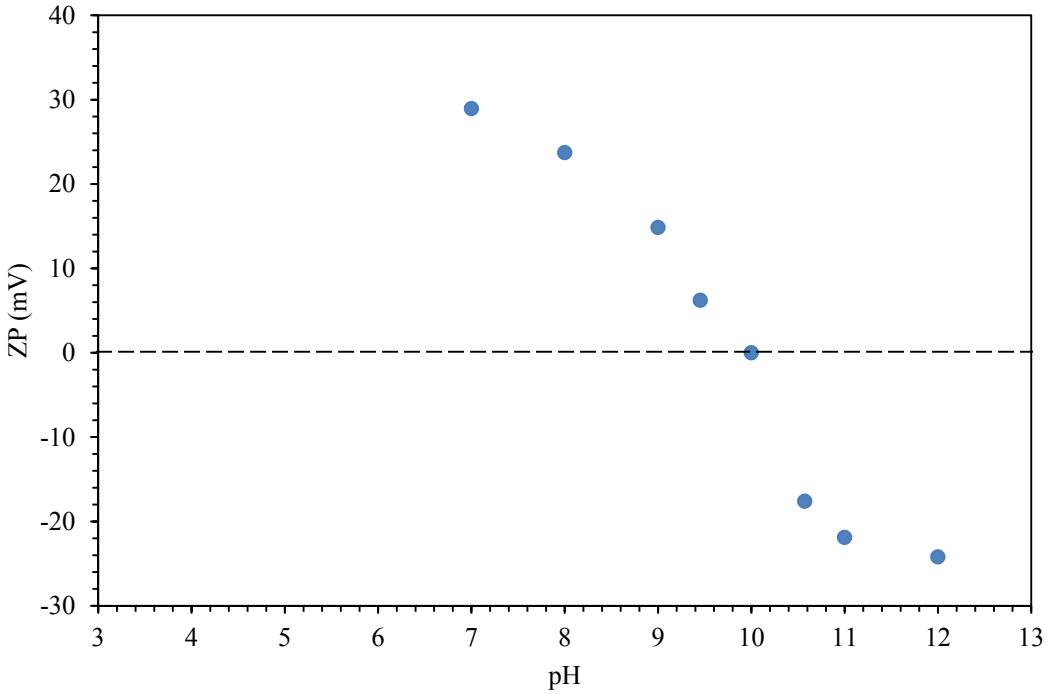

Fig. 6. ZP of 5 g/L X 5 hr MCS as a function of pH in DI water and 1 mM NaCl.

The figures above also show that the high PZC MCS sorbents remain positively charged under basic conditions as high as pH 10.0 whereas the Mn_2O_3 surface is negatively charged. This explains the wider pH range for Cr (VI) adsorption found for the MCS sorbents in the pH study. New and X 5hr MCS show a drastic decrease in the adsorption of Cr (VI) anions at pH > PZC in Figures 1, 2, and 3, respectively. This indicates that the extent of adsorption is dependent on the electrostatic attraction between the negatively charged Cr (VI) anions and the sorbent surface to form an outer sphere complex. In this case, adsorbate and surface interactions would be limited by the electron orbital symmetries and the sorbent PZC after Cr (VI) should not change. In addition, the decrease in the uptake of Cr (VI) on sorbents at higher pH could be due to an increase in competing hydroxyl ions (OH^-) for adsorption sites with increasing pH which can cause a reduction in adsorption [1, 9,10,11].

Specific inner-sphere anion adsorption can decrease the PZC and reverse electrophoretic mobility with increasing anion concentration [12]. An inner-sphere complex allows the necessary orbital overlap for a chemical reaction between the adsorbate and the surface to change the surface charge of the sorbent [13]. Shifts in the PZC of oxide minerals have been observed with the adsorption of the following anions: phosphate [14], arsenate [15,16,17], arsenite [18], chromate [19], carbonate [20], selenite [21], selenate, molybdate [22,23], and borate [24,25]. This phenomenon or change in PZC was also observed in the present study at varying degrees for Mn_2O_3 and MCS.

Figures 7 and 8, show that the surface charge of Mn_2O_3 was substantially altered in Cr (VI) solution and proves the adsorption of Cr (VI) onto the surface of Mn_2O_3. The influence of Cr (VI) was noticed to decrease the PZC of the sorbent to 3.61, decrease the zeta-potential values to negative values (charge reversal), and positive values were only observed between pH 2.095 to 3.61. Also, the anionic $HCrO_4^-$ and CrO_4^{2-} species are the predominant Cr (VI) species in the pH range 2.0–7, which can contribute negative charge on the surface of the sorbent. Hence, the shift in the PZC value to acidic side can be attributed to the formation of negatively charged inner-sphere complexes by specific adsorption of $HCrO_4^-$ and CrO_4^{2-} anions onto Mn_2O_3 [26,27]. Furthermore, a significant amount of Cr (VI) adsorption can be observed in Figure 1 at pH > PZC (6.56), which also suggests that the formation of an inner-sphere complex as the major mechanism for Cr (VI) adsorption at pH values above the PZC [10].

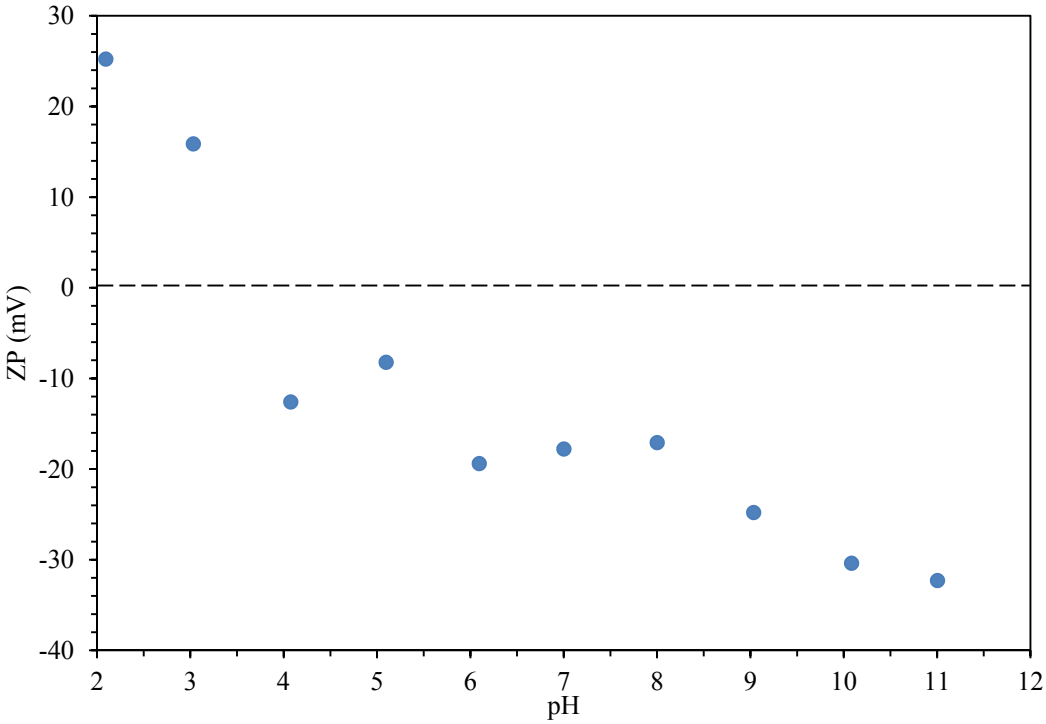

Fig. 7. ZP of 0.2 g/L Mn_2O_3 as a function of pH in 1 mg/L Cr (VI) and 1 mM NaCl.

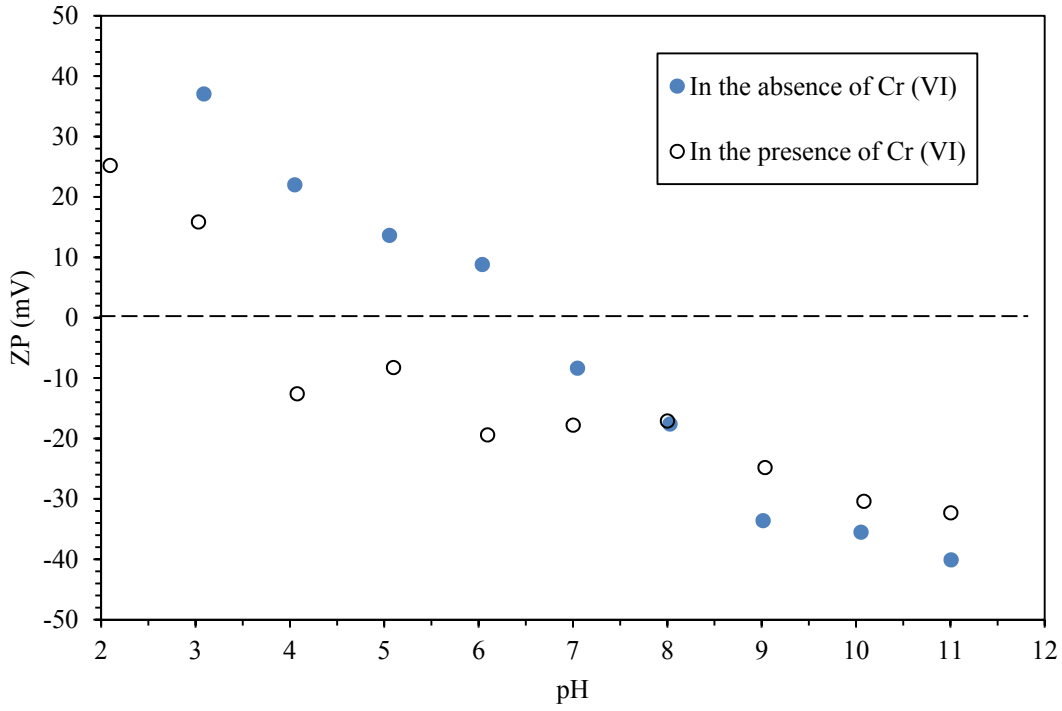

Fig. 8. ZP of 0.2 g/L Mn_2O_3 as a function of pH in the absence and presence of 1 mg/L Cr (VI).

In Figures 9 to 12, the presence of $HCrO_4^-$ and CrO_4^{2-} anions are noticed to only slightly decrease the PZC of New and X 5hr MCS to 9.42 and 9.17, respectively. Also, there was no reversal in surface charge with Cr (VI) adsorption as there was with Mn_2O_3; there was only a slight decrease in zeta potential. This difference can also be explained the different surface topography, where a monolayer coverage on Mn_2O_3 would disperse the negative charge whereas cluster formation would not. Based on these results, the formation of outer sphere complex again may be more predominant during Cr (VI) adsorption on New and X 5hr MCS. In comparison, the CrO_4^{2-} ions were reported to form monodentate surface complexes and surface nucleated Cr oxyhydroxides on silica [28], inner-sphere surface complexes on hydrous ferric oxide [29], and monodentate surface at low surface coverage and bidentate at high surface coverage on goethite [30].

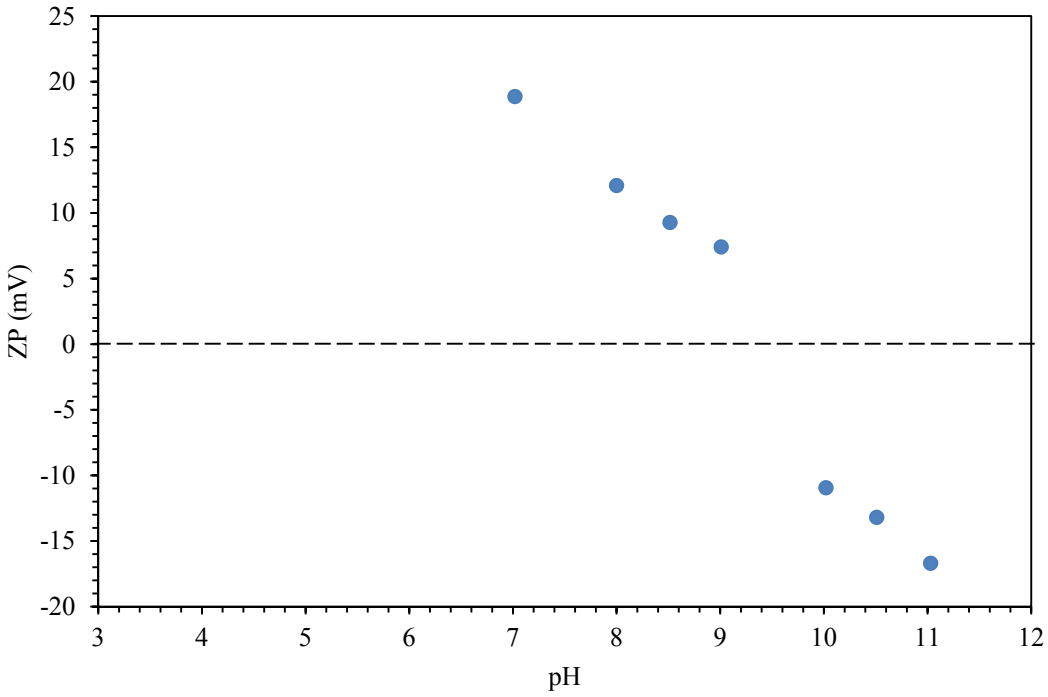

Fig. 9. ZP of 5 g/L NEW 5 hr MCS as a function of pH in 1 mg/L Cr (VI) and 1 mM NaCl.

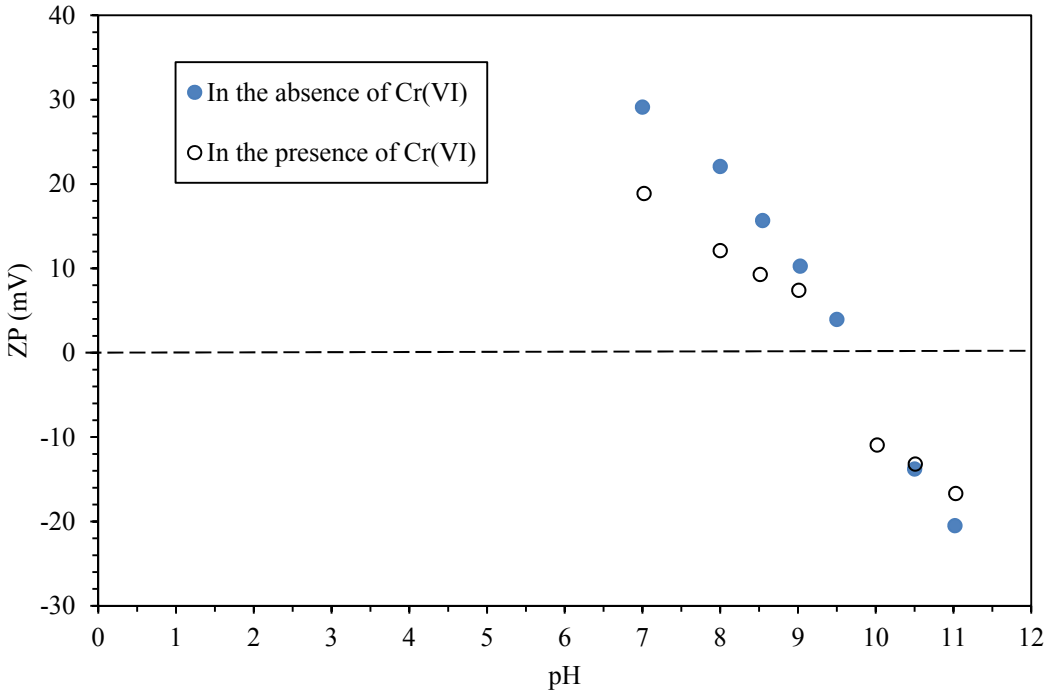

Fig. 10. ZP of 5 g/L NEW 5 hr MCS as a function of pH in the absence and presence of 1 mg/L Cr (VI).

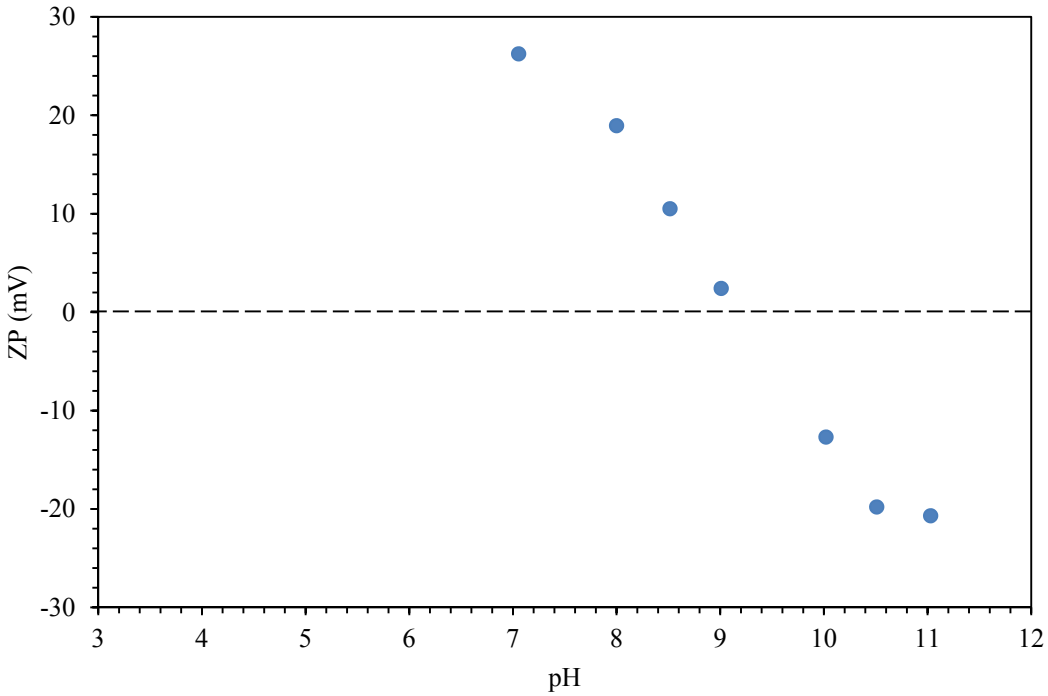

Fig. 11. ZP of 5 g/L X 5 hr MCS as a function of pH in 1 mg/L Cr (VI) and 1 mM NaCl.

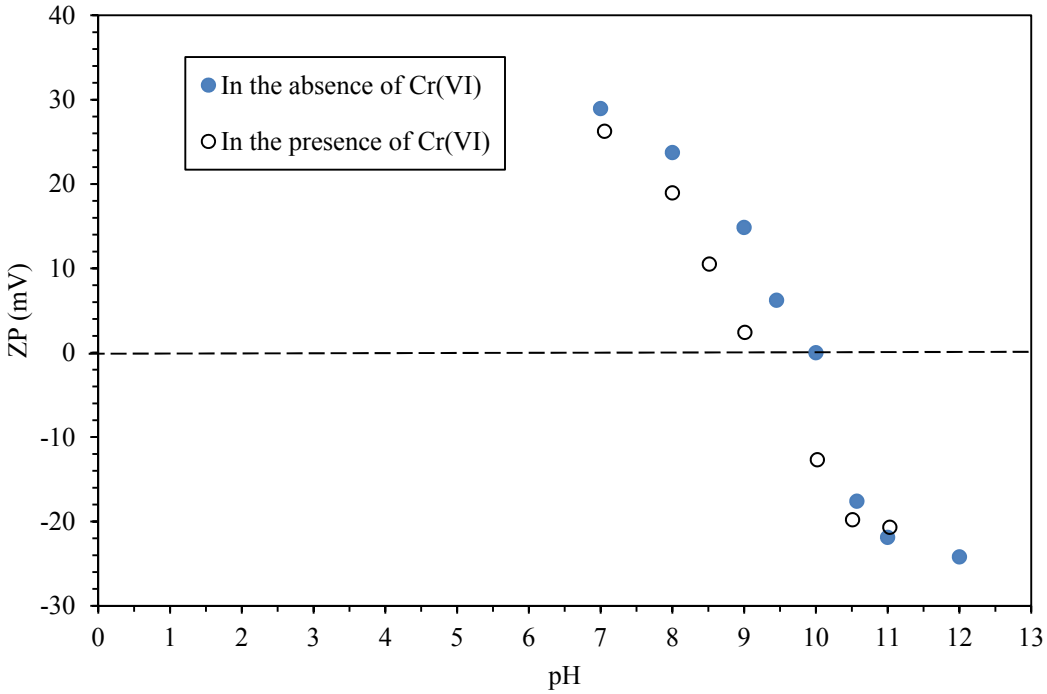

Fig. 12. ZP of 5 g/L X 5 hr MCS as a function of pH in the absence and presence of 1 mg/L Cr (VI).

Due to the nature of the Cr (VI) solution in DI water, which is not a buffered solution, the final pH of the solution after adsorption could change considerably during the experiments. Adding the sorbent to the solution is expected to shift the pH towards the point of zero charge; for pH > PZC, the pH shifts to the lower end and for pH < PZC, the pH shifts to the higher end. For the Mn_2O_3 study, the measurements of final pH of the solutions with different initial pH given in Table 1 confirmed this claim. This trend, however, was not followed in pH range 7.0 to 9.5 for New and X 5hr MCS sorbent studies, which may be explained by the competitive adsorption of OH^- ions above pH 7.0 (Tables 1, 2, and 3).

The measured specific conductance values of the samples are reported in Tables 4 to 6. It can be observed that the highest values of specific conductance were obtained at low and high pH values. Also, the specific conductance values were highest for X 5hr MCS followed by New 5hr MCS.

Table 4. Zeta potential conductance readings for Mn_2O_3.

pH	Conductance (us/cm)	
	In absence of Cr (VI)	**In presence of Cr (VI)**
3	405	1107
4	162	118
5	125.7	159.2
6	129	68
7	121.3	130
8	128.8	128.4
9	127	124.7
10	142.9	49.7
11	380	934

Table 5. Zeta potential conductance readings for NEW 5 hr MCS.

pH	Conductance (us/cm)	
	In absence of Cr (VI)	In presence of Cr (VI)
7	977	934
8	981	939
8.5	999	951
9	994	950
9.5	1007	965
10.0	1032	993
10.5	1084	1050
11	1224	1213

Table 6. Zeta potential conductance readings for X 5 hr MCS.

pH	Conductance (us/cm)	
	In absence of Cr (VI)	In presence of Cr (VI)
7	1185	1092
8	1141	1070
9	1166	1083
9.5	1189	1090
10	1164	1122
11	1429	1421
12	32700	31500

3.3.3. Effect of coexisting ions on adsorption of Cr (VI)

The presence of other ions, such as calcium, sulfate, bicarbonate, and phosphate, which are usually present in natural water may affect the Cr (VI) removal efficiency of the adsorbents as the co-adsorption of these ions implies competition for the available surface sites and a change in surface charge. The effect of these ions was therefore investigated at concentrations ranging from 0.5 mM to 2 mM for Ca^{2+} and SO_4^{2-}, from 0.5 mM to 5.5 mM for HCO_3^-, and from 0.05 mM to 0.5 mM for PO_4^{3-}. An initial Cr (VI) concentration of 1 mg/L was used in all solutions with a sorbent dosage of 20 g/L. The effect of Ca^{2+} ions on Cr (VI) adsorption is shown in Figures 13, 14, and 15 for sorbents Mn_2O_3, New 5hr MCS, and X 5hr MCS, respectively.

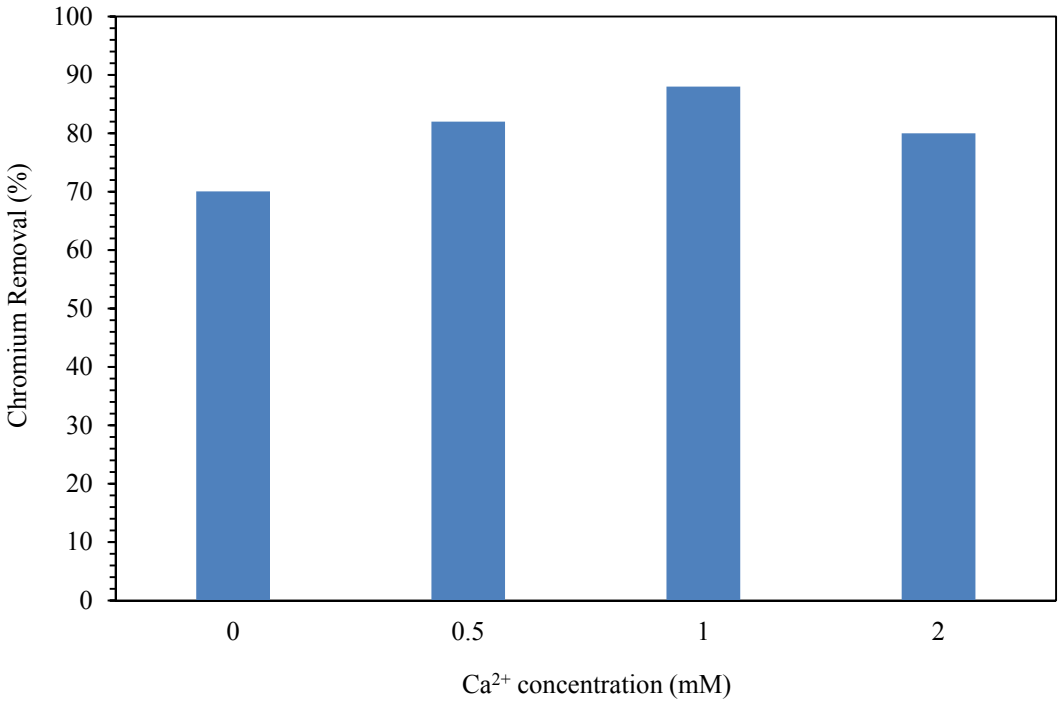

Fig. 13. Effect of Ca^{2+} ions on the adsorption of Cr (VI) onto Mn_2O_3.

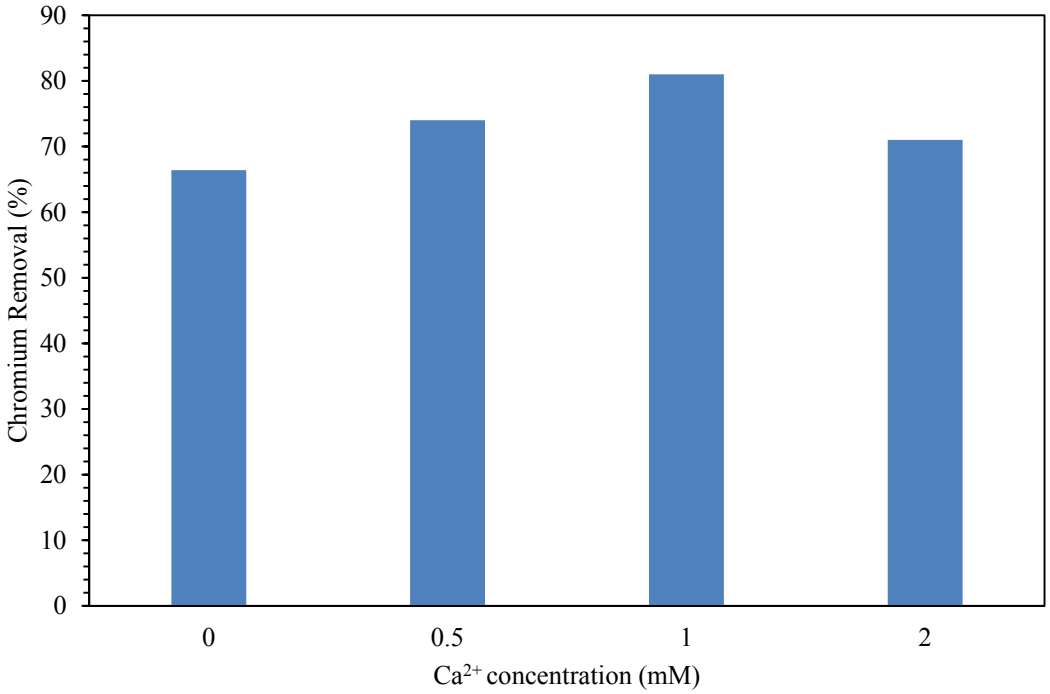

Fig. 14. Effect of Ca^{2+} ions on the adsorption of Cr (VI) onto NEW 5 hr MCS.

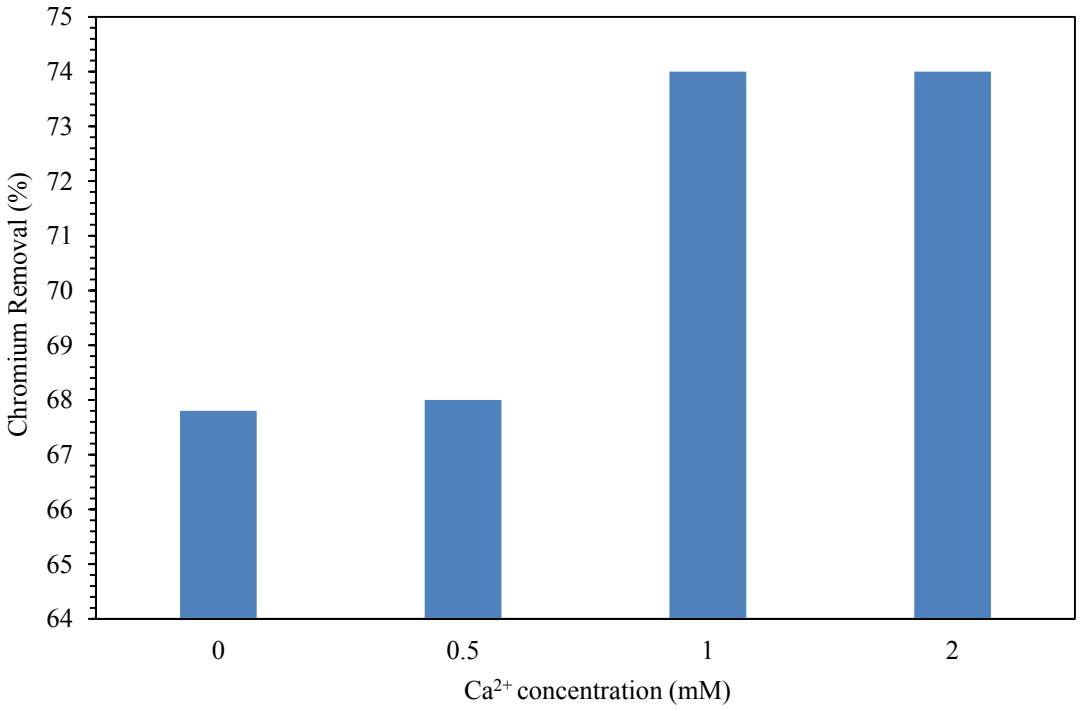

Fig. 15. Effect of Ca^{2+} ions on the adsorption of Cr (VI) onto X 5 hr MCS.

The figures above show that Cr (VI) adsorption was enhanced in the presence of Ca^{2+} and was optimum at the 1 mM Ca^{2+} concentrations. In the case of Mn_2O_3, the Cr (VI) removal was 88% at 1 mM Ca^{2+} whereas 80% at 2 mM The New 5 hr MCS sorbent displayed the same trend with 81% Cr (VI) removal at 1 mM Ca^{2+} and 71% Cr (VI) removal at 2 mM Ca^{2+}. For X 5hr MCS, the Cr (VI) removal was 74% at 1 mM Ca^{2+} and at 2 mM Ca^{2+}. The millimolar concentrations of other major cations have been reported to have a similar influence on Cr (VI) adsorption. The favorable electrostatic adsorption of anions can be attributed to the sorption of cations enhancing the positive sorbent surface charge [4]. Also, the metal hydroxides partially formed below the sorbent point of surface zero charge may increase anion exchangeable sites [31]. In one study, the adsorption of Cr (VI) on iron (III) hydroxide had similarly increased in the presence of cations Cu^{2+} and Zn^{2+} with increasing concentration of these cations [31].

The SO_4^{2-}, HCO_3^-, and PO_4^{3-}anions, on the other hand, had a significant negative effect on Cr (VI) adsorption that can be explained by the competition between these anions and the Cr (VI) anions for the limited available adsorption sites on the sorbent surfaces. The competing effect varies, depending on anion affinities for the solid surface and on the concentrations of surface sites, competing anions, and Cr (VI) anions [4]. The co-presence of SO_4^{2-} was found to moderately interfere with Cr (VI) adsorption on Mn_2O_3, New 5hr MCS, and X 5hr MCS as shown in Figures 16, 17, and 18, respectively.

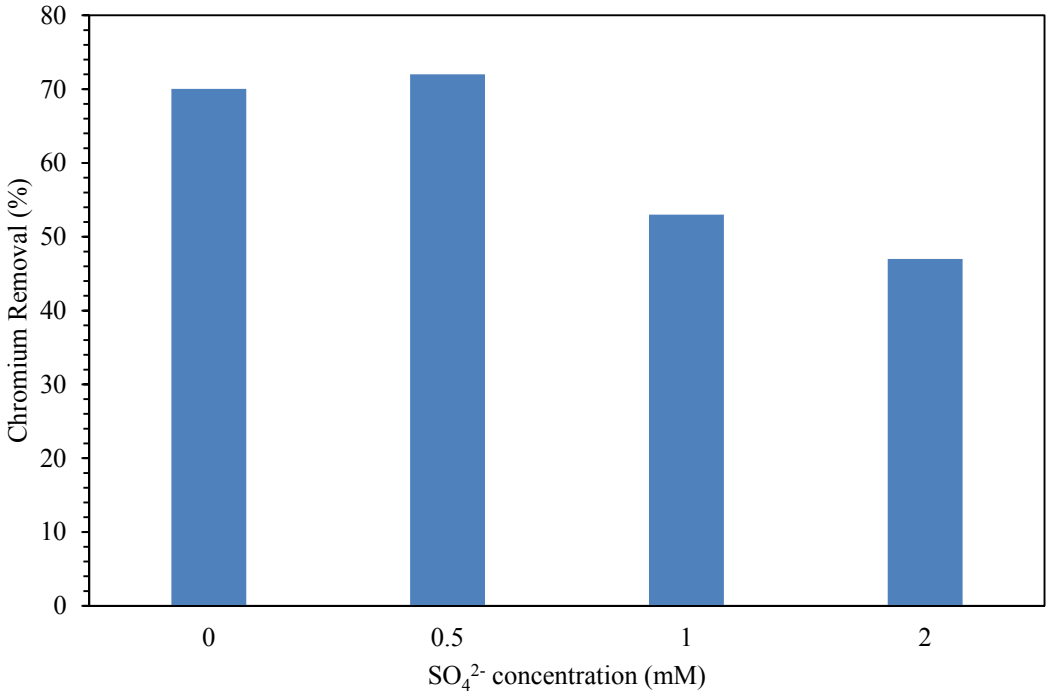

Fig. 16. Effect of SO_4^{2-} ions on the adsorption of Cr (VI) onto Mn_2O_3.

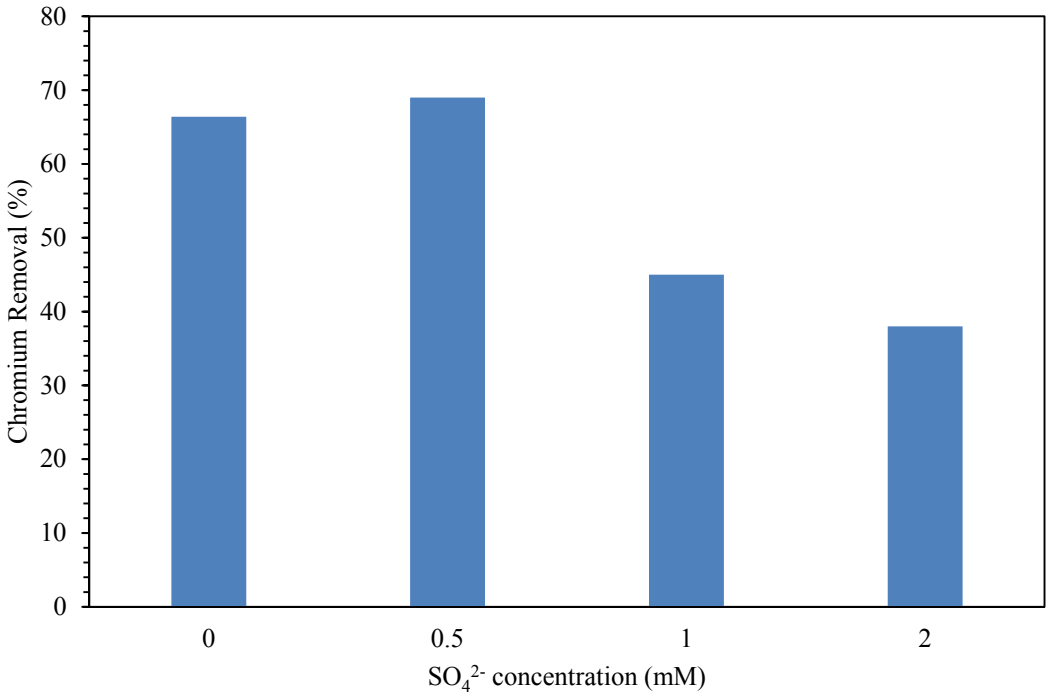

Fig. 17. Effect of SO_4^{2-} ions on the adsorption of Cr (VI) onto NEW 5 hr MCS.

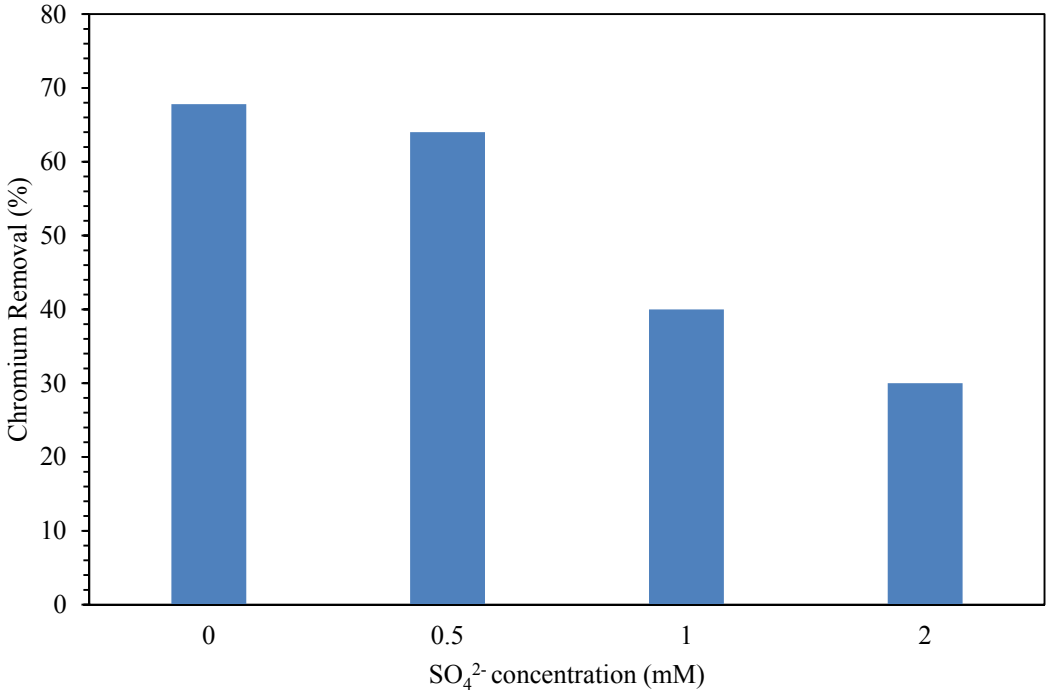

Fig. 18. Effect of SO_4^{2-} ions on the adsorption of Cr (VI) onto X 5 hr MCS.

In all three cases, the SO_4^{2-} ions become competitive at 1 mM and show a slight increase in competitive effect at 2 mM suggesting that Cr (VI) ions were more strongly bound. It should be noted that the SO_4^{2-} species present at high concentration may be favorable for specific adsorption as inner-sphere complexes. The increase in SO_4^{2-} concentration from 0 to 2 mM decreased Cr (VI) removal from 72% to 47 % for Mn_2O_3, from 69% to 38 % for New 5hr MCS, and from 64% to 30 % for X 5hr MCS. Similar results were observed with activated red mud and iron (III) hydroxide [3,31]. It also appears that Cr (VI) adsorption was slightly enhanced or not influenced at 0.5 mM SO_4^{2-}. The enhanced Cr (VI) adsorption may be suggestive of a complex bridging behavior of SO_4^{2-} with other anions or noncompetitive and weakly bound as outer-sphere complexes at the low concentration [8]. Spectroscopic studies have shown that SO_4^{2-} ions

similarly form both outer and inner-sphere complexes with γ-Al_2O_3 [32] and goethite [33] whereas inner-sphere complexes exclusively formed on hydrous ferric oxide [34]. However, the effect of co-existing SO_4^{2-} anions were modest in comparison to the effect of co-existing HCO_3^- anions shown next in Figures 19, 20, and 21 for sorbents Mn_2O_3, New 5hr MCS, and X 5hr MCS, respectively.

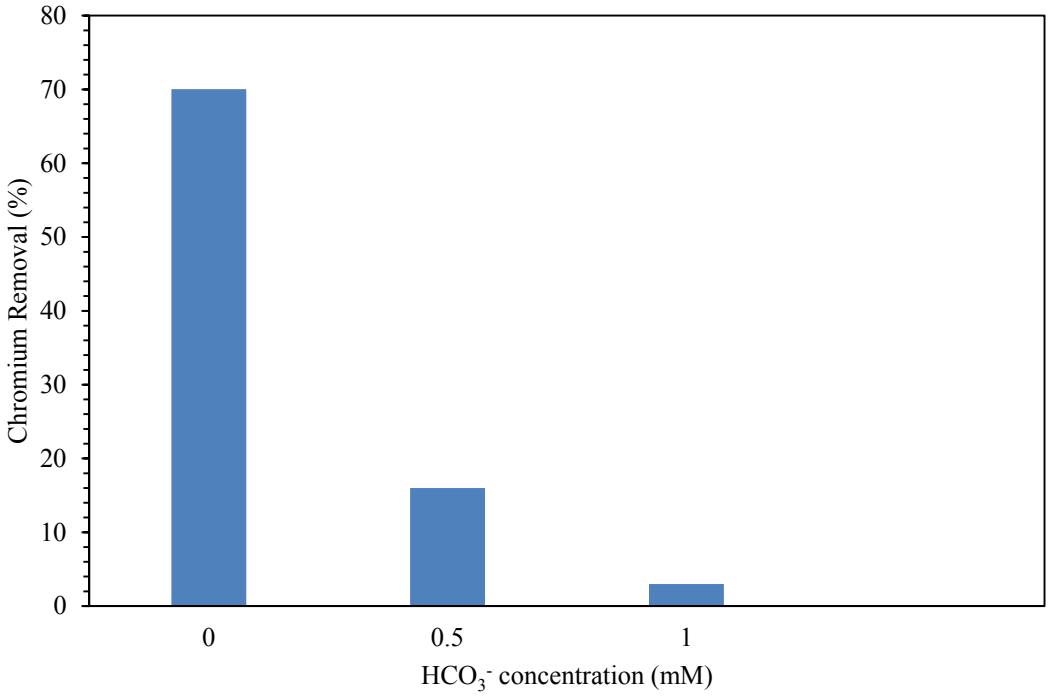

Fig. 19. Effect of HCO_3^- ions on the adsorption of Cr (VI) onto Mn_2O_3.

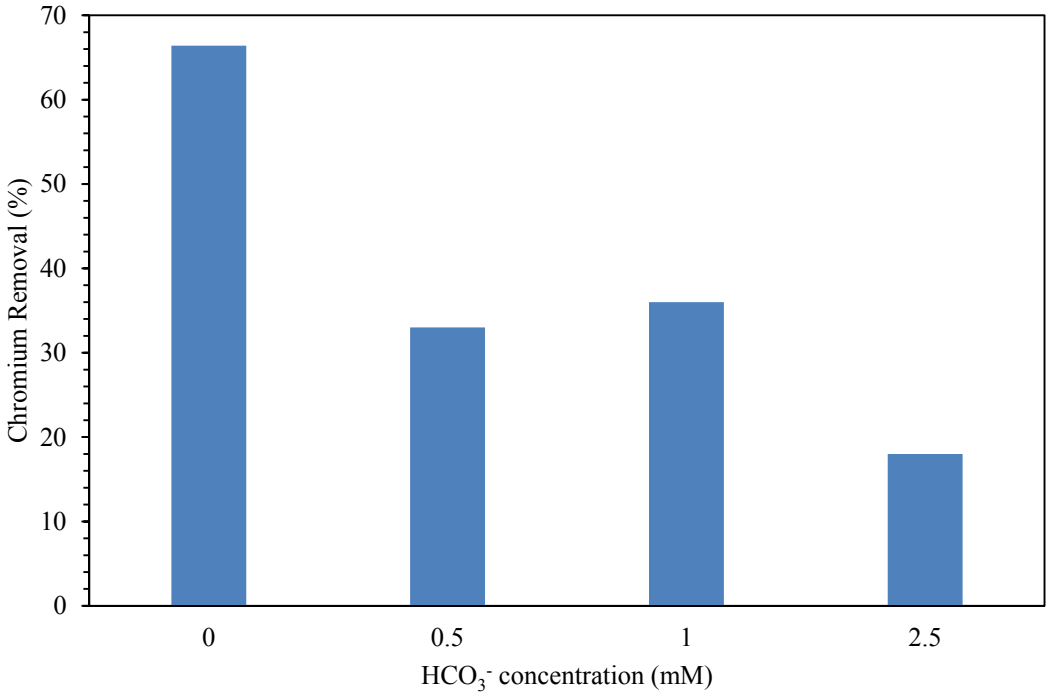

Fig. 20. Effect of HCO_3^- ions on the adsorption of Cr (VI) onto NEW 5 hr MCS.

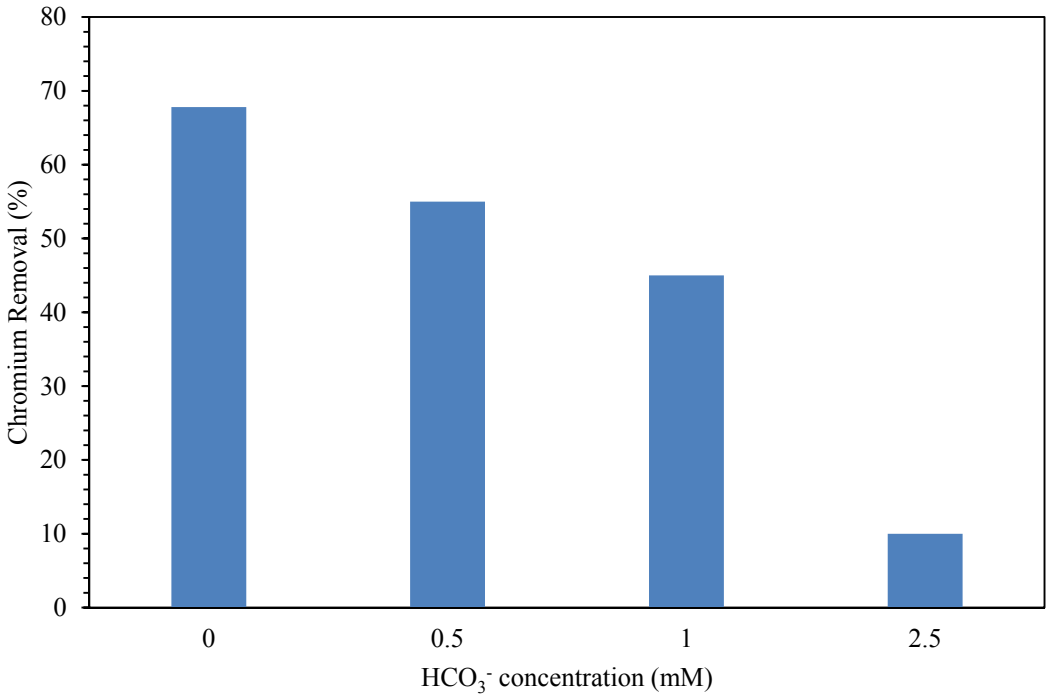

Fig. 21. Effect of HCO_3^- ions on the adsorption of Cr (VI) onto X 5 hr MCS.

The adsorption of Cr (VI) was significantly depressed at 0.5 mM HCO_3^- until negligible at 2.5 mM HCO_3^- and 5.5 mM HCO_3^- for Mn_2O_3 and MCS, respectively. These results can be attributed to both the competing effects and the unfavorably high pH conditions (pH 7.572 to 8.784 as shown in Table 9). In the Mn_2O_3 study, increasing the HCO_3^- concentration from 0.5 mM to 1 mM decreased removal of Cr (VI) from 16% to 3 %. The effect was less pronounced for New MCS and X MCS where an increase of 0.5 mM to 2.5 mM HCO_3^- decreased the removal of Cr (VI) from 33% to 18 % and 55% to 10 %, respectively. The relative stability of Cr (VI) adsorption on MCS can be explained by higher positive surface potential and greater availability of surface sites with Al content. In either case, the bicarbonate ions clearly exhibit strong binding, which is consistent with previous spectroscopic evidence indicating inner-sphere monodentate complexation on γ-Al_2O_3, amorphous Al oxide, gibbsite, and goethite [35,36,37]. The strongest competitive effect was observed with PO_4^{3-} in Figures 22, 23, and 24 for Mn_2O_3, New 5hr MCS, and X 5hr MCS, respectively, at the lowest anion concentrations studied.

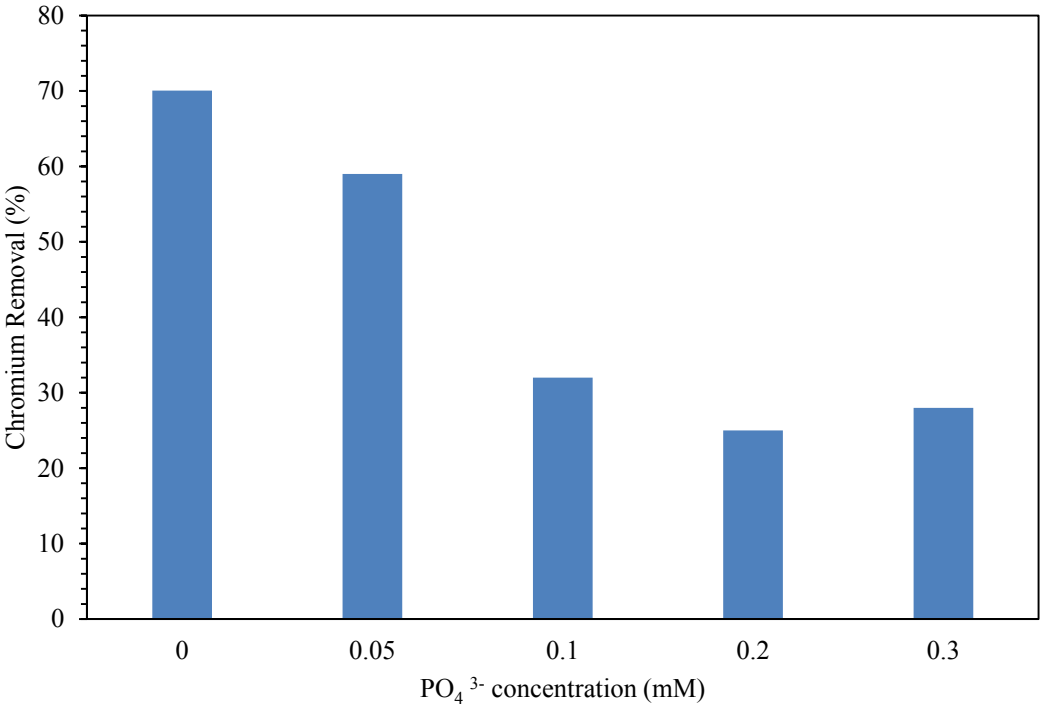

Fig. 22. Effect of PO_4^{3-} ions on the adsorption of Cr (VI) onto Mn_2O_3.

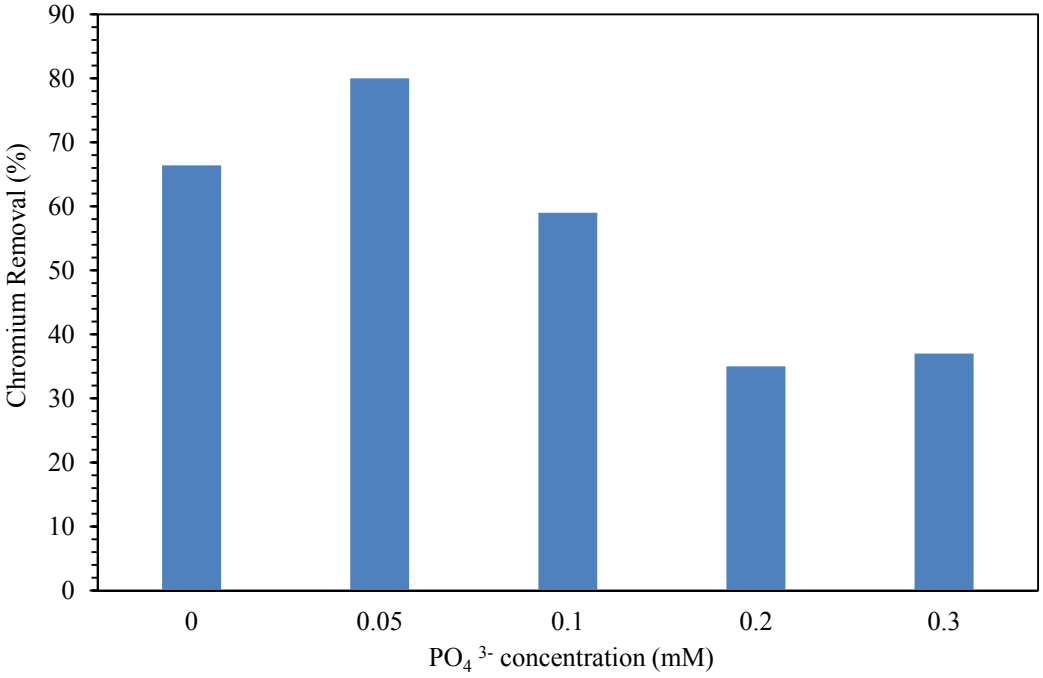

Fig. 23. Effect of PO_4^{3-} ions on the adsorption of Cr (VI) onto NEW 5 hr MCS.

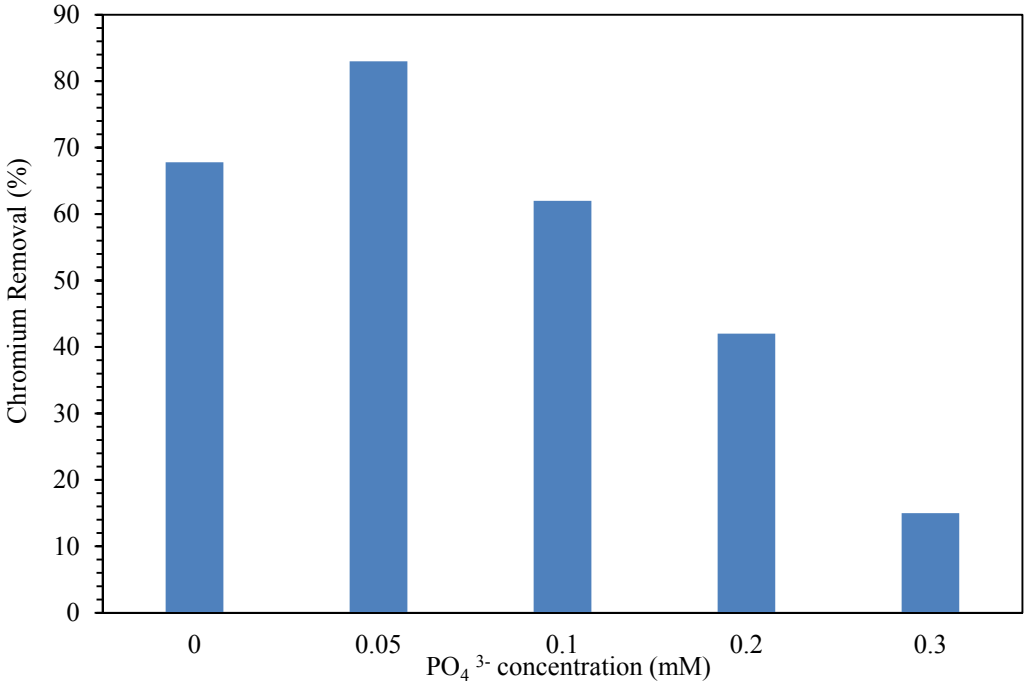

Fig. 24. Effect of PO_4^{3-} ions on the adsorption of Cr (VI) onto X 5 hr MCS.

The PO_4^{3-} ions were found to be competitive at 0.05 mM and 0.1 mM on Mn_2O_3 and MCS, respectively. These co-existing ion concentrations are more comparable to that of Cr (VI) found in solution indicating that the binding strength of Cr (VI) anions may be comparable to that of PO_4^{3-}. The adsorption of Cr(VI) was again less inhibited on the MCS absorbents than on Mn_2O_3 suggesting that the Mn_2O_3 adsorbent is highly selective for PO_4^{3-} anions as mentioned in numerous literature [38]. Moreover, enhanced adsorption of Cr (VI) on MCS was notable at 0.05 mM PO_4^{3-} again suggesting the complex bridging behavior of the anions. The Cr (VI) removal at 0.2 mM PO_4^{3-} was 25%, 35%, and 42% for the respective Mn_2O_3, New MCS, and X MCS studies and by 0.5 mM PO_4^{3-}, Cr (VI) adsorption was found to be negligible. The high interference of PO_4^{3-} on the adsorption of Cr (VI) can be attributed to the types of surface-complexes formed by PO_4^{3-} and sorbent surfaces [39]. It has been reported that protonated–nonprotonated bridging

bidentate, nonprotonated bridging monodentate, and monodentate complexation occurs between PO_4^{3-} and goethite and more generally inner-sphere complexation with pseudoboehmite [40,41,42]. These types of strong complexes may have formed with the sorbents in this study. Also, the SO_4^{2-} and PO_4^{3-} ions have been reported to show a similar affinity sequence for adsorption on activated red mud [3].

The pH readings of the stock solutions recorded in Tables 7 to 10 suggest that the presence of other ions interfere in the reaction mechanism through the determination of respective acidity. When the 1 mg/L Cr (VI) DI solution is mixed with either Ca^{2+}, SO_4^{2-} or PO_4^{3-} ions, the pH of the stock solution decreases and increases the positive sorbent potential, which decreases the electrostatic repulsion between sorbent surface and anions and increases reactions with $HCrO_4^-$. In contrast, the addition of HCO_3^- ions increased the stock solution pH and especially depressed Cr (VI) adsorption onto Mn_2O_3, the lower PZC sorbent. The HCO_3^- study also differs from all other co-existing ion studies with respect to final pH suggesting a different adsorption behavior; the final pH values had decreased instead indicating the co-adsorption of competing OH^- ions (Table 6). The SO_4^{2-} and PO_4^{3-} anions, on the other hand, were found to adsorb on Mn oxides the same way as $HCrO_4^-$ since the final pH values also increased to suggest a ligand exchange mechanism [31]. The similarity in size and symmetry of the CrO_4^{2-}, SO_4^{2-}, and PO_4^{3-} anions would also support similar adsorption behavior [39].

Table 7. Co-existing ion pH readings for Ca^{2+} ion.

Ca^{2+} (mM)	Stock	Mn_2O_3	New 5hr MCS	X 5hr MCS
0.5	5.730	6.795	6.449	6.470
1	5.480	6.298	6.136	6.364
2	5.641	6.023	6.364	6.328

Table 8. Co-existing ion pH readings for SO_4^- ion.

SO_4^- (mM)	Stock	Mn_2O_3	New 5hr MCS	X 5hr MCS
0.5	5.657	5.873	6.380	6.622
1	5.623	5.970	6.489	6.485
2	5.701	5.991	6.325	6.473

Table 9. Co-existing ion pH readings for HCO_3^- ion.

HCO_3^- (mM)	Stock	Mn_2O_3	New 5hr MCS	X 5hr MCS
0.5	7.572	7.186	7.184	7.143
1	7.876	7.462	7.519	7.368
2.5	8.342	7.920	8.032	8.065
5.5	8.784	8.467	8.058	8.223

Table 10. Co-existing ion pH readings for PO_4^{3-} ion.

PO_4^{3-} (mM)	Stock	Mn_2O_3	New 5hr MCS	X 5hr MCS
0.05	5.645	6.006	6.678	6.499
0.1	5.519	6.168	6.530	6.439
0.2	5.505	6.016	6.538	6.247
0.3	5.374	5.991	6.548	6.487
0.5	5.459	5.766	6.523	6.409

In Figures 25, 26, 27, and 28, the adsorption of Cr (VI) onto all three sorbents in terms of each competing ion is compared. It can be concluded that Cr (VI) adsorption onto the Mn_2O_3 sorbent was least influenced by the presence of SO_4^{2-} anions, however, most influenced by the Ca^{2+}, HCO_3^-, and PO_4^{3-} ions. The more significant impact of Ca^{2+} cations (Figure 25) can be explained by the near neutral PZC of Mn_2O_3 allowing for the adsorption of both cations and anions. Also, the lower affinity of the Mn_2O_3 surface for SO_4^{2-} anions may be attributed to a lower abundance of outer-sphere complexes whereas the higher affinity for competing PO_4^{3-} ions (Figure 28) and negligible ionic strength dependence can be due to inner-sphere complexation. In contrast, the better stability of the MCS sorbents to both the competing PO_4^{3-} and HCO_3^- anions, yet greater sensitivity to SO_4^{2-} anions (Figure 26) can be explained by the availability of additional surface sites resulting from the Al content and a mixture of inner and outer-sphere complexes. In several literature, Al oxides and hydroxides have been reported to form outer-sphere complexes with Cr (VI) anions [43]. Therefore, it is likely that Cr (VI) ions form a greater abundance of outer-sphere complexes on MCS, which is consistent with the adsorption edge and PZC shift results in the previous studies. Additionally, the ionic strength dependence, particularly for X MCS, may also be a factor in the decrease in Cr (VI) adsorption on MCS with increasing concentration of competing anions, which would also support the prevalence of outer-sphere complexation. The New MCS sorbent may be less susceptible to ionic dependence because of aging and greater abundance of inner-sphere complexes. Overall, it was found that the binding affinity for competing anions on all studied adsorbents follow the sequence PO_4^{3-} □ HCO_3^- □ SO_4^{2-}. Recently, the exact same order of Cr(VI) adsorption suppression on MnO_2 has been reported [44].

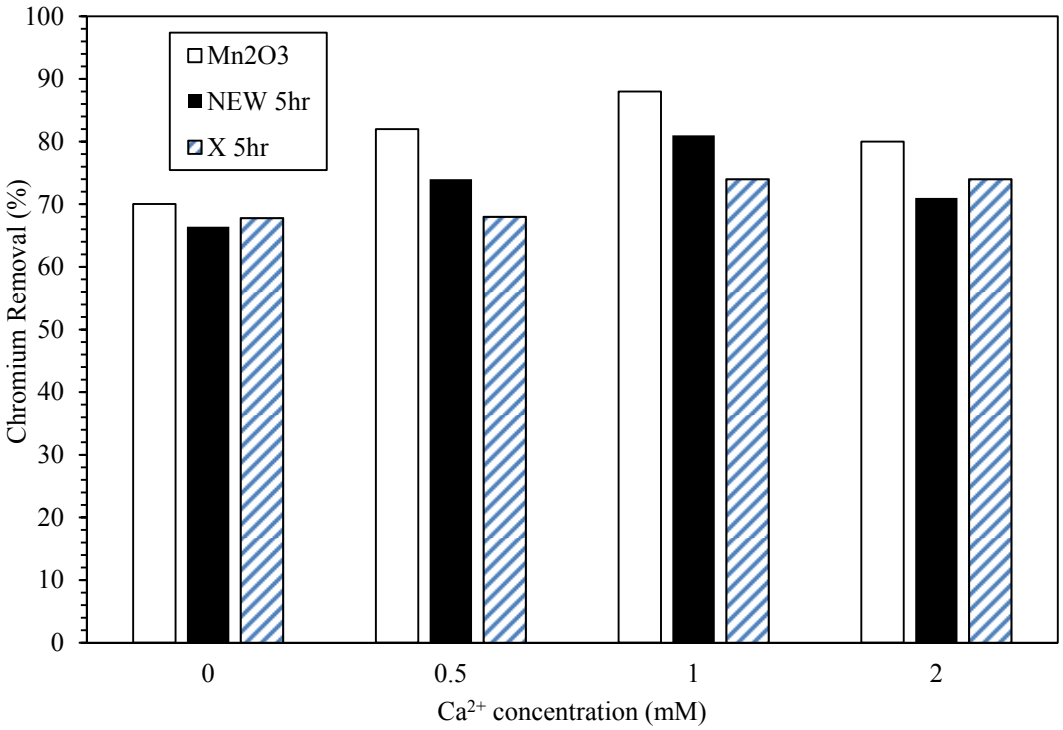

Fig. 25. Mn_2O_3, NEW 5 hr MCS, and X 5hr MCS percent removal comparison in different Ca^{2+} concentrations.

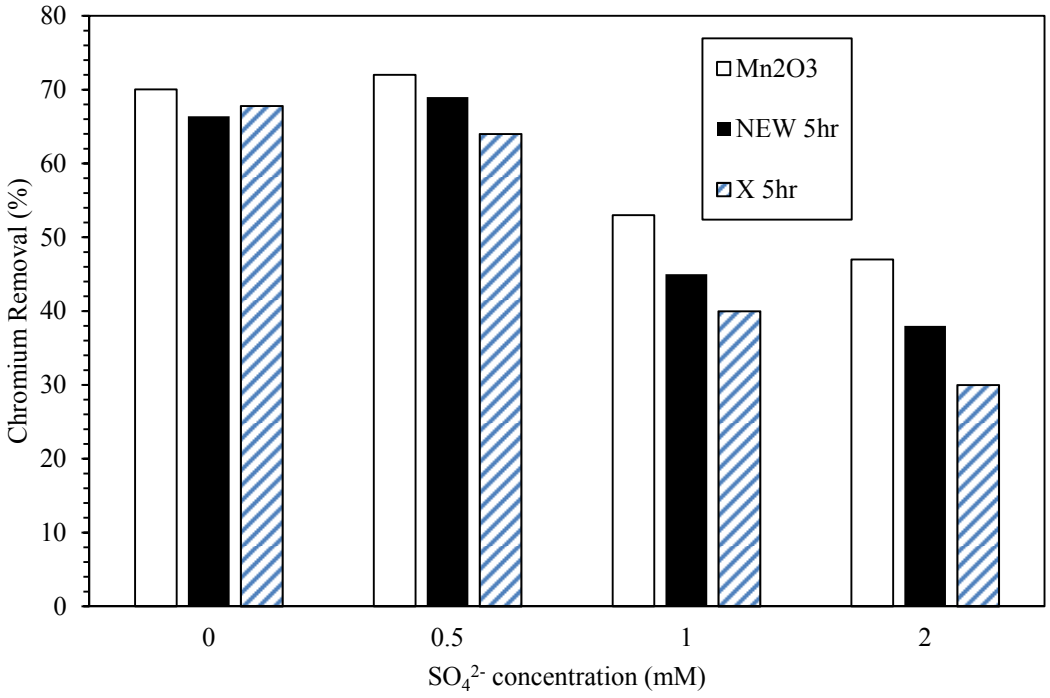

Fig. 26. Mn_2O_3, NEW 5 hr MCS, and X 5hr MCS percent removal comparison in different SO_4^{2-} concentrations.

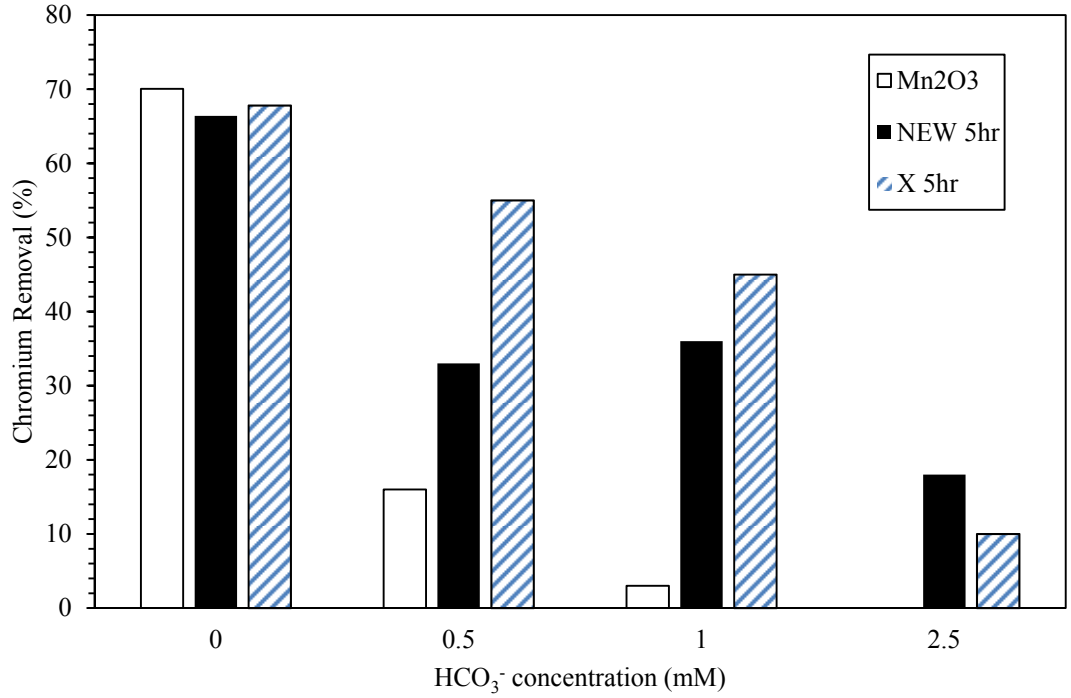

Fig. 27. Mn_2O_3, NEW 5 hr MCS, and X 5hr MCS percent removal comparison in different HCO_3^- concentrations.

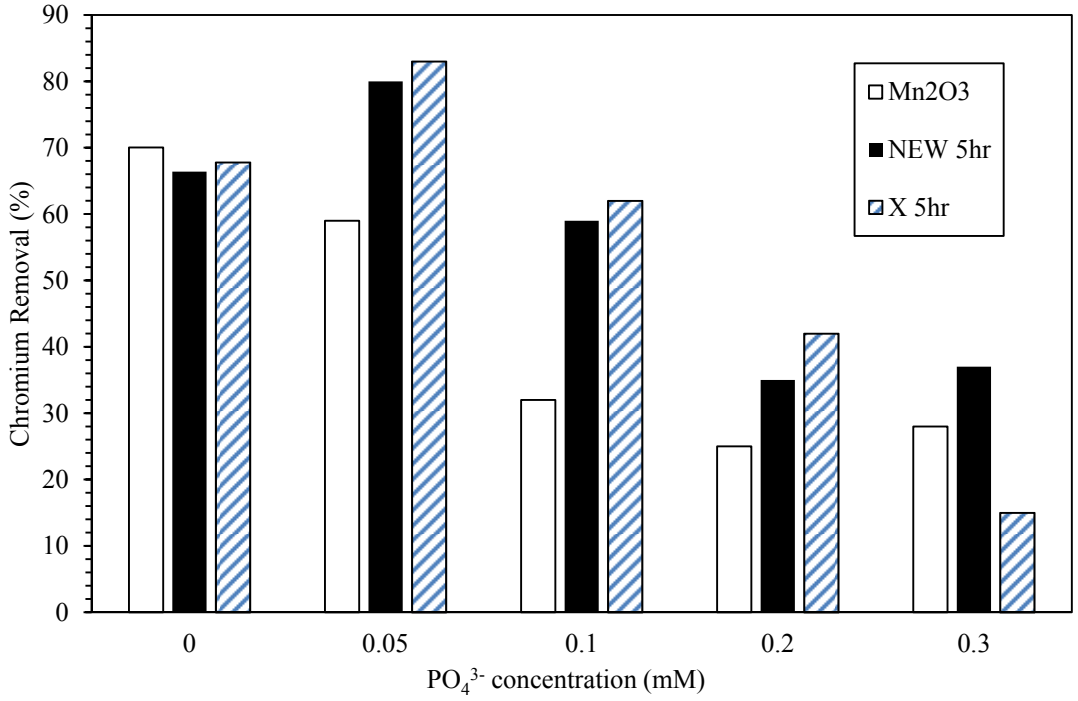

Fig. 28. Mn_2O_3, NEW 5 hr MCS, and X 5hr MCS percent removal comparison in different PO_4^{3-} concentrations.

3.3.4. Sorbent recycling

A “low cost” sorbent can further be cost effective if it can be reused in multiple cycles of operation. The effect of recycling on adsorption capacity of each sorbent was studied by exposing the same 1 g mass of sorbent to 1 mg/L of Cr (VI) solutions for three consecutive cycles of adsorption. The percent uptake of Cr (VI) by each sorbent from DI water for each adsorption cycle is presented in Figures 29, 30, 31, which show a general decrease in percent removal with each additional cycle of adsorption for all sorbents. The total Cr (VI) uptake, however, was substantial, particularly for New and X 5hr MCS sorbents.

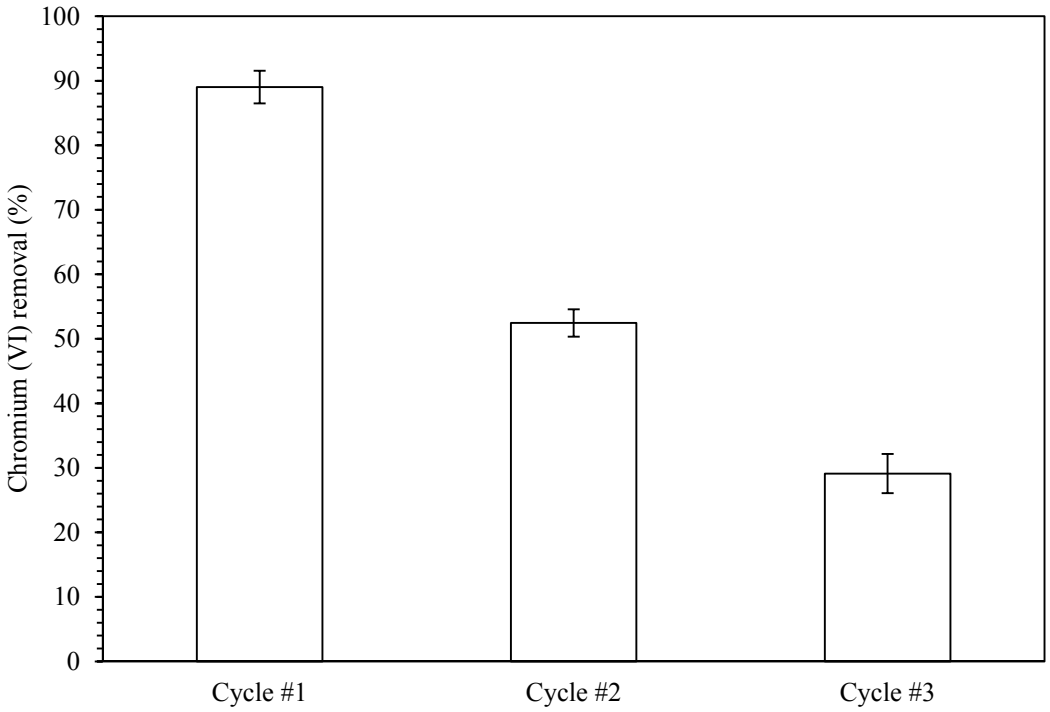

Fig. 29. Effect of Mn_2O_3 recycling on average Cr (VI) removal.

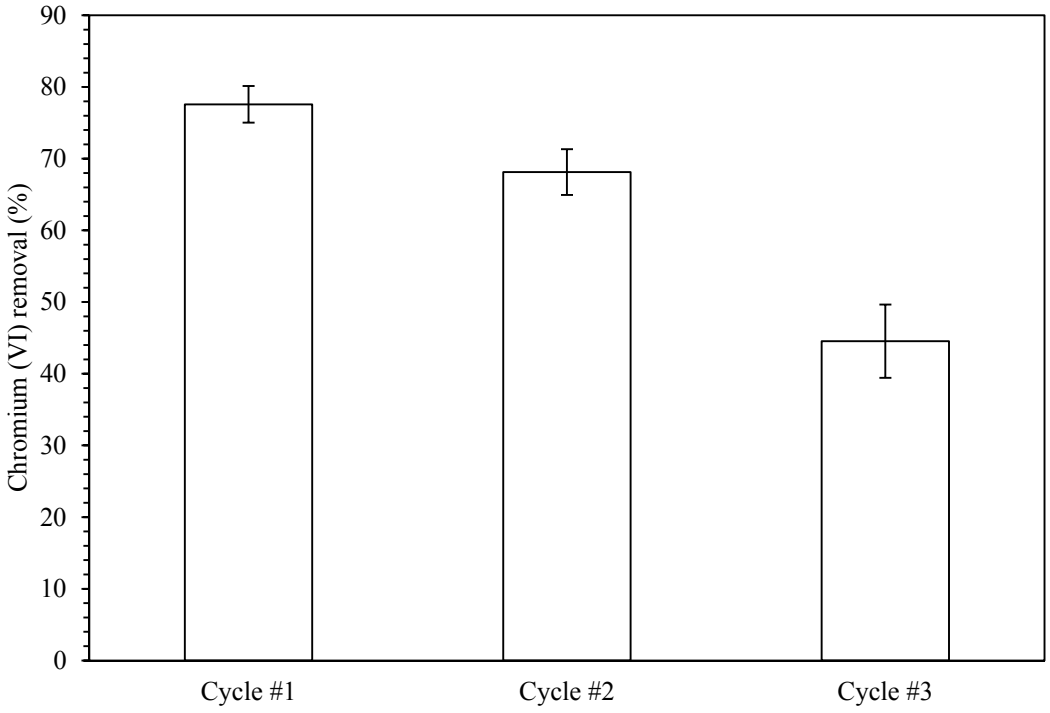

Fig. 30. Effect of New 5hr MCS recycling on average Cr (VI) removal.

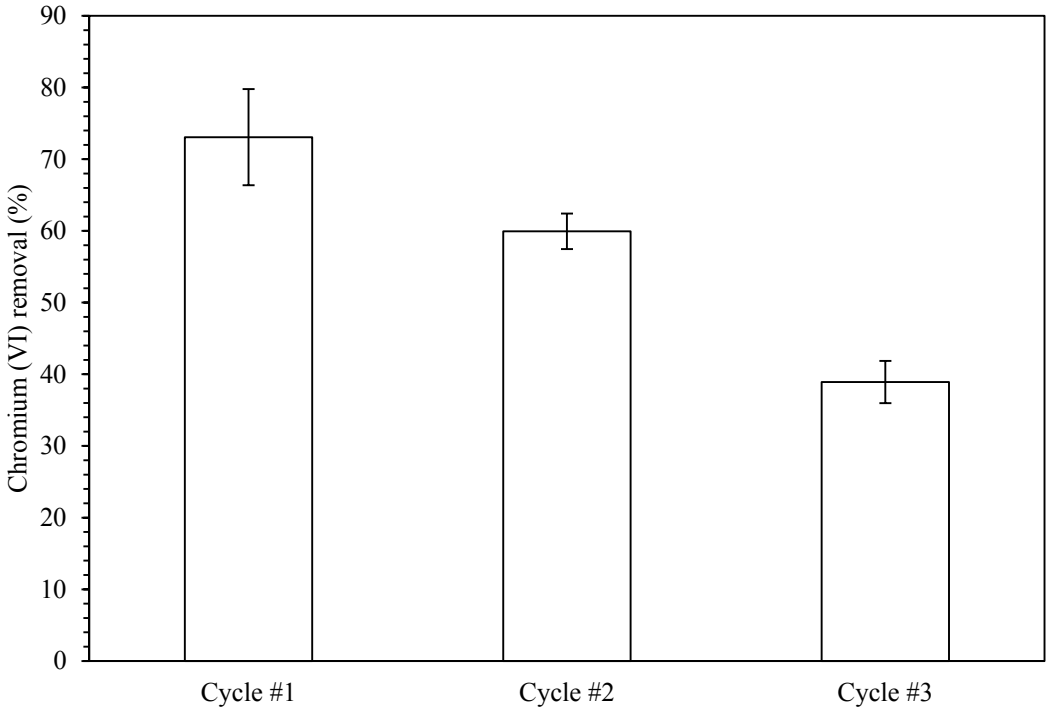

Fig. 31. Effect of X 5hr MCS recycling on average Cr (VI) removal.

The average percent uptake of Cr (VI) by 1 g of Mn_2O_3 from DI water for each cycle was 89%, 52.5%, and 29% for the first, the second, and the third cycles of adsorption and totaled 170.6%. The first cycle contributed to 52.2 % of the total Cr (VI) uptake (100%) while the second and third cycles accounted for only 30.8% and 17.1% of the total removed. The significant decrease in uptake with additional cycles can be explained by the decrease in available surface sites or monolayer saturation and by the decrease in sorbent positive potential with adsorption of Cr (VI) anions and subsequent increase electrostatic repulsion.

For 1 g of New 5hr MCS, on the other hand, Cr (VI) uptake totaled 190.3% with an average Cr (VI) uptake of 77.6%, 68.1%, and 44.5% for the first, the second, and the third cycles of adsorption, respectively. The percent of total Cr (VI) uptake achieved in each consecutive cycle thus corresponds to 40.8 %, 35.8%, and 23.4%. The additional cycles, in this case, account for the majority of Cr (VI) uptake with nearly 60% of the total Cr (VI) uptake found. The higher total removal can be attributed to the contributing Al sites and higher sorbent PZC.

The average percent uptake of Cr (VI) by 1 g of X 5hr MCS from DI water for each cycle was 73%, 59.9%, and 38.9% for the first, the second, and the third cycles of adsorption, respectively and totaled 171.9%. This corresponds to 42.5 %, 34.9%, and 22.6% of the total Cr (VI) uptake achieved during the three consecutive cycles of adsorption. Similar to New MCS, 57.5% of the total uptake of Cr (VI) was achieved during the additional cycles of adsorption. However, the lower total removal can be due to less aging or discontinuity of coating on sand.

The final pH of the triplicate samples after each adsorption cycle is given in Tables 11, 12, and 13 for Mn_2O_3, New MCS, and X MCS, respectively. The final pH results for New and X MCS followed previous trends; the final pH increased with increasing adsorption. The pH increase became less pronounced with MCS reuse as the percent Cr (VI) uptake also decreases. Mn_2O_3 also followed the same trend for the additional cycles implying a change in the adsorption mechanism after the first adsorption cycle, which may explain the significant decrease in Cr (VI) uptake with reuse.

Table 11. pH readings of triplicate samples for Mn_2O_3 recycling.

	pH
Cycle # 1	
Sample #1	5.714
Sample #2	5.698
Sample #3	5.656
Cycle # 2	
Sample #1	6.067
Sample #2	5.986
Sample #3	5.933
Cycle #3	
Sample #1	6.119
Sample #2	6.086
Sample #3	5.989

Table 12. pH readings of triplicate samples for New 5hr MCS recycling.

	pH
Cycle # 1	
Sample #1	6.182
Sample #2	6.028
Sample #3	6.079
Cycle # 2	
Sample #1	6.569
Sample #2	6.343
Sample #3	6.505
Cycle #3	
Sample #1	6.5
Sample #2	6.67
Sample #3	6.597

Table 13. pH readings of triplicate samples for X 5hr MCS recycling.

	pH
Cycle # 1	
Sample #1	6.173
Sample #2	6.678
Sample #3	6.287
Cycle # 2	
Sample #1	6.745
Sample #2	6.544
Sample #3	6.587
Cycle #3	
Sample #1	6.449
Sample #2	6.615
Sample #3	6.581

In summary, Mn_2O_3 had shown the highest percent removal for the first cycle, but the least percent removal by the third cycle. New 5 hr MCS showed highest percent removal for the second cycle and third cycle and was found to overall achieve the most removal with reuse. The reuse of X 5hr MCS was also found to be comparable to that of Mn_2O_3.

3.3.5. Regeneration study

A "low cost" sorbent can further be cost effective if it can be regenerated for additional reuse and if Cr (VI) ions can be recovered for reuse. The regeneration of New 5 hr MCS using three different concentrations of NaOH regenerant (0.001 N, 0.01 N, and 0.1 N) was studied at initial Cr (VI) concentrations of 1, 3, and 5 mg/L. The percent Cr (VI) uptake by virgin New 5hr MCS and regenerated New 5hr MCS for the 1, 3, and 5 mg/L Cr (VI) stock solutions are shown in Figures 32, 33, and 34, respectively. Several observations can be made from these results in terms of trends and sorbent performance.

First and foremost, it can be observed that although percent removal generally decreased after regeneration, the additional removal of Cr (VI) remained substantial, particularly for the 1 mg/L Cr (VI) DI solution. For initial Cr (VI) concentrations of 1 mg/L, 3 mg/L, and 5 mg/L, the average Cr (VI) removal before regeneration was 54.8%, 42.4%, and 35.7%, respectively and after regeneration decreased to a maximum of 45.9%, 29.1%, and 28.5%. Secondly, Cr (VI) removal for both virgin and regenerated New MCS declined with increasing initial Cr (VI)

concentration and tended to stabilize towards 5 mg/L of Cr (VI). Thirdly, there were no significant changes in Cr (VI) uptake when increasing NaOH concentration from 0.001 to 0.1 N; the Cr (VI) uptake for New 5hr MCS regenerated using 0.001, 0.01, and 0.1 N NaOH, respectively, was 45.9%, 39%, and 40.7% at 1 mg/L Cr (VI), 29.9%, 26.8%, and 26.4% at 3 mg/L Cr (VI), and finally 24.1%, 28.5%, and 27.5% at 5 mg/L Cr (VI). Therefore, sorbent regeneration using 0.001 N of NaOH is the most efficient option as it is just as effective as the higher NaOH concentrations if not more effective and most economical.

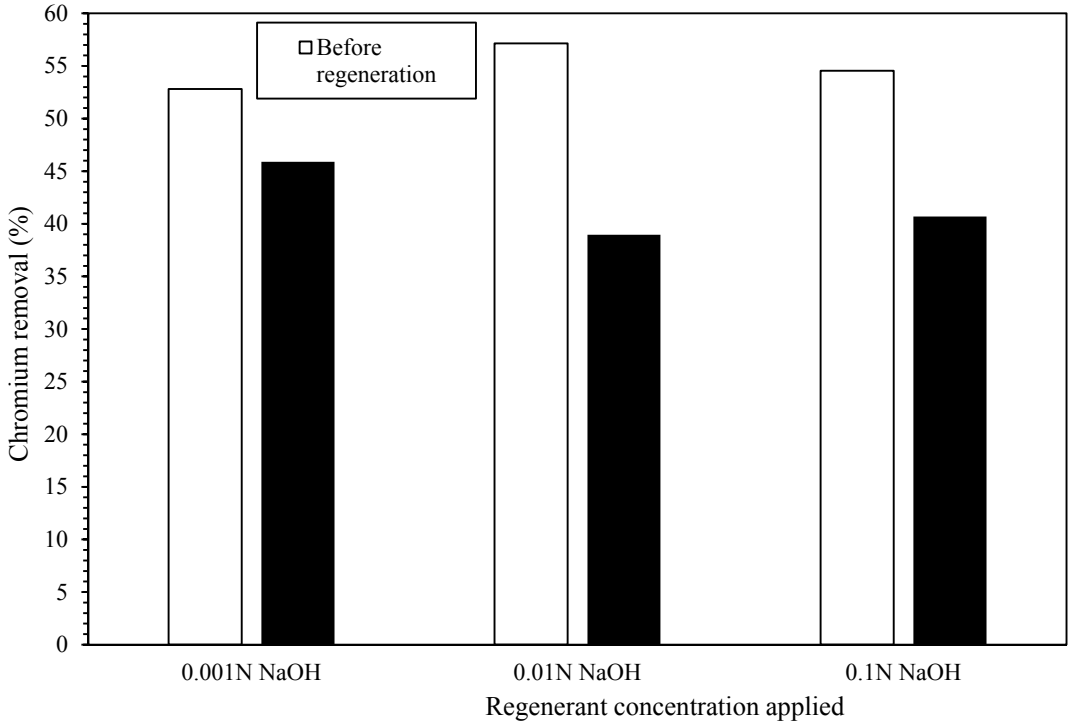

Fig. 32. Effect of eluent concentration on the regeneration of New 5 hr MCS using a 1 mg/L Cr(VI) solution.

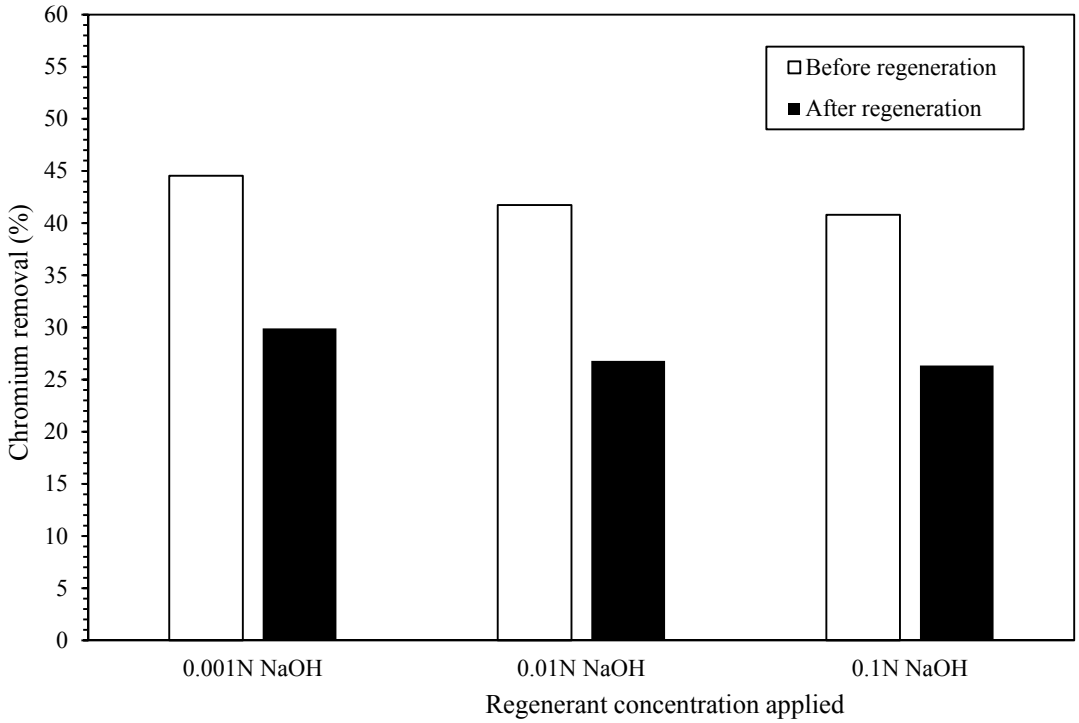

Fig. 33. Effect of eluent concentration on the regeneration of New 5 hr MCS using a 3 mg/L Cr(VI) solution.

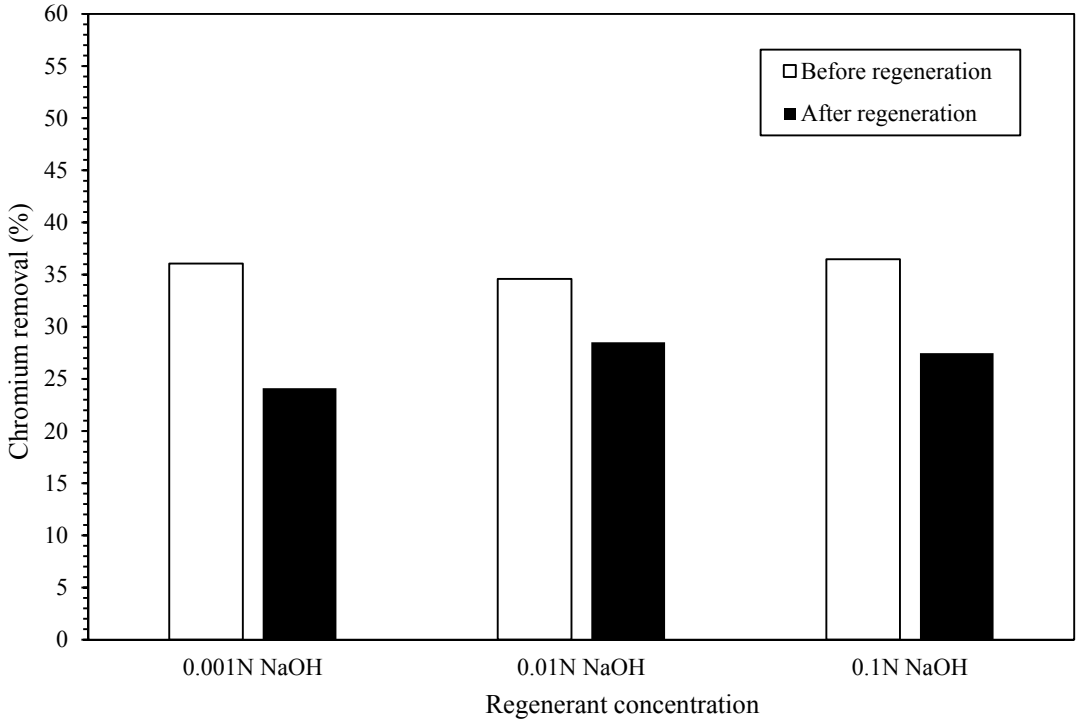

Fig. 34. Effect of eluent concentration on the regeneration of New 5 hr MCS from a 5 mg/L Cr(VI) solution.

The results are also given in terms of calculated regeneration efficiencies (RE%) and Cr (VI) recovery/desorption percent in Tables 14 and 15 and compared to the reported values for other alternate sorbents. The maximum regeneration efficiencies for New 5hr MCS at 1, 3, and 5 mg/L Cr (VI) studies were 86.9%, 67.1 %, and 82.4 % respectively. These results were specifically observed at 0.001 N NaOH for 1 and 3 mg/L Cr (VI) and at 0.01 N NaOH for 5 mg/L Cr (VI) indicating that at high Cr (VI) concentrations, the best results can be obtained at the intermediate NaOH concentration. The maximum New 5hr MCS regeneration efficiencies are much higher than those reported for peat where a maximum regeneration efficiency of only 35.5% was found using 1 M of NaOH and are rather comparable to iron oxide coated sand regenerated at pH 9.5 having regeneration efficiencies of 41.4%, 91.4%, and 84.7% at cycle 1, 5, and 10, respectively [45,46].

The maximum recovery of Cr (VI) ions found was 100%, 82.6%, and 60% in 0.001 N NaOH regenerant solution for the 1, 3, and 5 mg/L initial Cr (VI) loadings, respectively (Table 15). Similar maximum recovery percents have been reported for several alternate sorbents under different initial conditions. Udaybhaskar et al. reported a maximum Cr (VI) recovery of 63.5% in 1 M NaOH regenerant solution for chitosan at an initial Cr (VI) loading of 5 mg/L [47]. Moreover, Mallick et al. reported 99% in 0.04 M NaOH for Mn nodule leached residue at 10 mg/L Cr (VI) [10]. For a bagasse fly ash study at 500 mg/L Cr (VI), 98% Cr (VI) recovery in a 3 M NH_3 regenerant solution was also reported [1]. It can be seen that comparable Cr (VI) recovery can be obtained at much lower regenerant concentrations in the present study.

Table 14. New 5hr MCS regeneration efficiencies (RE%) for initial 1,3, and 5 mg/L Cr (VI).

	1 mg/L Cr (VI) solution	3 mg/L Cr (VI) solution	5 mg/L Cr (VI) solution
0.001 N NaOH	86.9	67.1	66.9
0.01 N NaOH	68.2	64.2	82.4
0.1 N NaOH	74.6	64.6	75.3

Table 15. Percent Cr (VI) recovered (%) during New 5hr MCS regeneration cycle.

	1 mg/L Cr (VI) solution	3 mg/L Cr (VI) solution	5 mg/L Cr (VI) solution
0.001 N NaOH	100	82.6	60
0.01 N NaOH	100	72.2	53.5
0.1 N NaOH	100	63.2	54.8

The resultant pH values for adsorption cycles before and after regeneration as well as for the regeneration cycle itself are given in Tables 16,17, and 18. The maximum New 5hr MCS regeneration efficiencies for 1 and 3 mg/L Cr (VI) observed at 0.001 N NaOH correspond to regenerant solution pH values of about 10 as shown in Tables 16 and 17. Thus, the relatively low values of regenerant solution pH may explain the higher regeneration efficiencies for 1 and 3 mg/L Cr (VI) indicating that regeneration efficiency is pH dependent. Bailey et al. similarly found that Cr (VI) adsorption by iron-oxide-coated sands regenerated at pH 9.5 was higher than at 1 N NaOH and confirmed that sorbent exposure to high pH solution causes loss of adsorptive capacity [21]. These findings are, however, contrary to those found for Mn nodule leached residues where the Cr (VI) percent recovery increased with increasing NaOH concentration suggesting that the abundance of OH^- caused increased hindrance to Cr (VI) ion diffusion [10].

Tables 16 to 18 also show that the resultant increase in pH due to the release of hydroxyl ions with Cr (VI) adsorption is less drastic for 5 mg/L Cr (VI) solutions than for 1 and 3 mg/L Cr (VI) solutions supporting earlier observations that Cr (VI) adsorption is reduced with increased adsorbate concentration. A similar behavior was also observed in peat column studies with adsorbent reuse [48].

Table 16. New 5 hr MCS regeneration study pH readings for 1 mg/L Cr(VI) solution.

	Before regeneration	**After regeneration**	**NaOH regeneration**
Sample #1 (0.001 N)	6.755	7.266	10.212
Sample #2 (0.01 N)	6.238	7.456	12.034
Sample #3 (0.1 N)	6.287	7.503	12.966

Table 17. New 5 hr MCS regeneration study pH readings for 3 mg/L Cr(VI) solution.

	Before regeneration	**After regeneration**	**NaOH regeneration**
Sample #1 (0.001 N)	6.533	7.344	10.23
Sample #2 (0.01 N)	6.59	6.974	12.034
Sample #3 (0.1 N)	6.511	7.736	13.002

Table 18. New 5 hr MCS regeneration study pH readings for 5 mg/L Cr(VI) solution

	Before regeneration	**After regeneration**	**NaOH regeneration**
Sample #1 (0.001 N)	6.454	6.634	10.128
Sample #2 (0.01 N)	6.338	6.741	12.055
Sample #3 (0.1 N)	6.59	6.958	12.991

3.4. Conclusion

In this chapter, it was shown that adsorption equilibria are quite labile and dependent on solution pH, which affects Cr (VI) speciation and sorbent surface charge and competing ions/ ionic strength conditions. The pH study showed typical anion adsorption; Cr (VI) adsorption decreased with increasing pH. However, a wider effective Cr (VI) adsorption range was found for Mn sorbents as compared to other oxides. Also from pH 2 to 9, Mn_2O_3 displayed far greater affinity than suggesting that both electrostatic and chemical interactions are likely.

The zeta potential results were also found to be consistent with pH study results as well as previous findings; the far greater change in Mn_2O_3 zeta potential is likely due to greater Cr (VI) adsorption and monolayer formation as opposed to lesser and weaker adsorption on MCS. Shifts in PZC were observed with Cr (VI) adsorption on Mn_2O_3, New and X MCS indicating specific inner-sphere anion adsorption possibly due to ligand exchange. Bhutani et al. (1992) has confirmed the chemical interaction of Cr (VI) on MnO_2 surface from infrared spectroscopy measurement and concluded that Cr (VI) sorption on MnO_2 occurs by a mechanism of ligand exchange is most likely. Yoon et al. (2012) also suggested outer-sphere complexation between Cr (VI) and surface of iron-manganese oxide coated sand. It was also found that Cr (VI) weakly adsorbed or formed an outer-sphere surface complex with the surface of iron-oxide coated sand from FT-IR measurement.

The co-existing ions study results also indicate either inner-sphere and/or outer-formation between Cr (VI) and sorbent surfaces since the co-adsorption of several anions implies not only

competition for available surface sites, but also affects surface equilibria by an altered surface charge. It was found that the co-existing Ca^{2+} cations enhanced electrostatic Cr (VI) anion adsorption while co-existing anions had a competitive effect in the order of PO_4^{3-} □ HCO_3^- □ SO_4^{2-} for Mn_2O_3, New and X MCS sorbents. Mn_2O_3 was found to have a stronger affinity for PO_4^{3-} and HCO_3^- than MCS again suggesting difference in surface site characteristics of two oxides. The possibility of adequate regeneration of sorbents is also indicated.

It was found that MCS sorbents had a much higher potential for reuse than Mn_2O_3 with New 5 hr MCS notably outperforming Mn_2O_3 by the third adsorption cycle and X 5hr MCS equaling Mn_2O_3 in performance. Moreover, New 5hr MCS showed potential for further reuse and Cr (VI) recovery after regeneration using 0.001 N NaOH, which was the lowest concentration studied. The regeneration efficiencies and Cr (VI) recovery/desorption percentages, particularly for 1 mg/L Cr (VI) loadings, were high and comparable to several other alternative adsorbents. The regenerated New 5 hr MCS could possibly continue to adsorb about 30% Cr (VI) for initial Cr (VI) solutions above 5 mg/L or likewise for five subsequent adsorption cycles at 1 mg/L Cr (VI). The desorption results also suggest that Cr (VI) adsorption is a reversible process clearly supporting physical adsorption as the dominant mechanism of Cr (VI) adsorption on MCS. Similar regeneration results can be expected for X 5 hr MCS due to the similarity in adsorption characteristics and perhaps slightly inferior results for Mn_2O_3 due to stronger Cr (VI) ion binding to sorbent surface and lower reuse efficiency.

REFERENCES

[1] Gupta, Vinod K., et al. "Removal of chromium (VI) from electroplating industry wastewater using bagasse fly ash—a sugar industry waste material." *Environmentalist* 19.2 (1998): 129-136.

[2] Namasivayam, C., and K. Ranganathan. "Waste Fe (III)/Cr (III) hydroxide as adsorbent for the removal of Cr (VI) from aqueous solution and chromium plating industry wastewater." *Environmental Pollution* 82, no. 3 (1993): 255-261.

[3] Pradhan, Jyotsnamayee, Surendra Nath Das, and Ravindra Singh Thakur. "Adsorption of hexavalent chromium from aqueous solution by using activated red mud." *Journal of Colloid and Interface Science* 217.1 (1999): 137-141.

[4] Richard, Françoise C., and Alain CM Bourg. "Aqueous geochemistry of chromium: a review." *Water Research* 25.7 (1991): 807-816.

[5] Guertin, Jacques, James A. Jacobs, and Cynthia P. Avakian. *Chromium (VI) Handbook*. Boca Raton, FL: CRC Press, 2005.

[6] Tandon, R. K., P. T. Crisp, J. Ellis, and R. S. Baker. "Effect of pH on chromium (VI) species in solution." *Talanta* 31, no. 3 (1984): 227-228.

[7] Davis, James A., and James O. Leckie. "Surface ionization and complexation at the oxide/water interface. 3. Adsorption of anions." *Journal of Colloid and Interface Science* 74.1 (1980): 32-43.

[8] Schulthess, C. P., and D. L. Sparks. "Competitive ion exchange behavior on oxides." *Soil Science Society of America Journal* 53.2 (1989): 366-373.

[9] Weng, C. H., J. H. Wang, and C. P. Huang. "Adsorption of Cr (VI) onto TiO_2 from dilute aqueous solutions." *Water science and technology* 35.7 (1997): 55-62.

[10] Mallick, Sujata, S. S. Dash, and K. M. Parida. "Adsorption of hexavalent chromium on manganese nodule leached residue obtained from NH_3–SO_2 leaching." *Journal of colloid and interface science* 297.2 (2006): 419-425.

[11] Gupta, Vinod K., Arshi Rastogi, and Arunima Nayak. "Adsorption studies on the removal of hexavalent chromium from aqueous solution using a low-cost fertilizer industry waste material." *Journal of Colloid and Interface Science* 342, no. 1 (2010): 135-141.

[12] Hunter, R.J. 1981. Zeta potential in colloid science: Principles and applications. Academic Press, London.

[13] Fendorf, Scott E., Robert J. Zasoski, and Richard G. Burau. "Competing metal ion influences on chromium (III) oxidation by birnessite." *Soil Science Society of America Journal* 57, no. 6 (1993): 1508-1515.

[14] Anderson, M.A., and D.T. Malotky. 1979. The adsorption of protolyzable anions on hydrous oxides at the isoelectric point. J. Colloid Interface Sci. 72:413–427.

[15] Anderson, M.A., J.F. Ferguson, and J. Gavis. 1976. Arsenate adsorption on amorphous aluminum hydroxide. J. Colloid Interface Sci. 54:391–399.

[16] Harrison, J.B., and V.E. Berkheiser. 1982. Anion interactions with freshly prepared hydrous iron oxides. Clays Clay Miner. 30:97–102.

[17] Suarez, D.L., S. Goldberg, and C. Su. 1999. Evaluation of oxyanion adsorption mechanisms on oxides using FTIR spectroscopy and electrophoretic mobility. Am. Chem. Soc. Symp. Ser. 715:136–178.

[18] Pierce, M.L., and C.B. Moore. 1980. Adsorption of arsenite on amorphous iron hydroxide from dilute aqueous solution. Environ. Sci. Technol. 14:214– 216.

[19] Lumsdon, D.G., A.R. Fraser, J.D. Russell, and N.T. Livesey. 1984. New infrared band assignments for the arsenate ion adsorbed on synthetic goethite (α-FeOOH). J. Soil Sci. 35:381–386.

[20] Su, C., and D.L. Suarez. 1997. In situ infrared speciation of adsorbed carbonate on aluminum and iron oxides. Clays Clay Miner. 45:814–825.

[21] Su, C., and D.L. Suarez. 2000. Selenate and selenite sorption on iron oxides: An infrared and electrophoretic study. Soil Sci. Soc. Am. J. 64:101–111.

[22] McKenzie, R.M. 1983. The adsorption of molybdenum on oxide surfaces. Aust. J. Soil Res. 21:505–513.

[23] Goldberg, S., H.S. Forster, and C.L. Godfrey. 1996. Molybdenum adsorption on oxides, clay minerals, and soils. Soil Sci. Soc. Am. J. 60:425–432.

[24] Goldberg, S., H.S. Forster, and E.L. Heick. 1993. Boron adsorption mechanisms on oxides, clay minerals, and soils inferred from ionic strength effects. Soil Sci. Soc. Am. J. 57:704–708.

[25] Su, C., and D.L. Suarez. 1995. Coordination of adsorbed boron: A FTIR spectroscopic study. Environ. Sci. Technol. 29:302–311.

[26] Sushree Swarupa Tripathy, Ashok M. Raichur, Enhanced adsorption capacity of activated alumina by impregnation with alum for removal of As (V) from water, Chemical Engineering Journal .138 (2008) 179–186.

[27] W. Stumm, Chemistry of the Solid–Water Interface, Wiley–Interscience, New York, 1999.

[28] Fendorf, S.E., G.M. Lamble, M.G. Stapleton, M.J. Kelley, and D.L. Sparks. 1994. Mechanisms of chromium (III) sorption on silica: 1. Cr (III) surface structure derived by extended X-ray absorption fi ne structure spectroscopy. Environ. Sci. Technol. 28:284–289.

[29] Fendorf, S.E., M.J. Eick, P. Grossl, and D.L. Sparks. 1997. Arsenate and chromate retention mechanisms on goethite: I. Surface structure. Environ. Sci. Technol. 31:315–320.

[30] Hsia, T.H., S.L. Lo, C.F. Lin, and D.Y. Lee. 1993. Chemical and spectroscopic evidence for specific adsorption of chromate on hydrous iron oxide. Chemosphere 26:1897–1904.

[31] Aoki, T., and M. Munemori. "Recovery of chromium (VI) from wastewaters with iron (III) hydroxide—I: adsorption mechanism of chromium (VI) on iron (III) hydroxide." *Water Research* 16, no. 6 (1982): 793-796.

[32] Wijnja, H., and C.P. Schulthess. 2000. Vibrational spectroscopy study of selenate and sulfate adsorption mechanisms on Fe and Al (hydr)oxide surfaces. J. Colloid Interface Sci. 229:286–297.

[33] Peak, D., R.G. Ford, and D.L. Sparks. 1999. An in-situ ATR-FTIR investigation of sulfate bonding mechanisms on goethite. J. Colloid Interface Sci. 218:289–299.

[34] Hug, S.J. 1997. In situ Fourier transform infrared measurements of sulfate adsorption on hematite in aqueous solutions. J. Colloid Interface Sci. 188:415–422.

[35] Wijnja, H., and C.P. Schulthess. 1999. ATR-FTIR and DRIFT spectroscopy of carbonate species at the aged γ-Al2O3/water interface. Spectrochim. Acta A Mol. Biomol. Spectrosc. 55:861–872.

[36] Villalobos, M., and J.O. Leckie. 2001. Surface complexation modeling and FTIR study of carbonate adsorption to goethite. J. Colloid Interface Sci. 235:15–32.

[37] Wijnja, H., and C.P. Schulthess. 2001. Carbonate adsorption mechanism on goethite studied with ATR-FTIR, DRIFT and proton co-adsorption measurements. Soil Sci. Soc. Am. J. 65:324–330.

[38] Post, Jeffrey E. "Manganese oxide minerals: Crystal structures and economic and environmental significance." Proceedings of the National Academy of Sciences 96.7 (1999): 3447-3454.

[39] Cieślak-Golonka, Maria, and Marek Daszkiewicz. "Coordination geometry of Cr (VI) species: Structural and spectroscopic characteristics." *Coordination Chemistry Reviews* 249.21 (2005): 2391-2407.

[40] Tejedor-Tejedor, M.L., and M.A. Anderson. 1990. Protonation of phosphate on the surface of goethite as studied by CIR-FTIR and electrophoretic mobility. Langmuir 6:602–611.

[41] Persson, P., N. Nilsson, and S. Sjöberg. 1996. Structure and bonding of orthophosphate ions at the iron oxide-aqueous interface. J. Colloid Interface Sci. 177:263–275.

[42] Bleam, W.F., P.E. Pfeffer, S. Goldberg, R.W. Taylor, and R. Dudley. 1991. A 31P solid-state nuclear magnetic resonance study of phosphate adsorption at the boehmite/aqueous-solution interface. Langmuir 7:1702–1712.

[43] Handzlik, Jarosław, Robert Grybos, and Frederik Tielens. "Isolated Chromium (VI) Oxide Species Supported on Al-Modified Silica: A Molecular Description." The Journal of Physical Chemistry C 120.31 (2016): 17594-17603.

[44] Gheju, Marius, Ionel Balcu, and Giannin Mosoarca. "Removal of Cr (VI) from aqueous solutions by adsorption on MnO_2." Journal of hazardous materials 310 (2016): 270-277.

[45] Sharma, D. C., and C. F. Forster. "Removal of hexavalent chromium using sphagnum moss peat." *Water Research* 27.7 (1993): 1201-1208.

[46] Bailey, R. P., T. Bennett, and M. M. Benjamin. "Sorption onto and recovery of Cr (VI) using iron-oxide-coated sand." *Water Science & Technology* 26, no. 5-6 (1992): 1239-1244.

[47] Udaybhaskar, P., Leela Iyengar, and A. V. S. Rao. "Hexavalent chromium interaction with chitosan." *Journal of Applied Polymer Science* 39.3 (1990): 739-747.

[48] Sharma, D. C., and C. F. Forster. "Continuous adsorption and desorption of chromium ions by sphagnum moss peat." *Process Biochemistry* 30.4 (1995): 293-298.

Chapter IV

IV. CONCLUSIONS AND RECOMMENDATIONS

1. Conclusions

The technical feasibility of Mn_2O_3 and MCS application for Cr (VI) removal from DI water has been investigated in batch systems at room temperature. The Langmuir, Freundlich, and D-R isotherms models were used to interpret the generated equilibrium adsorption data. It was found that the Freundlich model generally captures the effects of the Cr (VI) sorption process on all three Mn oxides studied for the concentration range and most accurately estimates the adsorption capacities. The sorbents can therefore be compared using Freundlich parameters; Mn_2O_3 showed the highest correlation and strongest binding of Cr (VI) ions with a 1/n value closest to zero followed by New MCS and X MCS. The adsorption capacity decreased in order X MCS □ Mn_2O_3 □ New MCS. Also, all three adsorbents displayed similar and low mean free energy indicative of predominating physical adsorption. The Freundlich model also correlates with a physical adsorption process. The Langmuir model conformed only to the Mn_2O_3 adsorption data; this observation implies that monolayer adsorption and heterogeneous surface conditions may co-exist under applied experimental conditions. Hence, the overall sorption of Cr (VI) on the Mn_2O_3 is complex and may involve more than one mechanism, such as ion exchange, surface complexation, and electrostatic attraction. The weak binding and multi-layer adsorption onto MCS sorbents can be attributed to the irregular and multi-phase surface whereas the crystalline and smooth surface of Mn_2O_3 allows for stronger binding and monolayer adsorption.

Furthermore, to justify the validity of Mn oxides as adsorbents for Cr (VI) ions adsorption, the obtained adsorption capacitates were compared with other alternative adsorbents and were found to be higher than that of bentonite, manganese dioxide, and more costly adsorbents such as GAC and commercial AC. In general, Mn oxides were found to be promising alternative adsorbents for Cr (VI) removal from DI water at low concentration.

Next, it was found that the adsorption of Cr (VI) onto Mn adsorbents was rapid for the first 30 to 60 minutes and then slowed as the equilibrium approached to depict a two-step reaction mechanism that was best described by a simple pseudo-second order rate expression. This finding suggests chemisorption is a possible alternative mechanism or that more than one rate-controlling step may exist. The pseudo second order rate constants and initial adsorption rates were in the order of X MCS □ New MCS □ Mn_2O_3, were found to correlate with adsorbent surface properties, and were similar to those reported for Mn nodule leached residue, montmorillonite, & iron-manganese coated sand. The comparatively slower second-order rate constant and initial adsorption rate obtained for Mn_2O_3 supports chemisorption as the overall rate-limiting step whereas the rapid adsorption on MCS is considered physical and reversible in nature with either external mass transfer or chemisorption or both as rate-limiting in the adsorption process.

Moreover, the adsorption and kinetics results were consistent with other observed phenomena including the results from pH studies and remaining studies. Specifically, Mn_2O_3 demonstrated a far greater affinity for Cr (VI) from pH 2 to 9 than MCS suggesting both electrostatic and chemical interactions likely occur at the interface while the MCS adsorbents demonstrated an

even wider effective adsorption range than Mn_2O_3. Although Cr (VI) adsorption generally decreased with increasing pH for the studied Mn adsorbents following typical anion adsorption, the effective Cr (VI) adsorption range was much wider in comparison to other reported oxides, which suggests that Mn adsorbents can be applied in water treatment processes without the need for pH adjustment.

From the coexisting ion studies, Ca^{2+} cations were found to slightly enhance electrostatic Cr (VI) anion adsorption while co-existing anions exhibited a competing effect in the order of PO_4^{3-} □ HCO_3^- □ SO_4^{2-} for all sorbents. The decrease in Cr (VI) adsorption was generally more pronounced with an increase in competing anion concentration in the case of MCS whereas Mn_2O_3 showed little change at the higher concentrations. Mn_2O_3 was also found to have a stronger affinity for PO_4^{3-} and HCO_3^- than MCS. These findings again suggest a difference in surface site characteristics of two oxides. Therefore, it can be hypothesized that Cr (VI) form both inner and outer-sphere complexes on Mn_2O_3 and weakly bind as outer-sphere complexes on MCS surface, which can be easily recovered. The possibility of adequate MCS regeneration then is also indicated.

All previous findings were found to be consistent with zeta potential measurements and observed PZC shifts of adsorbents after Cr (VI) adsorption. Mn_2O_3 showed a far greater change in zeta potential and in PZC likely due to greater Cr (VI) adsorption and specific inner-sphere anion adsorption by ligand exchange with OH^- groups at the surface. Bhutani et al. (1992) also confirmed the chemical interaction of Cr (VI) on MnO_2 surface from infrared spectroscopy measurement.

Finally, the reuse capacity of the MCS adsorbent was found to be greater than that of Mn_2O_3. This may be explained by the monolayer saturation of the Mn_2O_3 surface sites or creation of new adsorption sites and multi-layer formation on MCS. Moreover, New MCS showed potential for further reuse and Cr (VI) recovery after regeneration using 0.001 N NaOH, which was the lowest concentration studied. The regeneration efficiencies and Cr (VI) recovery percentages were high and comparable to several other alternative adsorbents. The desorption results also suggest that Cr (VI) adsorption is a reversible process clearly supporting physical adsorption as the dominant mechanism of Cr (VI) adsorption on MCS. In general, the MCS adsorbent is considered the more cost-effective as it can be reused in multiple cycles of adsorption and as the Cr (VI) can also be recovered for reuse.

In summary, the application of MCS adsorbents for Cr (VI) removal can offer the following advantages: wider effective pH range, greater stability under competing conditions, higher reuse capacity, and successful Cr (VI) recovery, and much cheaper preparation cost. However, the MCS adsorbent must be developed further and additional studies are needed in order to improve the Cr (VI) adsorption capacity and meet the 0.1 mg/L MCL requirement.

2. Recommendations

The coating solution pH and consistency can be optimized to enhance adsorption capacity of the MCS adsorbent while spectroscopic studies can confirm surface complex structures and stoichiometry directly for future optimization of adsorption mechanism pathways. Moreover, the

simultaneous removal of other contaminants can also be investigated to assess sorbent multi-functionality and decrease costs. To test sorbent stability in multiple regeneration cycles and to minimize costs further, additional eluents can be studied for Mn_2O_3 and MCS regeneration. Column studies are required to further evaluate the practical application for Cr (VI) removal from actual wastewater in a continuous flow system.

VITA

NAME: Snover Kaur Punia

EDUCATION:

M.S., Civil and Materials Engineering, University of Illinois at Chicago, Chicago, Illinois, 2017

B.S., Biology, Loyola University Chicago, Chicago, Illinois, 2010

B.S., Psychology, Loyola University Chicago, Chicago, Illinois, 2008

HONORS: Graduate Teaching Assistant, University of Illinois at Chicago, Chicago, Illinois, 2014-2015

MEMBERSHIP: American Society of Civil Engineering

PUBLICATIONS:

Punia, Snover, Kamel Babaeivelni, Lisha Wu, and Amid P. Khodadoust. "Removal of Arsenic from Coal Fly Ash Leachate Using Manganese Coated Sand." Geotechnical Special Publication, Vol. 2016-January, Issue 273 GSP, 62-69.

Wu, Lisha, Snover Punia, and Amid P. Khodadoust. "Removal of Chromium, Copper, and Arsenic from Contaminated Water Using Manganese Oxide Based Adsorbents." Geotechnical Special Publication, Vol. 2016-January, Issue 273 GSP, 2016, 53-61.